Doctoral Thesis

Efficient Bi-Directional Communications for Low-Power Wireless Mesh Network

Ryota Okumura
Graduate School of Informatics, Kyoto University

March 2021

Preface

With the spreading of the Internet of things (IoT), wireless communication technologies for transferring sensing or actuating information between IoT terminals are becoming more important. The receiver-initiated transmission (RIT) protocol, which is a receiver-initiated media access control (MAC) protocol standardized in the Institute of Electrical and Electronics Engineers (IEEE), is a promising technology for constructing low-power mesh networks. Such networks are operated under strong constraints to achieve long battery life, but the transmission performance should be enhanced for emerging advanced applications. This thesis aims to provide efficient bi-directional communications on the low-power wireless mesh networks based on the RIT protocol.

The MAC protocol is a crucial technology on low-power wireless mesh networks to achieve better transmission performance and interoperability. Therefore, as the first topic of this thesis, a concrete RIT protocol is analyzed to reveal its feature. For gas and water smart metering systems, the RIT protocol was standardized in the Wi-SUN Alliance as the Japan Utility Telemetering Association (JUTA) profile. However, the transmission performance of the concrete MAC protocol based on the JUTA profile has not been reported. In this thesis, the transmission performance of the Wi-SUN JUTA-profile compliant feathery RIT (F-RIT) protocol with the communication sequence of the U-Bus Air is designed and examined through theoretical analysis, computer simulations, and experiments with actual Wi-SUN dongles. The evaluations prove the feasibility of the Wi-SUN JUTA-profile compliant F-RIT protocol. Furthermore, through detailed analyses with the experimental results, the features of the implemented protocol on the performance of the carrier sense and the incident of the timeout are revealed.

Then, this thesis discusses the enhancement of the bi-directionality for efficient communications. This thesis focuses on communication traffics and tackles different problems depending on traffics. In the usual time, it is important to save the battery, so the communication traffic is not high. For data collections in the usual time, polling can be a better way to achieve dependable communications because it can avoid the collisions of data transmissions. However, the delay and current consumption due to the round-trip operation should be improved. Besides, for gas and water smart

metering systems, the emergency notification function is also important for safety. In such unusual cases as disasters, frequent calling traffic may occur. A higher transmission success rate is required under high traffic bi-directional communications in which each terminal tries to transfer data.

For the problem in the usual time, this thesis presents efficient polling communications for low-power data collections. The efficient polling communications are achieved from two proposals based on the cross-layered design. The first is the enhanced source routing scheme for downlink communications. The proposed scheme enables the flexible route selection to shorten the waiting time to transfer the data. The second is the round-trip delay reduction scheme focusing on the bi-directionality of polling communications. By simple and temporary parameter setting after the downlink communications, each terminal can wait for uplink communications by efficient operations. These two proposals are designed from independent viewpoints. The computer simulation results show that low-power and low-delay polling communications are achieved by the combined use of the two proposals.

This thesis proposes the enhanced F-RIT (eF-RIT) protocol for high traffic bi-directional communications in urgent cases. In relation to this subject, experiments of high traffic bi-directional communications of a standard-compliant RIT protocol are conducted. From the analysis of the communication failure cases, it is found that the incident of the timeout is the dominant factor for communication failures under high traffic conditions. The proposed eF-RIT protocol suppresses the timeout incidents by introducing the operation as the receiver during the waiting time as the sender. The feasibility of the proposed eF-RIT protocol is also shown by experiments with actual dongles.

The chapters of this thesis are listed as follows. Chapter 1 outlines the background of low-power wireless mesh networks and the overview of this thesis. In Chapter 2, wireless technologies for low-power IoT systems are discussed. The Wi-SUN JUTA profile-compliant F-RIT protocol is analyzed in Chapter 3. The efficient polling communications for power-efficient data collections in the usual time are presented in Chapter 4. Chapter 5 proposes the eF-RIT protocol for high traffic bi-directional communications for urgent cases. Finally, Chapter 6 concludes this thesis.

Acknowledgement

First of all, I would like to express my sincere gratitude to my supervisor, Professor Hiroshi Harada, for his helpful guidance and support in my research. Without his persistent help and constructive instruction, this work would have never been completed.

I also express my deep appreciation to Professor Masahiro Morikura and Professor Eiji Oki for their valuable advices and incisive comments on this thesis. Their advice and comments have been a great help in improving this thesis.

I express my great gratitude to Associate Professor Keiichi Mizutani for his strong support and guidance. Without his consistent and constructive instruction, this thesis could not have reached its present form.

I would also like to thank Associate Professor Hidekazu Murata, Dr. Takeshi Matsumura, and Ms. Hiroko Masaki for their helpful comments on my research.

I am deeply grateful to Dr. Jun Fujiwara of Antenna Giken Co., Ltd. and Mr. Takuya Kawata of Tokyo Gas Co., Ltd. for helpful discussions on my research.

I am also very grateful to laboratory secretaries and student members of Digital Communication Laboratory of Graduate School of Informatics, Kyoto University.

Finally, I would like to thank my parents and family for their support and encouragement throughout my work.

Contents

List of Figures

List of Tables

Abbreviations

Abbreviation	Description
6LoWPAN	IPv6 over low-power wireless PAN
6TiSCH	IPv6 over the TSCH mode of IEEE 802.15.4e
ACK	acknowledgement
AMI	advanced metering infrastructure
AODV	ad-hoc on-demand distance vector
ARIB	Association of Radio Industries and Businesses
BAN	body area network
CAP	contention access period
CFP	contention-free period
CSL	coordinated sampled listening
CSMA/CA	carrier sense multiple access with collision avoidance
CTS	clear to send
DACK	DATA ACK
DAO	destination advertisement object
DIO	DODAG information object
DODAG	destination oriented directed acyclic graph
DSSS	direct sequence spectrum spread
ETX	expected transmission count
F-RIT	feathery-RIT
FAN	field area network
FFD	full function device
GFSK	Gaussian frequency-shift keying
HAN	home area network
High-MAC	higher part of the MAC layer
IC	integrated circuit
IE	information element
IEEE	Institute of Electrical and Electronics Engineers
IEICE	Institute of Electronics Information and Communication Engineers
IETF	Internet Engineering Task Force
IP	Internet protocol
IPv6	IP version 6

Abbreviation	Description
IRDT	intermittent receiver-driven data transmission
ISM	industry science and medical
IoT	Internet-of-things
JUTA	Japanese Utility Telemetering Association
L2	layer 2
L2R	L2 routing
L3	layer 3
LFD	limited function device
LIFS	long interframe spacing
LPL	low power listening
LPWA	low-power wide-area
LQM	link quality metric
LTE	long term evolution
LTE-M	LTE category M
Low-MAC	lower part of the MAC layer
MAC	media access control
MANET	mobile ad-hoc network
NB-IoT	narrow-band IoT
NET	network
O-QPSK	offset phase-shift keying
OF	objective function
OFDM	orthogonal frequency-division multiplexing
OLSR	optimized link state routing
P2P	peer-to-peer
PAN	personal area network
PC	personal computer
PHY	physical
PQM	path quality metric
PSDU	physical layer service data unit
PSM	power save mode
Pre-CS	pre-carrier sense
QoS	quality of service
RACK	request ACK
RFC	request for comment
RI-MAC	receiver-initiated MAC

Abbreviation	Description
RICER	receiver-initiated cycled receivers
RIT	receiver-initiated transmission
RNACK	request negative ACK
RNO	radio number
RPL	IPv6 routing protocol for low-power and lossy networks
RSSI	received signal strength indicator
RSW	received signal weakness
RTS	request to send
SREQ	send request
SRM	spectrum resource management
SUN	smart utility network
TDMA	time division multiple access
TSCH	time slotted channel hopping
UART	universal asynchronous receiver/transmitter
USB	universal serial bus
WG	working group
Wi-SUN	wireless SUN
WAN	wide-area network
WuR	wake-up radio
eDRX	extended discontinuous reception
eF-RIT	enhanced F-RIT

Chapter 1
Introduction

1.1 Background

In the Internet-of-things (IoT) era, various things are being connected to the Internet to collect and utilize a variety of information. A typical IoT system is the smart metering system for electric power infrastructure. In Japan, smart power meters are being introduced widely to gather a huge number of power meter readings and to analyze the electricity usage information in real-time [1], [2]. A fundamental technology for the IoT systems is wireless communication that connects a large number of devices to the Internet at low-cost with high reliability. Cellular-based systems (e.g., narrow-band IoT (NB-IoT) [3]) is one of the solutions. While the NB-IoT can provide highly reliable transmission by operating in licensed bands, a higher service cost is required when all devices communicate directly with a base station by only a cellular-based system. Low-power wide-area (LPWA) systems using unlicensed bands (e.g., industry science and medical (ISM) bands or sub-GHz bands) like the SigFox [4] and the LoRaWAN [5] are also candidates for the IoT systems because they have the advantage of a lower cost than the cellular-based systems. However, these LPWA systems have the drawback that blind zones (i.e., no service area due to shadowing effects) are generated in their service range installing in urban areas with dense buildings. To resolve the blind zone problem, the introduction of multi-hop transmissions is necessary. For these reasons, the IEEE 802.15.4-based personal area network (PAN) system supporting multi-hop transmissions is suitable for IoT systems like smart metering systems in urban areas. In Japan, the 920 MHz-bands are allocated for the smart metering systems [6]: thus, many devices for the smart power meters support the 920 MHz-band operations and the multi-hop transmissions based on the IEEE 802.15.4g-compliant physical (PHY) layer [1], [7].

Similarly, the smart meters have been introduced in gas and water infrastructures (e.g., the wireless M-Bus [8] in Europe). The biggest difference between the smart power meter and the smart gas or water meters is the driving power of the wireless communication device. Generally, the wireless communication device for the smart

power meter is driven by a fixed power supply. On the other hand, the device for smart gas or water meter has to be driven by a battery for a long period, such as over ten years. Therefore, media access control (MAC) protocols to operate with low-power consumption have been developed. For example, the U-Bus Air [9], [10], which is a Japanese domestic wireless specification supporting multi-hop transmissions for gas and water utilities developed by the Japanese Utility Telemetering Association (JUTA) [11], adopts the receiver-initiated MAC protocol [12].

The origin of the receiver-initiated MAC protocol in the U-Bus Air is the wireless communication protocol called the intermittent receiver-driven data transmission (IRDT) [13], [14]. The IRDT specifies from the PHY layer to the network (NET) layer, and the MAC protocol is regarded as a receiver-initiated protocol. The IRDT can achieve low-power operation and has the robustness for the fluctuations in the wireless environment, so it is suitable for sensor networks. However, it was necessary to achieve the lower cost, stable module supply, and higher interoperability in the large-scale deployment for gas and utilities. Therefore, the standardization efforts were made towards the development of the U-Bus Air. In 2009, the PHY and MAC layer of the IRDT were proposed in IEEE [15], [16]. As a result, the PHY layer and a simple linking method in the MAC layers were adopted in IEEE 802.15.4g [7] in 2012 and IEEE 802.15.4e [17] in 2012, respectively. The linking method is called the receiver-initiated transmission (RIT) [17]. Moreover, in 2015, some components of the RIT operation related to the U-Bus Air were adopted in the IEEE 802.15.4-2015 [18]. Also, the complex link control in the MAC layer, the routing in the NET layer, and various functions of the U-Bus Air were summarized and released as drafts of domestic specification [9], [10]. However, the interoperability cannot be ensured only the standardization. Hence, the JUTA has standardized the IEEE standard-based PHY layer and a part of the MAC layer (i.e., a concrete MAC protocol, partially recognized the feathery-RIT (F-RIT) protocol [19], [20] developed based on the RIT protocol) to support the U-Bus Air in the Wi-SUN Alliance [21]. This specification is called the Wi-SUN JUTA profile. Also, in the Wi-SUN Alliance, the products are certified by taking the conformance and the interoperability tests [1]. To sum up, the network using the receiver-initiated MAC protocol was subdivided from the IRDT and standardized for the spreading. For constructing a communication system by combining technologies, it is very important to reveal the characteristics of each technology [20].

Moreover, developments to accommodate practical IoT traffic is also important. In the society with IoT technologies, not only sensing but also actuating information are required to be exchanged to control things or feedback information. For such sensing and actuating, uplink and downlink communication technologies are required. In smart metering systems, downlink communications are generally required for actuating such as meter reading control based on contract information or energy supply control under emergency situations [22]. However, in IoT systems with limited resources for communications, uplink communications for sensing information are often taken precedence, and downlink communications for actuating tend to be neglected. This problem is remarkable in LPWA systems that often specialize in sensing from a wide area. Therefore, expansion of downlink communications is essential for the next generation IoT systems, and multi-hop networks are suitable for such use cases. Focusing on multi-hop networks based on receiver-initiated MAC protocols, most of the researches have focused on uplink communications [13], [14], [23]–[27]. Hence, researches for bi-directional communications in practical scenarios are required. From the viewpoint of subdivided and simplified standardized technologies, it is also necessary to reconsider each elemental technology or combination of technologies for practical bi-directional communications.

1.2 Research Challenges

This thesis aims a low-power mesh networks by receiver-initiated MAC protocols. Figure 1.1 illustrates a typical concept of the low-power wireless mesh network targeted in this thesis. The mesh network assumes IoT systems like gas smart metering systems, and consists of battery-powered terminals, i.e., low-power communications between terminals are required. Battery-powered terminals communicate with each other using IEEE 802.15.4-based wireless PAN technologies. At least one terminal in the mesh network can be connected to the Internet using a wide-area network (WAN) like the long-term evolution (LTE). Collections of sensing data, instructions for actuation, or alarm reports of unusual situations are considered as traffics on such networks. Although there may be a stable power supply to some terminals in the practical case depending on applications, this thesis only considers that all terminals operate with the low-power MAC protocol.

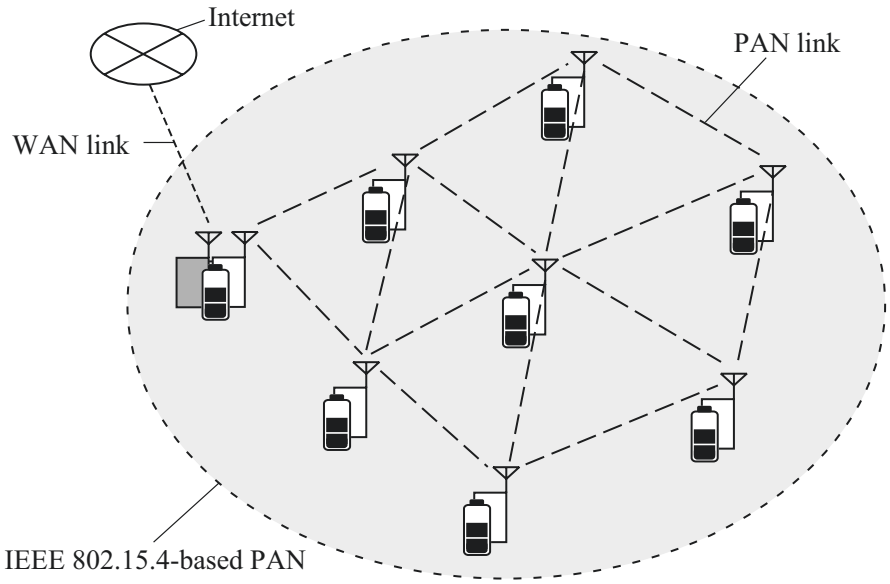

Figure 1.1: Concept of low-power wireless mesh network.

The main purpose of this thesis is to provide efficient and low-complexity communications with the RIT protocol on the wireless mesh network. To build a practical wireless network, it is necessary to operate concrete elemental technologies in an appropriate combination. In that sense, establishment of a concrete receiver-initiated MAC protocol, which has the interoperability required in IoT networks, is an essential point. It is also essential to achieve efficient and practical communications under the strong constraints to achieve battery-powered operation. In other words, it is desirable to be able to achieve low-power consumption or reliable communications in various traffic conditions. To deal with this, appropriate cross-layered designs are required for efficient operation.

The first research challenge in this thesis is the feasibility study of the standardized technology in the MAC layer. As described in the previous section, the technologies in the low-power wireless mesh network based on the receiver-initiated protocol are subdivided and standardized. For practical use, it is required to reveal the characteristics of each concrete standardized technology. This thesis studies the Wi-SUN JUTA profile-compliant F-RIT protocol by detailed analyses to prove its feasibility [28]. The overview of this challenge is also described in Sect. 1.2.1.

Although the studies on an elemental technology is important to validate the feasibility, the subdivided and simplified standardization does not always lead to practical network functions. It is necessary to improve the efficiency with the

practical use of the networks by reconsidering the technology or appropriate combination of the technologies. Hence, this thesis tries to enhance the communication characteristics focusing on bi-directionality of the practical communication traffics for IoT. This thesis focuses on bi-directional traffics in usual and emergency cases. For the data collections in the usual time, the polling communication can be used. It can avoid traffic concentration that deteriorates the communication reliability, but the larger delay and the power consumption due to bi-directional communications should be improved. This thesis proposes two schemes to improve the delay and the power consumption to achieve efficient polling communications [29]. The overview of this challenge is described in Sect. 1.2.2. In the communications in emergency cases, frequent calling traffic should be treated. This thesis evaluates the bi-directional frequent communications based on the F-RIT protocol and proposed the enhanced F-RIT (eF-RIT) protocol for reliable bi-directional communications [30]. The overview of this challenge is presented in Sect. 1.2.3.

1.2.1. Theoretical and Experimental Analyses of Wi-SUN JUTA Profile-Compliant F-RIT Protocol

For Wi-SUN systems, the communication characteristics of IEEE 802.15.4g-compliant systems and IEEE 802.15.4e-compliant F-RIT protocol have been evaluated by computer simulations and experiments [19], [20], [31]. However, these efforts are not concrete for the use in gas and water utilities. From the viewpoint of the PHY layer for utility use, the author has evaluated the transmission characteristic of the IEEE 802.15.4g-based communication system in water smart metering environments [32], [33]. In terms of the MAC layer, although the F-RIT protocol was standardized as the Wi-SUN JUTA profile for utility, there are no evaluations of its performance. In this thesis, the feasibility study of the Wi-SUN JUTA profile-compliant F-RIT protocol is conducted by analyzing the practical performance of the MAC layer in detail [28]. This thesis reveals the transmission performances of the Wi-SUN JUTA profile-compliant F-RIT protocol from theoretical analysis, computer simulations, and experimental evaluations. Also, the results are examined from viewpoints of the frame transmission performances and the timeout incidents. The analyses show that although sufficient transmission performance is achieved in actual modules, but the interference that cannot be detected by the carrier sense causes the continuous incidents of the timeout.

1.2.2. Efficient Polling Communications for Low-Power Data Collections

Multi-hop networks based on the receiver-initiated MAC protocols have a problem of low-reliability due to the collisions that occur when multiple terminals try to communicate with a receiver at the same time [13], [23]. Polling communications can avoid such collision problems and can achieve reliable data collections [34]. However, the round-trip operation causes a larger delay and a larger current consumption. This thesis improves the delay and the current consumption in polling communications by two proposed schemes that evoke the unique characteristics of receiver-initiated MAC protocols in round-trip communications [29]. The first is the enhanced source routing scheme that specifies multiple terminals as candidates of the relay terminal. With the proposed routing scheme, the advantage of opportunistic routing for RIT protocol can be also utilized in downlink communications to achieve low-delay and low-power consumption data collections. The second is the round-trip delay reduction scheme based on the wake-up interval modification, which focuses on the bi-directionality of polling communications. It can shorten the uplink communication delay by simple and temporary parameter modification. By the combined use of the two proposed schemes, data can be collected efficiently with the lower delay and the lower current consumption while maintaining high reliability of polling communications.

1.2.3. Enhanced F-RIT Protocol for High Traffic Bi-Directional Communications

The RIT protocol, in which the receiver-initiated MAC protocol is simplified for standardization, specifies behaviors for the sender and receiver separately. The previous two challenges also have a similar idea. However, taking the example of gas smart metering systems, emergency situations (e.g., gas leak detection and shut-off operation) can be assumed. In such cases, frequent communications occur. Also, the bi-directional communications are required for packets generated and transmitted individually by each terminal. Therefore, the case that each terminal has functions as both a sender and a receiver should be considered. In this challenge, the IEEE 802.15.4e-compliant F-RIT protocol in the bi-directional communication model is evaluated by computer simulations and experiments to show that the communication reliability decreases in high traffic bi-directional communications [30]. Also, the

experimental results are analyzed in detail and it is shown that the timeout incidents in bi-directional communications are the main factor of the communication failures. Then, this thesis proposes the eF-RIT protocol to suppress the timeout incidents in bi-directional communications [30]. The computer simulations and experiments with Wi-SUN dongles show the feasibility of the proposed eF-RIT protocol.

1.3 Outline and Contributions of This Thesis

The chapter overview of this thesis relevant to the challenges is shown in Fig. 1.2. In Chapter 2, the wireless technologies for IoT communication systems are presented. The status of multi-hop networks based on the IEEE 802.15.4 are introduced along with various IoT communication systems. Moreover, elemental technologies in the multi-hop networks based on the IEEE 802.15.4 such as MAC protocols and routing protocols are introduced. Also, the combinations of technologies into various system configurations are discussed, and the characteristics and the uniqueness of the wireless mesh networks based on the receiver-initiated MAC protocols are clarified.

In Chapter 3, the feasibility of the Wi-SUN JUTA profile-compliant F-RIT protocol is studied from theoretical analysis, computer simulations, and experiments with actual dongles [28]. From evaluations, it is proven that the Wi-SUN JUTA profile-compliant F-RIT protocol achieves the efficient communication characteristic in an interference environment. Moreover, the feature of the protocol is discussed based on detailed analysis results.

Polling communications for usual data collections are studied in Chapter 4 [29]. The two schemes are proposed to achieve efficient polling communications based on the F-RIT protocol. Results from computer simulations show the effectiveness of proposed schemes to improve the communication delay and the current consumption for reliable and low-power communications.

In Chapter 5, the eF-RIT protocol is proposed to achieve high traffic bi-directional push-type communications [30]. The conventional IEEE 802.15.4e-compliant F-RIT protocol and the proposed eF-RIT protocol are evaluated not only by computer simulations but also experiments with Wi-SUN dongles. The conventional IEEE 802.15.4e-compliant F-RIT protocol is analyzed in detail to show that the timeout problem occurs under high traffic conditions. The computer simulation and

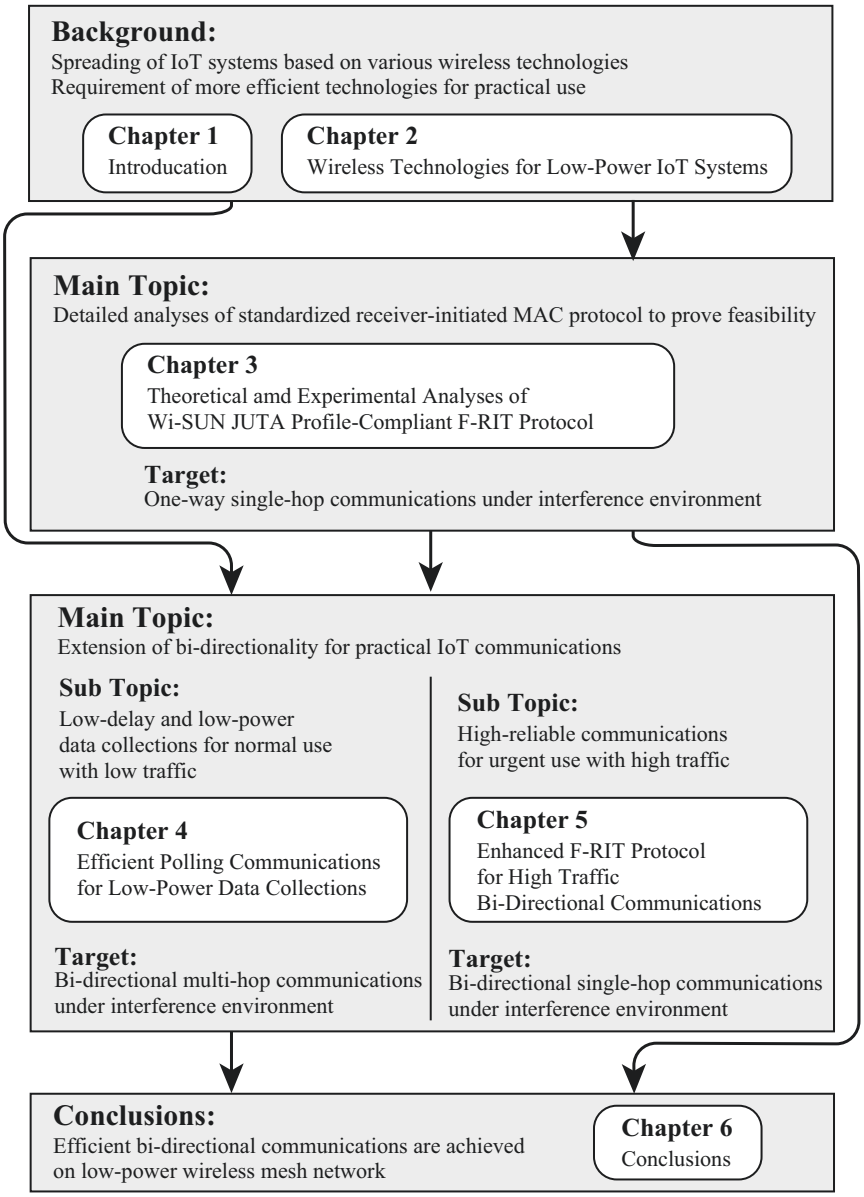

Figure 1.2: Chapter overview.

experimental results confirm that the eF-RIT protocol improves the transmission success rate by resolving the timeout problem.

Finally, Chapter 6 concludes this thesis by summarizing achievements and discussing future works.

Chapter 2
Wireless Technologies for Low-Power IoT Systems

This chapter describes wireless technologies for low-power IoT systems. From the overview of various technologies, the specificity of receiver-initiated MAC protocols and multi-hop networks based on receiver-initiated MAC protocols is emphasized. In Sect. 2.1, various wireless communication systems are discussed, and the advantage of the multi-hop systems based on the IEEE 802.15.4 is clarified. Then, standardized MAC and routing technologies for multi-hop systems are introduced in Sect. 2.2. The combined uses of MAC and routing technologies are discussed, and the uniqueness of the RIT protocol is emphasized. After that, the related researches and activities on the target of this thesis, receiver-initiated MAC protocols, are explained. In Sect. 2.3, the features of low-power wireless mesh networks based on receiver-initiated MAC protocols are discussed. Then, issues and challenges related to them are investigated in Sect. 2.4. Development challenges for the U-Bus Air with a highly interoperable RIT protocol are introduced in Sect. 2.5. Finally, Sect. 2.6 concludes this chapter.

2.1 Wireless Communication Systems for IoT

On-ground wireless communication systems for IoT are divided into two categories by the frequency band to use. First is the cellular-based LPWA systems like the NB-IoT [3] and the LTE category M (LTE-M) [35]. These systems use licensed bands, and communication cost for each terminal is required. As the low-power technology, the power save mode (PSM) and extended discontinuous reception (eDRX) are adopted to reduce the idle duration [36]. Also, to achieve wider coverage compared to the LTE, it supports repeated transmissions.

Second is the communication systems operated in unlicensed bands. These systems often adopt PAN technologies. A large merit of using unlicensed bands is lower cost, but interferences from other systems should be considered. The 2.4 GHz band and sub-

GHz bands are often used for IoT systems. Examples of systems in the 2.4 GHz band are the ZigBee and the Bluetooth [37]. Although the 2.4 GHz band has the advantage of being able to be used worldwide, it has a short communication range and is susceptible to interference from Wi-Fi and microwave ovens. As a result, the systems in the 2.4 GHz band are often used for short-range communications in homes and offices. For IoT use cases, efforts for practical use of wireless communication systems using the sub-GHz bands have made great progress [38]. Although the sub-GHz bands has a smaller bandwidth than the 2.4 GHz band, they can be used for long-distance communications due to the high radio reachability. Also, systems using sub-GHz can avoid interferences from Wi-Fi systems. Therefore, it is used for various IoT applications both indoors and outdoors in the countries where the sub-GHz bands are available by regulations. In Japan, the 920 MHz-band is regulated by the Association of Radio Industries and Businesses (ARIB) [6].

Systems in the sub-GHz bands can be further classified into star topology-based communication systems and multi-hop communication systems. Examples of formers are the SigFox [4], the LoRaWAN [5], and the Wi-Fi HaLow [39]. They aim wider coverage to accommodate huge IoT devices mainly in outdoors. To achieve wider coverage, lower data rates based on modulation for long-range communications are adopted. Some systems adopt diversity technics like the time diversity by repeated transmission and space diversity by reception at multiple base stations [4]. Examples of multi-hop communication systems are the Wi-SUN [1] and the Z-Wave [37]. Multi-hop systems in sub-GHz bands often adopt IEEE 802.15.4-based PHY and MAC [18] technologies. Although the transmission coverage is shorter than LPWA systems like the SigFox and the LoRaWAN, multi-hop networks can expand the coverage or eliminate the blind zone by multi-hop transmissions. Also, they have a merit of a relatively higher PHY layer throughput compared to LPWA systems in the star topology. In multi-hop networks, there are many combinations of the MAC and network layer technologies than in the star topology networks. Appropriate technologies should be selected to satisfy various network requirements. In the following sections, technologies for IEEE 802.15.4-based low-power multi-hop networks are discussed.

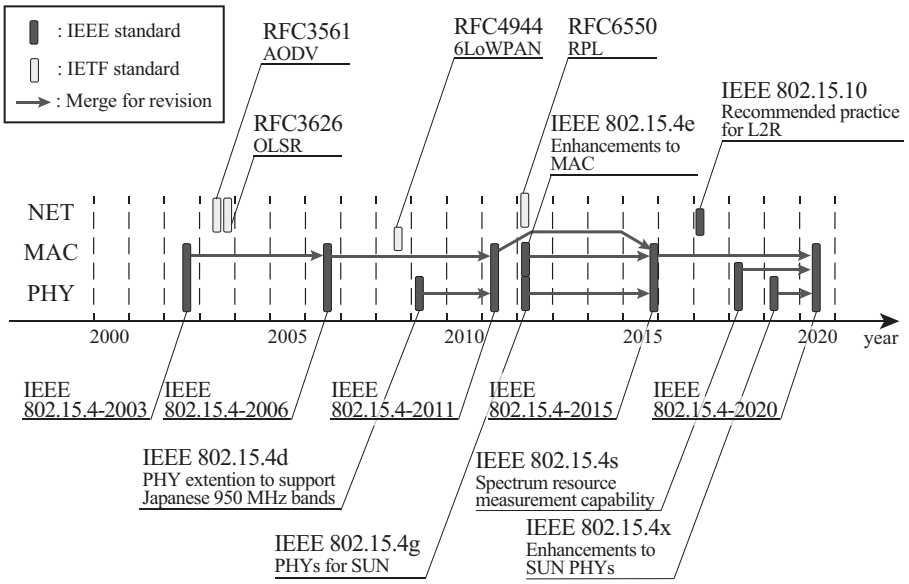

Figure 2.1: IEEE and IETF standards related to wireless multi-hop networks.

2.2 Standardized Technologies for Low-Power Multi-Hop Networks

In this section, the technologies for PAN-based low-power multi-hop networks are described. In general, PHY and MAC technologies for PAN are standardized in the IEEE. On the other hand, specifications related to Internet protocol (IP) are standardized in the Internet Engineering Task Force (IETF). Figure 2.1 shows major IEEE and IETF standards related PAN-based multi-hop networks. In 2003, the PHY and MAC standards for wireless sensor networks were started [40]. Besides, wireless routing protocols existed as IETF standards to be used mainly in mobile ad-hoc networks (MANETs). However, these technologies have been inadequate for IoT, which connects vast numbers of devices to the network. In the PHY layer, the specifications use the sub-GHz bands were developed. In Japan, the standards using sub-GHz bands have started from the IEEE 802.15.4d [41] standardized in 2009. In the MAC layer, the low-power operations are key technologies in IoT. From the beginning of the IEEE 802.15.4, there were the indirect transmission and the superframe-based MAC protocols. In the IEEE 802.15.4e [17] standardized in 2012, various low-power MAC protocols like the time-slotted channel hopping (TSCH), the coordinated sampled listening (CSL), and the RIT protocols, and so on were

Table 2.1: SUN FSK parameters for Japanese band [18].

Parameter	Operating mode			
	#1	#2	#3	#4
Data rate	50 kbps	100 kbps	200 kbps	400 kbps
Modulation	2-FSK	2-FSK	2-FSK	4-FSK
Modulation index	1.0	1.0	1.0	0.33
Channel spacing	200 kHz	400 kHz	600 kHz	600 kHz

standardized to enhance the options for low-power operations. For routing, the IP version 6 routing protocol for low-power and lossy networks (RPL) [42] was developed for IP-based IoT networks. Besides the IP-based networks, the IEEE 802.15.10 [43] was standardized to provide the lightweight layer 2 routing (L2R).

Since then, some elemental technologies have been standardized, such as the enhancements to PHYs for higher performance networks [44] and spectrum resource measurement (SRM) for effective spectrum utilization [45]. In addition, it is becoming more important for these technologies to be used efficiently. Therefore, cross-layered network designs depending on the purpose are developed in various organizations (e.g., the Wi-SUN Alliance [21] and the JUTA [11]).

2.2.1. PHY Technologies

In the IEEE 802.15.4 [18], various PHYs are defined as the offset phase-shift keying (O-QPSK), the Gaussian frequency-shift keying (GFSK), and the orthogonal frequency-division multiplexing (OFDM). For low-power systems, simple PHYs are often used to achieve power-efficient transmissions. For example, the ZigBee operated in the 2.4 GHz band based on the IEEE 802.15.4 adopts O-QPSK PHY with direct sequence spectrum spread (DSSS) and achieves a maximum data rate of 250 kbps [46]. Wi-SUN operated in sub-GHz bands adopts GFSK PHY for smart utility network (SUN). Table 2.1 shows parameters of SUN FSK for Japanese bands. The minimum data rate in the IEEE 802.15.4 is 50 kbps [1], and Japanese advanced metering infrastructure (AMI) systems often use a data rate of 100 kbps [47], [48].

2.2.2. MAC Protocol

MAC protocols are essential to the reduce wake-up time of terminals for long-term battery life. In the IEEE 802.15.4 [18], various protocols are standardized, and they

should be used properly for network requirements. In this section, the following protocols are introduced: the indirect transmission, the TSCH, the superframe, the CSL, and the RIT protocols. The indirect transmission protocol can be utilized in communications between a stable-powered terminal and a battery-powered terminal. Others can be used in communications between battery-powered terminals. The TSCH and the superframe protocols saves the power from synchronous way and the CSL and the RIT protocols reduces the current by asynchronous methods.

Indirect Transmission

The indirect transmission [49] is often adopted as the communication protocol between the stable powered terminal which listens to the channel always and battery-powered low-power terminal operated in the duty cycle. From battery-powered terminal to stable powered terminal, the normal carrier sense multiple access with collision avoidance (CSMA/CA) is performed to transmit the data. On the other hand, the stable powered terminal should perform queuing the data. The battery-powered terminal transmits a data request frame and performs a short time listening at the wake-up timing. At other times the terminal goes to sleep to save its battery. If the stable powered terminal receives a data request frame from the destination terminal, it notifies that a data is pending or not by transmitting an acknowledgement (ACK) frame. The data frame is transmitted after the ACK.

TSCH

The TSCH is one of the synchronous protocols adopted in the IEEE 802.15.4 [18]. In the TSCH-based networks, the timeslot is defined for the time axis. The time slot is common in the network and is long enough to exchange a data frame and an ACK frame. Also, the slotframe, which is several numbers of timeslots, is defined for scheduling. In a slotframe, pairwise direct communications between terminals are assigned. If a terminal has a frame to be transmitted, the terminal should wait for the link to the destination terminal. In the assigned timeslot to communicate with the destination, the terminal transmits a data frame at the designated timing in the timeslot. Channel hopping can mitigate the multipath fading effect, and schedules for channels and timeslot work to avoid contention [50].

The TSCH can be used in low-power operation. In a timeslot, a terminal can not only transmit or receive a frame but can also turn off the radio to save energy. Also, even if the reception operation is assigned to a timeslot, it is not necessary to receive in all the slot. This is because the frame transmission timing is synchronized, and the

wakeup duration can be limited. In the TSCH, time synchronization accuracy is a key for the operation. The terminal with a larger clock drift should enlarge the listening duration [51]. Therefore, high-accuracy network-wide time synchronization is required to achieve a lower duty-cycle. Although the high-accuracy synchronization can be achieved by some efforts, but high timing precision and low variance of the drift are required [52].

Superframe

The superframe is a format defined by a PAN coordinator in the beacon mode. Communication timings are bounded by beacon frames, which are transmitted at the beginning of each superframe. Active and inactive periods can be defined in a superframe, and terminals can sleep in the inactive periods to save the power. In the active period, the contention access period (CAP) is offered for random access by the slotted CSMA/CA. The PAN coordinator can allocate some periods for low-latency or quality of service (QoS) aware applications as the contention-free period (CFP). By adopting turned-off beacons and reducing the active period, the low-power operation enough for the long-term battery life can be achieved [53]. Also, the multi-hop can be realized when the full function device (FFD) defines other superframes for other FFDs or limited function devices (LFDs).

CSL

The CSL protocol is one of the asynchronous MAC protocols adopted in the IEEE 802.15.4 [18]. The operating principle is derived from the low power listening (LPL) [54], which adds a long preamble before transmitting a data frame so that the receiver in the low duty cycle can detect the frame transmission. In the IEEE 802.15.4, the long preamble is interpreted as the wake-up sequence. To satisfy the requirements in the IEEE 802.15.4 and radio regulations like ARIB STD-T108 [6] in Japan, the embodying CSL protocol is often used with the packetized wake-up sequence [55], [56].

The operational overview of the CSL protocol with the packetized wake-up sequence in the IEEE 802.15.4 is described in Fig. 2.2. The battery-powered low-power terminal performs the short time listening called the cannel sample at the interval of the MAC CSL period. A terminal that generates a data frame starts the wake-up sequence. In the wake-up sequence, the wake-up frames that consist of the destination address and the transmission timing of the data frame are transmitted continuously. When the CSL protocol is operated in asynchronous, the wake-up

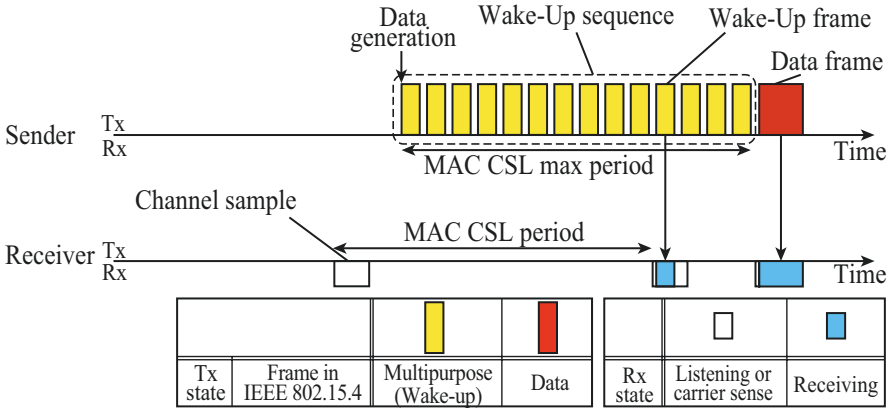

Figure 2.2: Operational overview of CSL protocol.

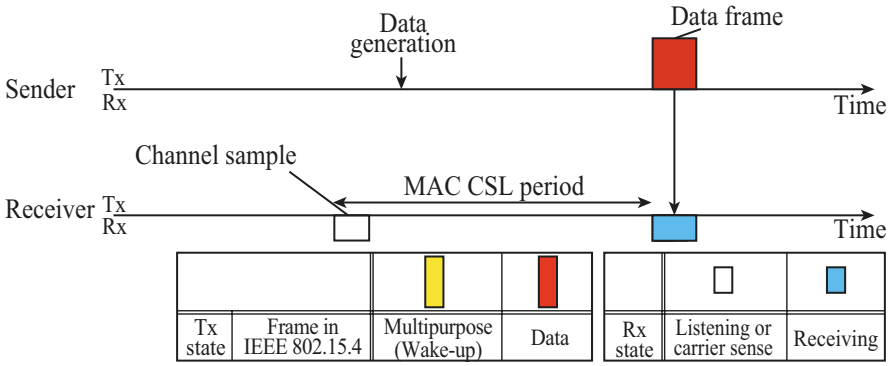

Figure 2.3: Operational overview of synchronous CSL protocol.

sequence length is set for longer than the MAC CSL period so that the destination terminal can receive the wake-up frame. The destination terminal that gets the transmission timing from the received wake-up frame performs the listening to receive a data frame according to the timing information in the wake-up frame. Also, the synchronous operation of the CSL protocol is defined in the IEEE 802.15.4 [55]. If the sender knows the receiver's wake-up timing, the wake-up sequence can be reduced unless the receiver can get the wake-up or data frame as shown in Fig. 2.3.

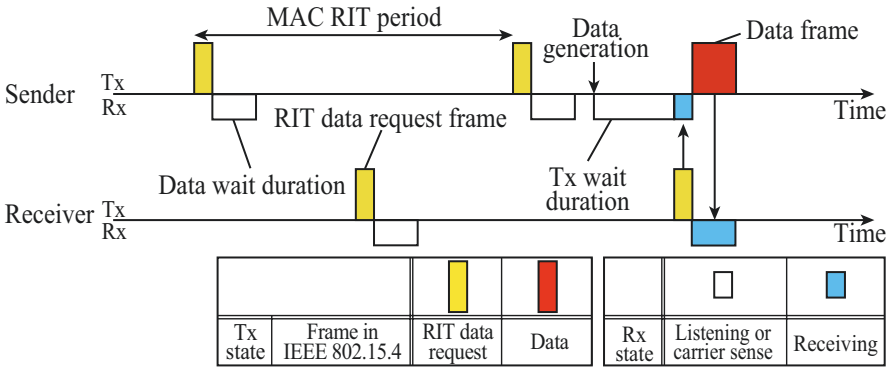

Figure 2.4: Operational overview of RIT protocol. ©2021 IEICE

RIT

The RIT protocol is an asynchronous MAC protocol adopted in the IEEE 802.15.4 [18]. The receiver-initiated operating principle is derived from the receiver-initiated MAC protocols like the RI-MAC and the IRDT, but the RIT protocol is standardized as an simple and basic protocol in the IEEE 802.15.4. A procedure of the RIT protocol defined in the IEEE 802.15.4 [18] is shown in Fig. 2.4. In the RIT protocol, all terminals periodically transmit a frame called the RIT data request frame. The transmission interval is called the MAC RIT period. After the transmission, the terminal listens to the channel for a short time to receive the frame addressed to itself. This period is called the data wait duration. A case is considered that a terminal illustrated as a sender in Fig. 2.4 generates a data frame and tries to transmit to a terminal illustrated as a receiver in Fig. 2.4. First, the sender starts listening to receive the RIT data request frame from the receiver. This state is called the Tx wait duration, and continued for the period of the MAC RIT Tx wait duration unless the sender succeeds to transfer the data frame. If the sender receives an RIT data request frame from the receiver, the sender transmits the data frame. The receiver can start to receive the data frame because the receiver should be in the listening state of the data wait duration.

2.2.3. Routing Protocol

In multi-hop networks, the routing protocol is also essential for efficient operations. Although there are various standardized routing protocols, some routing protocols like the ad-hoc on-demand distance vector (AODV) [57] and the optimized link state

routing (OLSR) [58] protocols are not suitable for IoT cases because of their large overhead to construct the routes. Therefore, lightweight routing protocols have been developed and standardized for the IoT, which often limit the route construction function [59].

RPL Based Layer 3 Routing

The RPL is a routing protocol supporting IPv6 [60] standardized as request for comments (RFC) 6550 [42] in the IETF. With the RPL, the layer 3 (L3) network called the destination oriented directed acyclic graph (DODAG) is constructed. In the DODAG, all paths are oriented toward a terminal called the root. The RPL uses a distance vector called the rank to evaluate each terminal's position in a DODAG. The rank is calculated from metrics defined in the objective function (OF). The expected transmission count (ETX) is a major metric used in the RPL [61], but various OFs are designed to meet the requirements in the network.

In the operation, a control message called the DODAG information object (DIO) has a key role to construct a DODAG. Each terminal advertises the metrics using the DIO and computes their parent and own rank from the neighbor terminal's metrics. The uplink communications toward the root are achieved by each node forwarding the data to their parent. Also, the control frames called the destination advertisement object (DAO) are sent toward the root from each terminal. The root can execute downlink communications referring to the accumulated parent information of each terminal loaded in the DAO.

IEEE 802.15.10 Based Layer 2 Routing

The IEEE 802.15.10 [43] offers a non-IP multi-hop network based on a L2R protocol. Such a multi-hop network is suitable for resource-limited environments for disaster prevention, structure monitoring, and agriculture. The non-IP-based communications achieve smaller overhead in comparison with the IP-based communications, so lower power consumption or higher data transfer efficiency than the RPL-based network is expected [62]. In the IEEE 802.15.10, terminals are organized into a hierarchical mesh that collects data to a root. The path quality metric (PQM) is defined as a metric to indicate the distance from the root to each terminal. Terminal information including the PQM is shared with neighbor terminals by broadcasting using information elements (IEs). Each terminal calculates its own PQM from information on the received IEs and a metric defined between terminals called the link quality metric

(LQM). Hence, the design of LQM dominant over the performances of the multi-hop network. For the LQM calculation, the hop count, the received signal weakness (RSW), the ETX, and the expected airtime are defined in the IEEE 802.15.10, but vendor-specific LQM can be adopted.

The MAC protocol is not specified in the IEEE 802.15.10, but the major CSMA/CA protocol is insufficient to achieve a long-life battery-operated network. This is because terminals should be in the listening state to wait for the packets from neighbor terminals. The RIT and the CSL protocols are given as examples to achieve a smaller duty cycle in the IEEE 802.15.10 [43].

Opportunistic Routing in U-Bus Air

For a routing protocol in U-Bus Air, an opportunistic routing protocol was prepared and standardized in a specification by the JUTA [9]–[11], [47]. The aim of the specification is to provide highly reliable communications by self-route selection on the install-easy networks by self-construction function [47]. A wireless mesh network can accommodate maximum of 50 battery-powered terminals.

In the current U-Bus Air, the routing is conducted using tables. Each terminal decides the adjacent terminals from the RSSI value of the received beacon frames (i.e., the frame with radio number command). Also, each terminal possesses a hop count table for the routing, in which adjacent terminals are handled as a hop count of one. The consistent of the hop count table is kept by a common update counter. Each node exchanges the hop count table, and updates the table referring to the adjacent terminal's table. By this process, the terminal can obtain hop numbers for all terminals in the network. Moreover, a routing table is defined for the peer-to-peer (P2P) multi-hop communications. For all terminals in the network, whether an adjacent terminal is a forwarding terminal, a backward terminal, a sideway terminal, or a non-adjacent terminal is recorded from the own and adjacent terminal's hop count tables. In the communication process, each terminal transfers the data to a forwarding terminal toward a final destination terminal referring to the routing table.

2.2.4. Combination of Technologies

In Sects. 2.2.2 and 2.2.3, various MAC and routing technologies were introduced. In this section, the combination of these technologies is discussed. First, simple and low-constraint networks are considered. Home area IoT networks are an example. In such networks, a large number of hops are not required. Also, requirements for traffics or

power consumption are not so high. The multi-hop function is often simplified and communications between battery-powered devices are not often considered. Therefore, the indirect transmission is often used for the low-power operation. Examples are wireless specifications using the 920 MHz band in Japan for the ECHONET Lite (i.e., protocol stacks for operation or monitoring of home appliances) based on the Wi-SUN or the ZigBee [63]. The Wi-SUN enhanced home area network (HAN) [64] (i.e., the enhanced version of Wi-SUN-based specification in [63]) has a simple relay function and the indirect transmission is adopted for low-power operation. Although the ZigBee IP (i.e., a ZigBee-based specification in [63]) supports multi-hop based on the RPL, communications between battery-powered devices are not supported and the indirect transmission is adopted in communications between battery-powered and stable power-supplied devices.

For large-scale multi-hop networks, the RPL or the IEEE 802.15.10-based L2R can be used to construct the network automatically. Here, both routing protocols use the broadcasts to neighboring terminals for exchanging metrics. Hence, it is important to support broadcasting in the low-power MAC protocol. From the viewpoint of being able to perform seamless broadcasting, the TSCH and the CSL protocols are suitable for these networks. Although the TSCH protocol tends to show better power consumption characteristics due to the synchronization [50], [65], it is necessary to choose the appropriate protocol considering the requirements like the clock accuracy of the terminal.

One major field for the RPL-based multi-hop networks is industrial networks including process automation and factory automation. In industrial fields, stringent requirements such as interference tolerance, low latency, and low power consumption should be satisfied. For such applications, deterministic wireless buses and networks such as the WirelessHART and ISA100 in 2.4 GHz-band have been used [66]. These specifications adopt wireless technologies based on the time division multiple access (TDMA), which is the base of the TSCH protocol adopted in the IEEE 802.15.4e. Also, to enhance the compatibility with the Internet, IP-enabled wireless networks are being developed. In this trend, a protocol stack with the TSCH in the MAC layer, the IPv6 over low-power wireless PAN (6LoWPAN) for adaptation, and the RPL for routing has become most popular. Network management and scheduling are important in the networks based on the TSCH and the RPL. Therefore, the IETF IPv6 over the TSCH mode of IEEE 802.15.4e (6TiSCH) working group (WG) [67] has standardized the scheduling mechanism and network access authentication for the TSCH and RPL-

based networks [68]. It is also important to develop a precise synchronization mechanism for the smooth operation of the TSCH protocol in the whole network [52].

Another deployment of the networks with the RPL is for field areas [69]. An example of practical and pervasive network development for field areas is the Wi-SUN field area network (FAN) standardized in the Wi-SUN Alliance [1], [21]. Note that the first version of the Wi-SUN FAN does not support the low-power operation for battery-powered terminals. The Wi-SUN FAN aims the networks for smart city, smart metering, and smart monitoring. The basic MAC operation is based on the CSMA/CA. In addition, the frequency hopping is used to periodically switch the channel to be used, although it does not adopt tight frame-level synchronization like the TSCH [70]. Now that the first version of the Wi-SUN FAN has been launched, the support of low-power operation in the Wi-SUN FAN node is being considered. Here, the basic idea is similar to the 6TiSCH, the sleep time can be ensured by synchronization. However, given the multi-vendor network construction and fewer synchronization opportunities for the low-power operation, MAC operation that relies on strict synchronization may be at a disadvantage. Hence, the authors have proposed to use the synchronous CSL protocol in a partially [71].

Compared with the RPL-based networks that support IP communications, the IEEE 802.15.10 L2R-based networks aim at lightweight configurations. Therefore, it is desirable to avoid adopting the complex mechanisms to maintain the synchronization when introducing the low-power operation. However, it is preferable to use the broadcast to exchange IEs, which is necessary for routing in the IEEE 802.15.10. Under these assumptions, the CSL protocol would be better suited for the low-power operation than the RIT protocol because of its seamless broadcast capability [56], [62].

As different from concepts in the hierarchical networks based on the RPL or the IEEE 802.15.10, the cross-layer design with the RIT protocol and the opportunistic routing has been developed in the U-Bus Air [9], [47]. An important feature of the opportunistic routing is that it does not specify a unique forwarding destination terminal as opposed to the RPL and the IEEE 802.15.10 that calculates one preferred destination terminal. This can be driven seamlessly in combination with a receiver-initiated MAC protocol, i.e., if the forwarding destination terminal is not specified in the routing process, the actual receiver can be defined uniquely by the receiver-initiated operation in the MAC layer. This feature enables to provide robust communications under unstable wireless environments where the link can be disabled due to the shadowing by humans or things. Although there are strong constraints on

network size and communication throughput in comparison with the hierarchical networks, the U-Bus Air is operated within the constraints [47].

From the above discussions, the RIT is characterized by robust communications based on the cross-layer techniques with the opportunistic routing protocol. This is a unique design and cannot be achieved by other standardized MAC and routing technologies. After this section, the features, historical background, challenges, and standardization of the multi-hop networks based on receiver-initiated MAC protocols are explained.

2.3 Features of Multi-Hop Networks Based on Receiver-Initiated MAC Protocols

As discussed in the previous section, there are various MAC and routing protocols for low-power multi-hop networks. Among them, the RIT protocol has a unique operating principle, and the entire network with the routing protocol should be designed according to their characteristics. Although only the RIT protocol is standardized, a number of receiver-initiated MAC protocols are being studied, including those that are not standardized [12]. In this section, the history and features of the multi-hop network using receiver-initiated MAC protocols are described.

2.3.1. PHY Layer

Receiver-initiated MAC protocols are often adopted in wireless sensor networks operated with limited energy. Such networks often adopt PAN technologies with simple PHY layers described in Sect. 2.2.1.

2.3.2. MAC Layer

Firstly, to clarify the feature of the receiver-initiated MAC protocols, the operation of receiver-initiated MAC protocols is discussed with an example of the RIT protocol. The data transfer from a sender is considered. Two terminals are considered as a candidate of the receiver. Once a sender starts the transfer process, the sender starts the Tx wait duration. At this point, the forwarding destination is not decided. If the sender receives an RIT data request frame from one of the candidates of the receiver, the sender transfers the data. If the sender can perceive the result of the transmission

(e.g., the ACK is introduced for transfer control), the sender ends the transfer process in the case that a candidate of the receiver successfully accepts the data. If the data transfer process fails (e.g., the sender perceives fails from non-arrival of the ACK), the sender can get back to the Tx wait duration. Then, the sender can forward the data to another candidate of the receiver. Note that if the sender does not catch an RIT data request frame from one of the candidates, the sender can transfer the data to another candidate. Summarizing the above, although there are multiple terminals as candidates of the receiver, the transmission with the receiver-initiated MAC protocol results in the unicast to a terminal.

The receiver-initiated operation can enhance the robustness in low-power sensor networks. This concept was first proposed in receiver-initiated cycled receivers (RICER) in 2004 [72]. In [72], the multiple candidates of the receivers were introduced as potential receivers. This research revealed that the receiver-initiated rendezvous scheme can show efficient characteristics under strong fading conditions. However, the RICER focused only on the rendezvous scheme in the MAC layer, and not reached cross-layer designs that include receiver-initiated MAC protocols [73].

After that, some protocols were proposed for multi-hop networks. Two main protocols are the basis for the subsequent studies. One is the IRDT proposed in 2007 in Japan [13], [14], [74]. This research starts from a simple linking protocol (i.e., the basis of the RIT protocol) and routing protocol adopting the concept of potential receivers [14]. Second is the receiver-initiated MAC (RI-MAC) proposed in 2008 [75]. The RI-MAC has a concrete and implementable MAC design based on IEEE 802.15.4 frames. Note that, hereafter all MAC protocols that adopts receiver-initiated mechanism in the MAC layer (e.g., the RIT protocol, the IRDT, and the RI-MAC) are called receiver-initiated MAC protocols [12]. Based mainly on these protocols, various derivative receiver-initiated MAC protocols have been proposed. Essential motivations and approaches are summarized in Sect. 2.4.

2.3.3. Network Layer

In multi-hop networks using the receiver-initiated MAC protocols, routing protocols that have a close cross-layer structure with the MAC layer are often used [76]. In general, the routing protocols belong to the opportunistic routing [77] for employing the MAC layer's feature that multiple candidates of the receiver can be considered. Hence, the selection of the best forwarding terminal, which is a major concern in the routing protocols like the RPL and the IEEE 802.15.10 L2R, is not a common problem.

In other works, the tree topology like the DODAG in the RPL is not required, and the routing is achieved flexibly on the mesh topology. For routing metric calculations, very simple metrics such as the hop counts are normally adopted. The network layer is often characterized by the definition of the network topology and the determination of neighboring terminals, which are necessary to configure the candidate of receivers.

There are two main definitions of the network type. One is the networks managed by the routing tables each terminal possesses. A major type is the opportunistic routing based on tables [48], which is similar to the routing in the U-Bus Air [9], [47] explained in Sect. 2.2.3. Hereafter, this network type is called the table-based network in this thesis. The routing is achieved by referring to the routing tables (e.g., hop count table) by each terminal. In the table-based networks, a problem is the scalability. The benefit of the table-based networks is P2P communication, but terminals should have the routing table which holds the information of all terminals. To achieve successful routing, the consistency of the routing tables of each terminal is maintained by exchanging the routing tables. In a large-scale network, the performances (e.g., the transmission success rate or the current consumption) would be decreased due to the large overhead of exchanging tables [23]. Therefore, table-based networks are often used on a small-scale.

The other is the networks managed by the centralized metrics (e.g., the minimum number of hops) from the coordinator to each terminal [25]–[27]. Hereinafter, this network type is called the centralized metric-based network in this thesis. In major cases, the metric information is loaded in the beacon frame (e.g., the RIT data request frame in the RIT protocol) and broadcasted to the neighbor terminals. The sender decides whether transfer the data frame or not by using the metric in the beacon frame. For example, in the networks that adopt the minimum number of hops as a metric, the data are collected to a coordinator by forwarding the data to the terminal which has a smaller metric [25]. The metric-based networks have scalability because each terminal autonomously calculates the metric and frequent exchange of tables is not required. However, the setting of the destination is limited since it is not possible to distinguish between non-coordinators by the metric.

2.4 Issues and Challenges in Multi-Hop Networks Based on Receiver-Initiated MAC Protocols

The receiver-initiated MAC protocols are used not only in gas and water smart metering but also various sensor networks. Although the details of the MAC protocols are different depending on the system, the research based on the unique operating principle of receiver-initiated MAC protocols can be divided into several approaches. In this section, the issues and challenges of the receiver-initiated MAC protocols are summarized into three important approaches of intermittent wake-up interval design, random access and retransmission, and wake-up timing adjustment. These approaches are based on the operation principle of the receiver-initiated MAC protocols, and please note that there are further problems such as broadcasting [78], flooding [79], and multi-channel operation [80]. Moreover, receiver-initiated MAC protocols may be used jointly with technologies like wake-up radio (WuR) [81], [82], and energy harvesting [26], [83].

2.4.1. Intermittent Wake-Up Interval Design

The performance of the receiver-initiated protocols is highly affected by the intermittent wake-up interval. One motivation for the interval design is to reduce or balance the power consumption. For the receiver with the smaller wake-up interval, the sender can transfer the data in the smaller delay. Therefore, the sender can reduce the power consumption in spite of the large power consumption of the receiver to wake up frequently. Conversely, the receiver can save the battery by setting a larger intermittent wake-up interval. However, the larger delay to access the receiver increases the sender's power consumption. Therefore, the optimal setting on the wake-up interval depending on the frequency of sender and receiver operations can achieve a better power consumption characteristic [13], [26].

Besides the power consumption, the reliability is also a major motivation to modify the wake-up interval. The larger intermittent wake-up interval induces frequent collisions between multiple senders. This problem occurs because the larger wake-up interval increases the probability that multiple senders possess its data, but the communication timing is limited, and the collision occurs. Therefore, a high communication reliability can be achieved by optimizing the wake-up interval according to the communication traffic [13], [23], [84]. However, frequent wake-up

operations to transmit many beacon frames may impair the communication quality by interferences.

Thus, the intermittent wake-up interval of the receiver-initiated MAC protocols has a significant impact on power consumption and communication reliability. There is a trade-off between setting smaller intervals to prevent frequent data collisions and reduce the sender's power consumption and setting larger intervals to prevent larger interferences and reduce the receiver's power consumption. Therefore, it is necessary to design the intermittent wake-up interval according to the priority objective (e.g., to reduce the listening state waiting for the available receiver under crowded conditions depending on the number of hops [85]).

2.4.2. Random Access / Retransmission

As mentioned before, collisions that occur when multiple senders have their data is a severe problem in the receiver-initiated MAC protocols, which limits the communication chances at the receiver's wake-up timing. There are some challenges that mitigate the collision problem by the random access or retransmission approaches. A main idea is to provide a sufficient listening duration of a receiver for the random access to be performed after the beacon transmission. Basically, the listening duration after the beacon transmission accounts for much of the power consumption required for the standby. Hence, enlarging the listening duration to avoid collisions to improve communication reliability, leads to an increase in power consumption.

Even if the random access to a certain duration after the beacon transmission is adjusted, collisions will inevitably occur when multiple terminals try to access a terminal. For such a case, retransmissions are also a solution to improve the reliability. It is a common case that a receiver that detects a collision does not immediately go to sleep but transmits a beacon for the retransmission.

The random access and retransmission approach appears in the use of various receiver-initiated MAC protocol. As a concrete example, in the RICER, multiple slots are defined after a beacon to accommodate a data and an ACK frame [72]. Also, in [73], the handshake with request to send (RTS)/clear to send (CTS) is proposed to reduce the slots in the listening state. In the RI-MAC, both the random access and the retransmissions are jointly employed [75]. The conflict of data transmissions is sorted out by the immediate beacon transmission and larger listening window after a collision, and the ACK control which also serves as a beacon. Similar approaches can be seen in the IRDT that the receiver sets smaller intermittent wake-up intervals when a

collision occurs to provide frequent communication chances [13]. Besides, in the IRDT, the retransmission control by the receiver is attempted in addition to a similar approach [86].

2.4.3. Wake-Up Timing Adjustment

Mainly, the receiver-initiated MAC protocol is operated in full asynchronous condition. However, the adjustment of the initial wake-up timing can be one way to improve the network performance. The main purpose of the adjustment of the wake-up timing is to shorten the communication delay and to reduce the power consumption.

There are some proposals to improve the transmission characteristics by scheduling or changing the wake-up timings by using the information on the data transmission flow according to the hop count or intercepted frame transmissions from neighbor terminals [27], [87]. Another example of the wake-up timing adjustment proposes the cooperatively overlapping of the wake-up timing with neighbor terminals to enables broadcasting [88]. As an alternative to adjusting the beacon timing of the receiver, a method by the sender is proposed that the sender predicts the receiver's transmission timing and delays to start the listening according to the predicted timing to save the energy [89].

2.5 Development of Highly Interoperable RIT protocol

For practical use of the technology, it is also essential to ensure feasibility. Especially for the utility systems that require sustainable device supply, the interoperability enhancement is also a key challenge. The U-Bus Air is being developed to realize smart metering systems adopting a receiver-initiated MAC protocol with high interoperability.

2.5.1. Protocol Stack Design

As explained in Sect. 1.1, the RIT protocol was proposed and adopted in the IEEE 802.15.4e from the U-Bus Air development team, but this standardization is not enough for interoperability. This is because the RIT protocol is conceptual, so concrete protocol should be designed for interoperability. Also, the protocol designs to embody complex communications in practical systems should be considered.

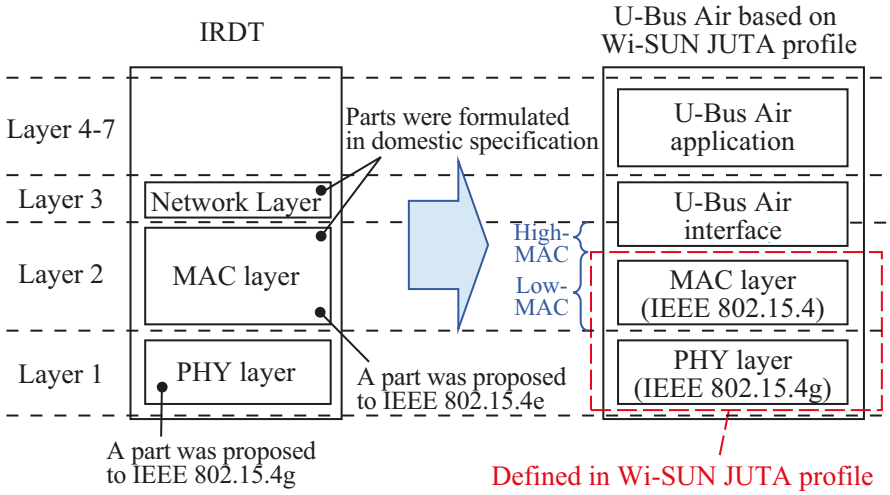

Figure 2.5: Protocol stack designs of IRDT and U-Bus Air based on Wi-SUN JUTA profile. ©2021 IEICE

With these backgrounds, the development of U-Bus Air was embarked on the protocol stack design that divides the MAC layer into two layers. Figure 2.5 shows the original IRDT protocol stack design, which is a base of the U-Bus Air, and the protocol stack design for interoperable-friendly U-Bus Air with the divided MAC layer. The MAC layer is divided into two parts: the lower part and the higher part. The lower part of the MAC layer is closely related to the specification of the integrated circuit (IC), where is the part that high interoperability is required. On the other hand, the higher part of the MAC layer is a part to cover the flexible link control. Therefore, the features of interoperability and flexibility, which can often conflict with each other, are managed, although the interpretation of some parameters and control between layers can be complicated. Hereafter, the lower and higher parts of the MAC layer is called the Low-MAC and the High-MAC, respectively.

2.5.2. Low-MAC

In the Low-MAC, concrete MAC protocol based on the RIT protocol in the IEEE 802.15.4 has been developed. First, the F-RIT protocol was proposed as an IEEE 802.15.4-compliant concrete MAC protocol [15], [16]. The F-RIT protocol is an embodying RIT protocol proposed for battery-powered terminals, which has two features [20]. First is the compaction of the RIT data request frame. The RIT data request frame length should be as short as possible to reduce the power consumption

and interferences. In the F-RIT protocol, only source terminal information is loaded in an addressing field of the RIT data request frame (i.e., information about the destination terminal is omitted). Second is the simplification of the CSMA/CA with a random backoff process to transmit the RIT data request frame. To reduce the power consumption for the transmission of the RIT data request frames in a crowded channel environment, a pre-carrier sense (Pre-CS), which is a simplified channel sampling process, is applied instead of the CSMA/CA process with a random backoff. When a terminal detects another transmission during the period of the Pre-CS, the terminal does not transmit the RIT data request frame until the next periodical wake-up timing.

Moreover, the F-RIT protocol was standardized in the Wi-SUN Alliance [21]. This specification is called the Wi-SUN JUTA profile and includes the PHY layer based on the IEEE 802.15.4g [7] and the Low-MAC based on the IEEE 802.15.4-2015 [18]. Also, the Wi-SUN Alliance provides opportunities for certification with the Wi-SUN JUTA profile for newly developed products by testing their interoperability.

The RIT protocol defined in the Wi-SUN JUTA profile uses three specified frames in the IEEE 802.15.4 [18]: an RIT data request frame, an RIT data response frame, and a data frame. The RIT data response frame was newly standardized in the IEEE 802.15.4-2015 [18]. When the RIT data response frame is used, the sender transmits the RIT data response frame in the data wait duration to inform the receiver that the sender is pending a data frame addressed to the receiver as shown in Fig. 2.6. If the receiver catches the RIT data response frame in the data wait duration, the listening duration is extended. Then, the sender and the receiver can transmit the data frames to each other in this duration.

In the JUTA profile, the RIT data request and the data frames are transmitted after the Pre-CS in the Low-MAC. The action after detecting the channel busy before the transmission of a data frame is issued from the upper layer. The RIT response frame is transmitted without performing the carrier sense so that the receiver can catch the frame within the data wait duration. The Wi-SUN JUTA profile determines some parameters to realize the low-power consumption of the F-RIT protocol within the IEEE standard. For example, the MAC RIT period and the MAC RIT Tx wait duration in the Low-MAC are defined to 5 s. To achieve successful interoperability, the sender should start to transmit the RIT data response frame within the duration from 0.8 ms to 1.25 ms after the reception of the RIT data request frame.

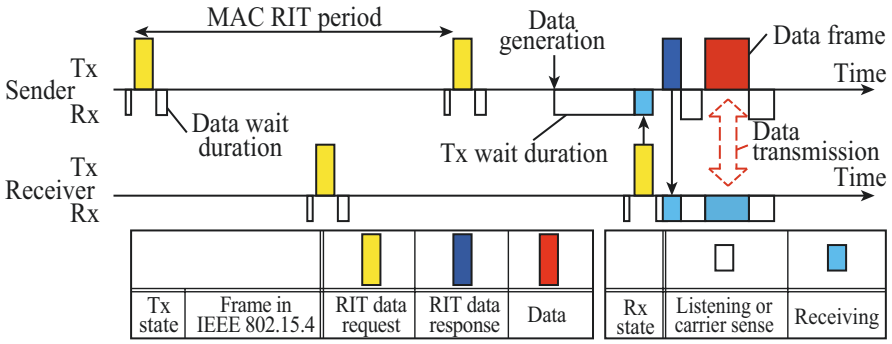

Figure 2.6: Communication sequence of F-RIT protocol based on Wi-SUN JUTA profile. ©2021 IEICE

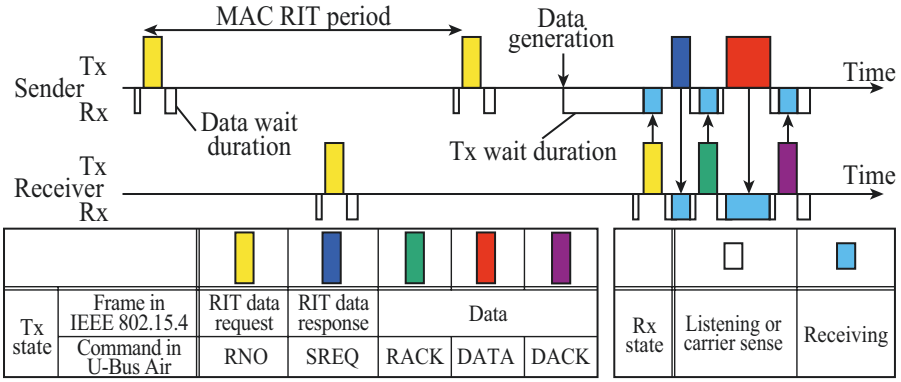

Figure 2.7: Major communication sequence in U-Bus Air to transfer data with DATA command. ©2021 IEICE

2.5.3. High-MAC

The MAC layer of the original U-Bus Air [9] defines practical communication sequences using several link control commands for actual services. Figure 2.7 illustrates the communication sequence which transfers data on a frame with the DATA command. This is a major communication sequence in the U-Bus Air [9], and corresponds to the sequence of the IRDT [13].

In the case that the communication sequence shown in Fig. 2.7 is achieved based on the Wi-SUN JUTA profile, a radio number (RNO) command and a send request (SREQ) command are applied to the RIT data request frame and the RIT data response frame, receptivity. The U-Bus Air defines the acknowledgement for the SREQ

command, and this is called a request ACK (RACK) command. The sender transmits the user data on a frame with the DATA command after receiving the RACK command. If the receiver accepts the data, it transmits a DATA ACK (DACK) command to the sender. Hereafter, the frame which loads a certain link control command is called by only the command name (e.g., RNO means the RIT data request frame with the RNO command). In the draft [9], which does not comply with the IEEE standard MAC, RNO and DACK are transmitted with a carrier sense, and SREQ is transmitted without any carrier sense. Here, when a carrier is detected by the carrier sense, a re-transmission is not performed. RACK and DATA are transmitted using the carrier sense, which waits for the carrier to be clear state for a certain period if it detects a carrier. Besides this normal sequence, the U-Bus Air defines various communication processes that are required in actual services. For example, the receiver can refuse the request for the communication link establishment by transmitting request negative ACK (RNACK). Besides that, the sender can re-transmit DATA if it does not receive DACK. Furthermore, not only single DATA transmission but also the multiple DATA transmissions, and the bidirectional exchange of DATA are supported.

2.6 Conclusion

In this chapter, the overview of wireless technologies for low-power IoT systems were introduced. Multi-hop networks with PAN technologies operated in sub-GHz bands were one of the solutions for low-power IoT systems. For such networks, there were many low-power MAC protocols to reduce the power consumption and routing protocols to relay packets. This thesis emphasized that the combination of these technologies is essential. The RIT protocol, one of the receiver-initiated MAC protocols, was suitable for ad-hoc networks, and the cross-layer technologies with opportunistic routings could provide unique characteristics on the wireless mesh network. Then this thesis presented various challenges on the receiver-initiated MAC protocols from both academic and practical viewpoints.

The academic and practical challenges are partly antithetical to each other (e.g., the MAC RIT period is completely fixed in the JUTA profile to ensure interoperability, but dynamic setting is a major approach to improve the performance in academic researches), and the author does not consider that practical development does not fully embrace the academic perspectives. In the next and beyond chapters, while this thesis contributes to the development of concrete technologies for practical use, this thesis

challenges to improve the communication characteristics based on practical use by re-examining and combining the technologies appropriately. As an addendum, although this chapter focused on relatively wide-area IoT networks, the concept of the receiver-initiated MAC protocols can be applied to other communication systems as well for the low-power operation and efficient handshake. Underwater communications [90], body area network (BAN) [91], and terahertz communications [92] are examples. The findings which reveal the specificity of the receiver-initiated MAC protocols may be applicable to other communication systems other than multi-hop networks using sub-GHz bands.

Chapter 3
Theoretical and Experimental Analyses of Wi-SUN JUTA Profile-Compliant F-RIT Protocol

3.1 Introduction

In this chapter, the feasibility of the Wi-SUN JUTA profile-compliant F-RIT protocol is studied comprehensively by theoretical analysis, computer simulations, and experiments with developed prototypes. To handle a system based on standardized technologies, it is essential to comprehend each elemental technology. As mentioned in Chapter 1, the IEEE 802.15.4e-compliant F-RIT protocol was theoretically, numerically, and experimentally evaluated in [19], [20], [30]. However, an evaluation sequence, packet usages, and various parameters in these previous works do not comply with the Wi-SUN JUTA profile and the U-Bus Air standard. In this chapter, the Wi-SUN JUTA profile-compliant F-RIT protocol supporting a communication sequence of the U-Bus Air is designed [28]. Hereinafter, the protocol evaluated in this chapter is called the JUTA F-RIT protocol. Through theoretical analysis, computer simulations, and experiments with Wi-SUN dongles, the JUTA F-RIT protocol is evaluated comprehensively. Moreover, the frame transmission performance and the timeout incident are analyzed from the experimental results to reveal the transmission performance of the JUTA F-RIT protocol in detail. The key contributions of this chapter are the follows:

- Transmission success rate of the JUTA F-RIT protocol is evaluated in a cochannel interference environment by theoretical analysis and computer simulations [28].
- The world's first Wi-SUN dongle-type prototype with the JUTA F-RIT protocol is developed [28]. The commercial dongle equipped with the IEEE 802.15.4g [7] and the ARIB STD-T108 [6] compliant Wi-SUN RF module is used for the implementation.
- By using the developed prototypes, the JUTA F-RIT protocol is evaluated

experimentally and its feasibility is demonstrated [28].

- The communication performance of prototypes from two viewpoints of the frame transmissions [28] and the timeout incident are considered for the reference of better implementation or upper layer design.

The rest of this chapter is organized as follows. In Sect. 3.2, the theoretical analysis of the JUTA F-RIT protocol is developed. Then, the transmission success rate is evaluated by theoretical analysis and computer simulations for the reference of the performance in the prototype. In Sect. 3.3, the world's first Wi-SUN dongle-type prototype that hosts the JUTA F-RIT protocol is developed and evaluated. Moreover, the performance of the prototype is considered in detail from the viewpoints of the frame transmissions and the timeout in Sect. 3.4. Finally, Sect. 3.5 concludes this chapter.

3.2 Theoretical Analysis and Evaluation of Wi-SUN JUTA Profile-Compliant F-RIT Protocol

In this section, the JUTA F-RIT protocol is designed as a Wi-SUN JUTA profile-compliant F-RIT protocol for evaluations. The performance of the JUTA F-RIT protocol is evaluated by theoretical analysis and computer simulations for references of experiments in next section. The theoretical analysis is developed based on the analysis scheme focusing on the carrier sense.

3.2.1. System Model

In this chapter, the one-way communication model in an interference environment as illustrated in Fig. 3.1 is considered. In the system model with N terminals, one specific terminal (i.e., sender) generates the data and transmits to a specific terminal (i.e., receiver) based on the JUTA F-RIT protocols. Other $N-2$ terminals do not transmit any data, namely, they transmit only RIT data request frames which acts as interferences. All terminals are operated in a single channel. In this system model, the transmission performances are evaluated under cochannel interferences of only RIT data request frames. This model can be considered as a part of a snapshot of the multi-hop polling communication from the center terminal coordinating a network, which is a function of the U-Bus Air [10].

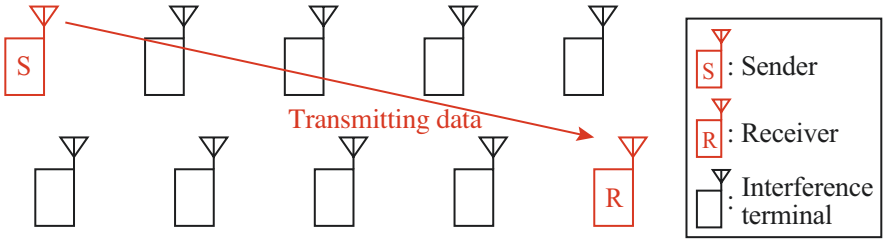

Figure 3.1: System model. ©2021 IEICE

To randomize the timing of the data generation, the next data generation timing is decided at the end of the data transmission operation. The interval of the data transmission operation is defined as the data generation interval, and the reciprocal numbers of the intervals follow to the Poisson distribution in this chapter. The MAC RIT period is not absolutely fixed and slightly randomized in the simulation in Sect. 3.2.5 since the actual modules are affected by the clock drift [55], and the RIT data request frames are not transmitted at intervals of the ideal MAC RIT period.

In this chapter, to focus on the communication in the MAC layer, especially in the Low-MAC, only the PHY and the Low-MAC are implemented in the actual module evaluated in Sect. 3.3. Therefore, the case is assumed that the data frames are transmitted from the High-MAC on the outside of the module as a minimum setup of the Wi-SUN JUTA profile, and the communication delay between the High-MAC and the Low-MAC based on the universal asynchronous receiver/transmitter (UART) is considered in the simulation.

3.2.2. Practical JUTA F-RIT Protocol for Evaluation

To evaluate the practical protocol with the features of the Wi-SUN JUTA profile in the Low-MAC, the practical JUTA F-RIT protocol for the evaluation is designed [28]. In this chapter, the typical communication sequence of the U-Bus Air, which is shown in Fig. 2.7 and designed based on the Wi-SUN JUTA profile, is considered.

Figure 3.2 shows the IEEE 802.15.4-2015-compliant frame structures defined by the Wi-SUN JUTA profile. In the Wi-SUN JUTA profile, the physical service data unit (PSDU) length of all frames should be less than 255 bytes. In the Low-MAC evaluated in this chapter, these frames and F-RIT communication sequence shown in

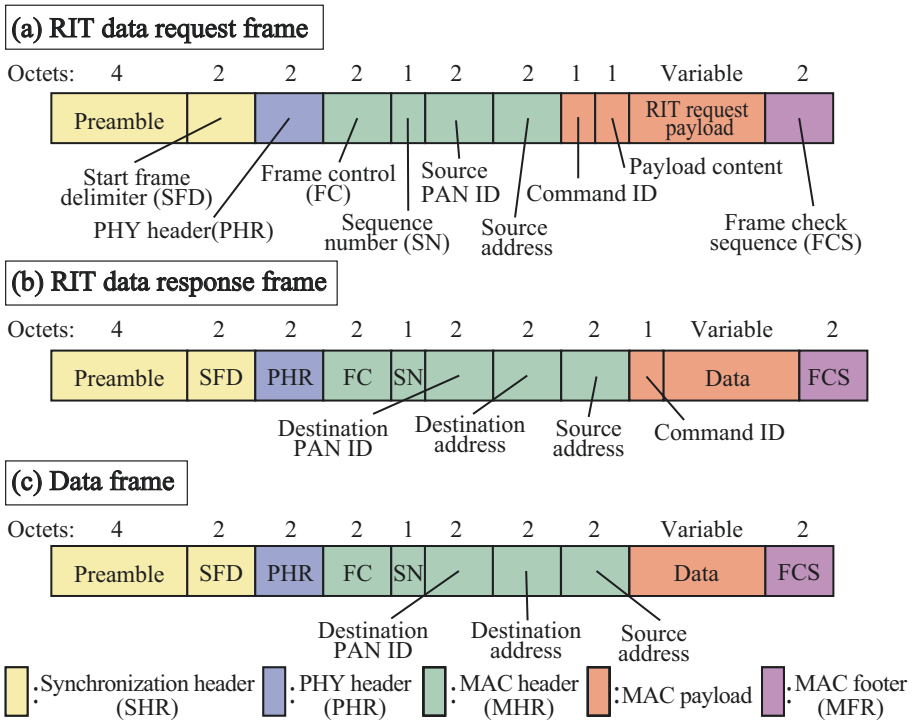

Figure 3.2: Detail of frame structures in Wi-SUN JUTA profile. ©2021 IEICE

Fig. 2.7 are assumed. The RIT data request frame shown in Fig. 3.2(a) loads only the source terminal information in the addressing field in accordance with the specification of the F-RIT protocol as described in Sect. 2.5.2. By using the data frame shown in Fig. 3.2(c) in the Low-MAC, the terminals can exchange RACK, DATA, and DACK.

The range of the MAC RIT Tx wait duration is set in the range from 5 to 25 s. Although the MAC RIT Tx wait duration is defined as same as the MAC RIT period evaluated in [19], [20], [30], the U-Bus Air sets the listening duration waiting for RNO as a guide as 5 times of the RNO transmission interval [9]. This means the RIT-based system with the High-MAC waits for the communication chances for several times of the RIT data request frame transmission from the receiver in the High-MAC. Taking the specification of the U-Bus Air that has the whole MAC layer into account, the MAC RIT Tx wait duration over 5 s can be applied in the Low-MAC.

In the communication sequence for the evaluation, two steps are considered for the successful communication as enabling the MAC RIT Tx wait duration over the MAC RIT period in the Low-MAC. The first step is the establishment of a communication link (i.e., the receiver and the sender receive SREQ and RACK, respectively). During

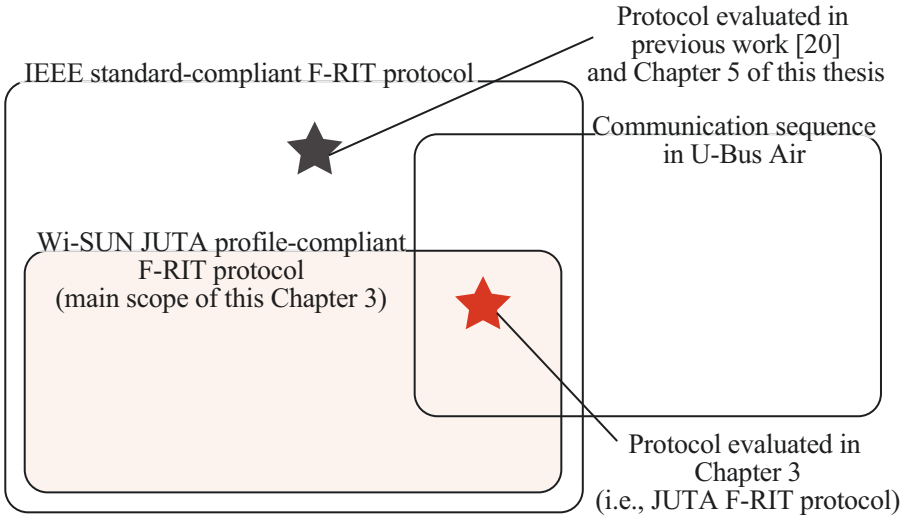

Figure 3.3: Relationship between standards and protocols.

the Tx wait duration, the sender attempts to establish the communication link and waits for the reception of RNO from the receiver until the successful communication link establishment. The second step is the successful execution of the communication link that the sender receives DACK and accomplishment of the communication link. If the communication sequence stops in the second step, the communication pair do not try to establish the communication link again after one successful communication link establishment because this chapter focus on the evaluation of the Low-MAC. During the link establishment, the re-transmission of the data frame is also not performed.

Figure 3.3 summarizes the relationship between standards and protocols for evaluations mentioned in this thesis. Since the Wi-SUN JUTA profile complied with the IEEE standard, the Wi-SUN JUTA profile-compliant F-RIT protocol should be included in the IEEE standard-compliant F-RIT protocol. Regardless of these international standards, we can also consider the communication sequence of the U-Bus Air. Although the IEEE 802.15.4e-compliant F-RIT protocol was included in the IEEE standard-compliant F-RIT protocol, it did not comply with the Wi-SUN JUTA profile and was not designed based on the communication sequence of the U-Bus Air. The main scope of this chapter is the Wi-SUN JUTA profile-compliant F-RIT protocol. The JUTA F-RIT protocol is designed within the Wi-SUN JUTA profile and supports the communication sequence in the U-Bus Air.

3.2.3. Interference Model and Analysis of Frame Transmissions

In this section, the frame transmissions are analyzed based on the interference model shown in Fig. 3.4. The interference model considers frame transmissions in an interference environment of RIT data request frames. At the same time, as the generation of the desired frame (i.e., the RIT data request or data frames), the terminal starts the carrier sense. At the Pre-CS, the channel state is assessed at the center of the sensing duration T_{CS}. If the channel state is clear, the terminal starts transmitting the frame after the Rx to Tx turnaround time T_{TA} from the end of the Pre-CS.

As shown in Fig. 3.4, the result of the transmission of the desired frame depends on the generation of interference frames. For simplicity of the analysis, the generation of multiple interference RIT data request frames during the desired frame transmission process is not considered. In the system model, the probability that an interference RIT data request frame is generated during the duration of t is $(N-2)/T_{RIT} \cdot t$. Here, T_{RIT} denotes the MAC RIT period (i.e., the generation interval of the RIT data request frame at a terminal).

As illustrated in Fig. 3.4(a), the carrier is detected at the Pre-CS if an interference frame is generated during the RIT data request frame length T_{Req}. Hence, the theoretical incident rate of carrier detection is described as follows:

$$p_{Detect} = \frac{N-2}{T_{RIT}} \cdot T_{Req}. \tag{3.1}$$

When an interference frame is generated during $2T_{TA} + T_{CS}$ as illustrated in Fig. 3.4(b), the sender or receiver cannot detect the carrier at the Pre-CS. In this case, the desired frame transfer fails because the collision occurs between the desired frame and an interference RIT data request frame. The theoretical incident rate of the collision is expressed by

$$p_{Collision} = \frac{N-2}{T_{RIT}} \cdot (2 \cdot T_{TA} + T_{CS}). \tag{3.2}$$

The transfer of the desired frame succeeds in the case that the carrier is not detected at the Pre-CS, and also the collision does not occur. Therefore, the probability of the successful transfer of the desired frame is expressed by

$$p_{wCS} = \left(1 - \frac{N-2}{T_{RIT}} \cdot T_{Req}\right) \cdot \left(1 - \frac{N-2}{T_{RIT}} \cdot (2T_{TA} + T_{CS})\right). \tag{3.3}$$

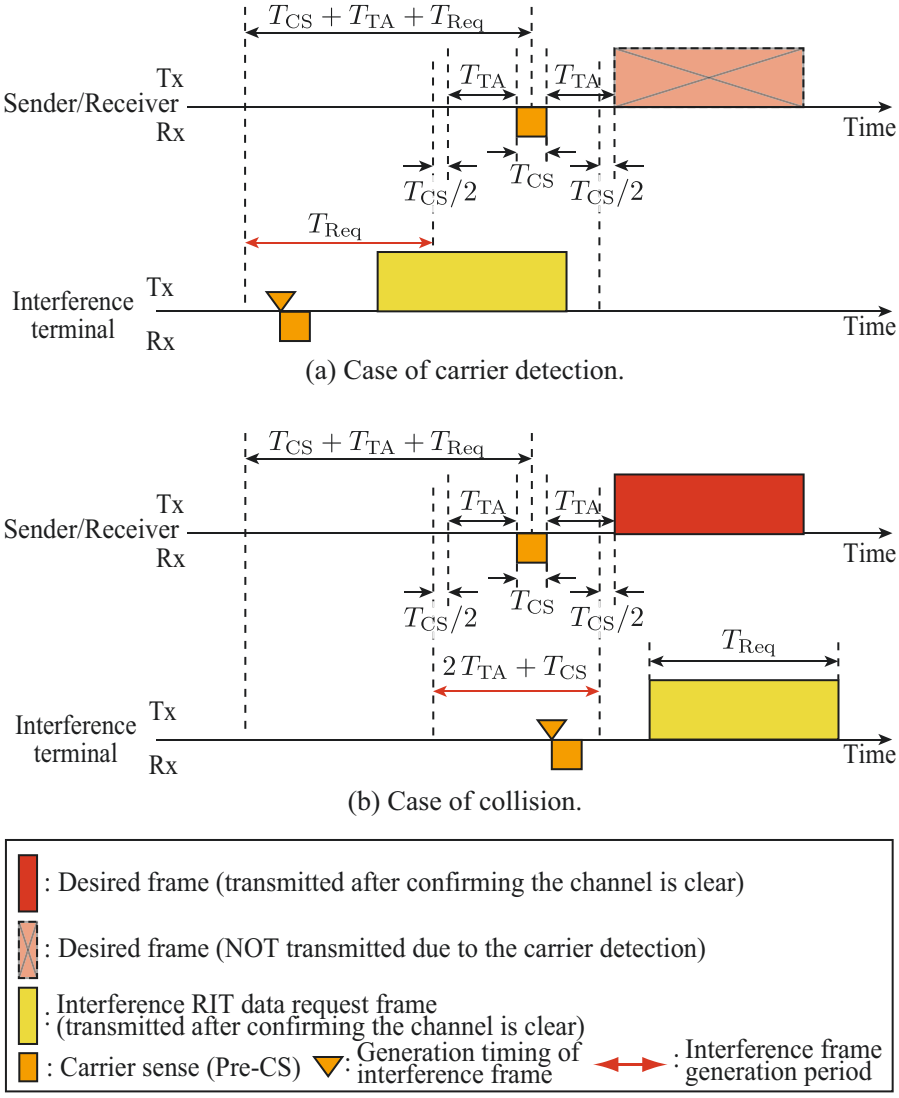

Figure 3.4: Interference model for analysis of frame transmissions. ©2021 IEICE

In the case that the desired frame is the RIT data response frame, only the collision case should be considered because the carrier sense is not performed as explained in Sect. 2.5.2. The collision occurs when the interference terminal performs the carrier sense at the duration that starts at the end of the RIT data request frame transmitted by the receiver and the start of the RIT data response frame transmitted by the sender. We define the turnaround time of the sender from the end of the reception of an RIT data request frame to the start of the transmission of an RIT data response frame as the RIT data response Tx ON T_{TxON}. The probability that the receiver catches the RIT data response frame successfully is described as follows:

$$p_{\mathrm{woCS}} = 1 - \frac{N-2}{T_{\mathrm{RIT}}} \cdot T_{\mathrm{TxON}}. \tag{3.4}$$

3.2.4. Theoretical Analysis of JUTA F-RIT protocol

In this section, the communication performance of the target JUTA F-RIT protocol is derived based on the analysis of frame transmissions in the previous section. In the JUTA F-RIT protocol, the communication link is established when transfers of the RIT data request frame (i.e., RNO), RIT data response frame (i.e., SREQ), and RACK succeed continuously as described in Sect. 3.2.2. Hence, the communication link establishment success probability for one trial is described as follows:

$$p_{\mathrm{Link}} = p_{\mathrm{wCS}} \cdot p_{\mathrm{woCS}} \cdot p_{\mathrm{wCS}}. \tag{3.5}$$

Then, if DATA and DACK transfers succeed continuously after the establishment of the communication link, the link results in successful execution. Therefore, the probability of successful execution of the communication link is expressed by

$$p_{\mathrm{Exec}} = p_{\mathrm{wCS}} \cdot p_{\mathrm{wCS}}. \tag{3.6}$$

In the JUTA F-RIT protocol described in Sect. 3.2.2, the case is assumed that the communication pair may have multiple chances (i.e., the number of timings to receive the RIT data request frames from the receiver may larger than one) to establish the communication link. The transmission success rate for n times of chances to establish the communication link is expressed by

$$p_{\mathrm{Suc}}(n) = \begin{cases} 0, & (n = 0) \\ \left\{ \sum_{k=0}^{n-1} (1 - p_{\mathrm{Link}})^k \right\} \cdot p_{\mathrm{Link}} \cdot p_{\mathrm{Exec}}. & (n \geq 1) \end{cases} \tag{3.7}$$

Here, the chances to establish the communication link depend on the MAC RIT Tx wait duration T_{TWD} (i.e., the maximum duration that the sender waits for the RIT data request frame from the receiver). n is expressed by $\lfloor T_{\mathrm{TWD}} / T_{\mathrm{RIT}} \rfloor$ or $\lfloor T_{\mathrm{TWD}} / T_{\mathrm{RIT}} \rfloor + 1$ for the probabilities of $1 - (T_{\mathrm{TWD}} / T_{\mathrm{RIT}} - \lfloor T_{\mathrm{TWD}} / T_{\mathrm{RIT}} \rfloor)$ and $T_{\mathrm{TWD}} / T_{\mathrm{RIT}} - \lfloor T_{\mathrm{TWD}} / T_{\mathrm{RIT}} \rfloor$, respectively. Therefore, the transmission success rate is expressed as follows with the MAC RIT Tx wait duration T_{TWD}:

$$\begin{aligned} p_{\mathrm{Suc},T_{\mathrm{TWD}}} = {} & p_{\mathrm{Suc}} \left(\left\lfloor \frac{T_{\mathrm{TWD}}}{T_{\mathrm{RIT}}} \right\rfloor \right) \cdot \left\{ 1 - \left(\frac{T_{\mathrm{TWD}}}{T_{\mathrm{RIT}}} - \left\lfloor \frac{T_{\mathrm{TWD}}}{T_{\mathrm{RIT}}} \right\rfloor \right) \right\} \\ & + p_{\mathrm{Suc}} \left(\left\lfloor \frac{T_{\mathrm{TWD}}}{T_{\mathrm{RIT}}} \right\rfloor + 1 \right) \cdot \left(\frac{T_{\mathrm{TWD}}}{T_{\mathrm{RIT}}} - \left\lfloor \frac{T_{\mathrm{TWD}}}{T_{\mathrm{RIT}}} \right\rfloor \right). \end{aligned} \tag{3.8}$$

Table 3.1: Parameters for evaluation.

Parameter	Values
Wireless transmission rate	100 kbit/s
Number of terminals N	10–50
RIT data request frame length (RNO command)	28 byte
RIT data response frame length (SREQ command)	25 byte
Data frame length (RACK command)	22 byte
Data frame length (DATA command)	250 byte
Data frame length (DACK command)	22 byte
MAC RIT period T_{RIT}	5 s
Data generation interval	30 s
MAC RIT Tx wait duration T_{TWD}	5.0–25 (s)
Pre-CS length T_{CS}	0.13 ms
Rx to Tx turnaround time T_{TA}	0.19 ms
RIT data response Tx ON T_{TxON}	0.8 ms
Long interframe spacing (LIFS)	1.0 ms
Baudrate	115200 baud

3.2.5. Evaluation of Transmission Performance

The transmission success rate characteristics of the JUTA F-RIT protocol is evaluated by theoretical analysis and computer simulations. Table 3.1 shows the parameters for the evaluation. The protocol is evaluated in several numbers of terminals N and MAC RIT Tx wait durations T_{TWD}. In a communication system including upper layers, DATA may contain accumulated user data and routing data. Therefore, assuming a large data size within the 255 byte PSDU length limit specified by the Wi-SUN JUTA profile, we set a frame length of 250 byte, which is the same as in the past evaluations of the IEEE 802.15.4e-compliant F-RIT protocol [20]. The data generation interval is set to only 30 s. This is a value to evaluate the basic communication performances, although it is high frequency compared to the actual communication traffic generation for smart metering systems. In the system model, only RIT data request frames are interference from the viewpoint of the communication pair. In other words, the transmission success rate is not affected by the data generation interval. To allow more trials in the experiments explained in Sect. 3.3.2, a small interval is set. Therefore, the same value is set in the computer simulations. In the computer simulations, the process delays which appear in the actual prototypes are considered.

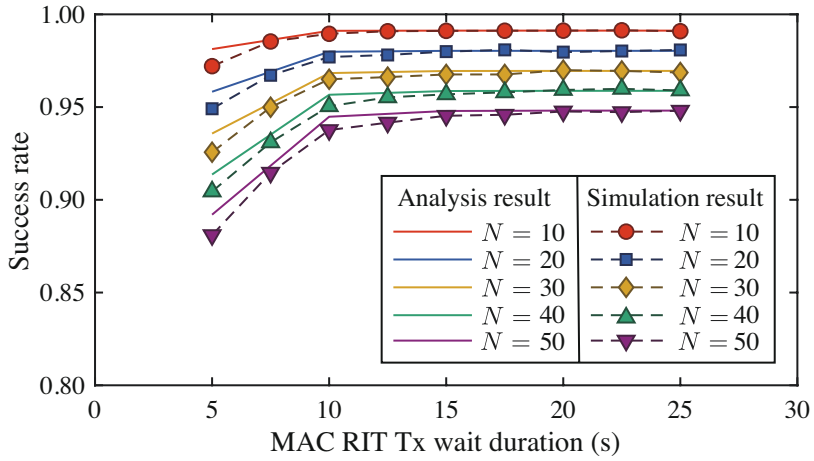

Figure 3.5: Transmission success rate characteristics by theoretical analysis and computer simulations. ©2021 IEICE

Rx to Tx turnaround time is given based on the ideal specification of the module and firmware used in the prototype described in Sect. 3.3.1. Following the assumption mentioned in Sect. 3.2.2 that considers the implementation, the delay between the reception and the transmission of frames (e.g., the delay at the sender after receiving RACK until transmitting DATA) is considered in the computer simulations. This assumes the waiting duration for UART communications between the Low-MAC and the High-MAC with the baudrate of 115200 baud. The number of transmission trials is set to 1.0×10^5 for each parameter in computer simulations. The transmission is judged as success when the sender receives DACK successfully.

Figure 3.5 shows the transmission success rate characteristics of the JUTA F-RIT protocols as a function of the MAC RIT Tx wait duration T_{TWD}. Both of the theoretical analysis results and the computer simulation results have similar characteristics: the transmission success rate tends to converge to a certain rate for each number of terminals as the MAC RIT Tx wait duration T_{TWD} extends. The chance to establish the communication link is given once when the MAC RIT Tx wait duration T_{TWD} is set equal to the MAC RIT period T_{RIT}, and the chance may fail due to the interference of RIT data request frames. By extending the MAC RIT Tx wait duration, the chance to establish the communication link increases. However, the transmission success rate does not approach 100% since the re-transmission of data frames and re-establishment of the communication link is not performed in this

evaluation focusing on the Low-MAC. In both of the analysis results and the simulation results, the JUTA F-RIT protocol can achieve the transmission success rate of about 95% when the MAC RIT Tx wait duration T_{TWD} is 5 s and the number of terminals N is 20, that is the typical interference condition of smart metering [30]. Although the theoretical analysis and the simulation results show a similar tendency, there is some divergence when the MAC RIT Tx wait duration T_{TWD} is small. This is because the timings to transmit RIT data request frames are described independently every time during the MAC RIT period in the analysis, while the RIT data request frames are transmitted in an interval in the practical protocol. On the other hand, the deviations between the theoretical analysis and the simulation results are within 0.1% when the MAC RIT Tx wait duration T_{TWD} is 25 s. This means that the analysis of the frame transmissions has high accuracy.

3.3 Development of Prototype and Experimental Evaluation of JUTA F-RIT Protocol

In this section, the world's first actual Wi-SUN dongle-type prototype that hosts the JUTA F-RIT protocol is developed and its transmission performance is evaluated experimentally.

3.3.1. Development of Prototype and Experimental Configuration

The Wi-SUN dongle-type prototype is developed by the commercial universal serial bus (USB)-type Wi-SUN dongle installing the JUTA F-RIT protocol. The commercial Wi-SUN dongle (BP35C2, ROHM Co., Ltd.) with the specification shown in Table 3.2 is used for the development. In the dongle, IEEE 802.15.4g-compliant [7] and Wi-SUN alliance-certified [21] radio module (BP35C0, ROHM Co., Ltd.) is integrated. The firmware that works as Low-MAC in the RF module and the application that acts as simple High-MAC for the evaluation on the personal computer (PC) are developed to evaluate the JUTA F-RIT protocol. The developed dongles are connected to the PC via USB cables and controlled by the application on the PC. In the implemented protocol, the RIT data request and RIT data response frames are transmitted from the Low-MAC in the module, and data frames are transmitted from the High-MAC on the PC application. The connection between the High-MAC on the

Table 3.2: Specification of Wi-SUN dongles.

Item	Specifications
USB dongle	ROHM Co., Ltd BP35C2
RF module	ROHM Co., Ltd BP35C0
Baud rate	115200 baud
Wireless standard	Based on ARIB STD-T108 [6]
Modulation	2-GFSK
Wireless frequency	920 MHz band
Transmission rate	100 kbit/s
Transmission power	+20 mW
Receiving sensitivity	–103 dBm (TYP.) (100 kbit/s, BER<0.1%)

PC and Low-MAC on the module is based on UART communication. In the developed protocol, there is no synchronization or clock correction between dongles. The protocol is implemented so that some parameters related to frame transmission timings (e.g, the Rx to Tx turnaround time, the RIT data response Tx ON, and the LIFS) are realized around the values shown in Table. 1. The data wait duration starts 0.7 ms after the transmission of the RIT data request frame and continues for 1.2 ms. This is to ensure that the RIT data response frame is received correctly even if there is some variance in the RIT data response Tx ON in the prototypes.

In an experimental configuration shown in Fig. 3.6, N terminals are placed in a plane of 50 cm × 12 cm. The system model is as same as shown in Fig. 3.1, and the two dongles placed in a diagonal position of the plane are the sender and the receiver. Others are interference terminals since all terminals are operating in a single channel. This experimental configuration is designed to evaluate the basic transmission performance as similar as in Sect. 3.2. In this environment, the sender or the receiver is located farther away from each other than any other interference terminal. This is to prevent the received power of the desired frame from being sufficiently larger than the received power of the interference frame. In other words, the dongles are arranged so that the collision likely occurs if the desired and the interference frames are transmitted simultaneously as assumed in Sect. 3.2.

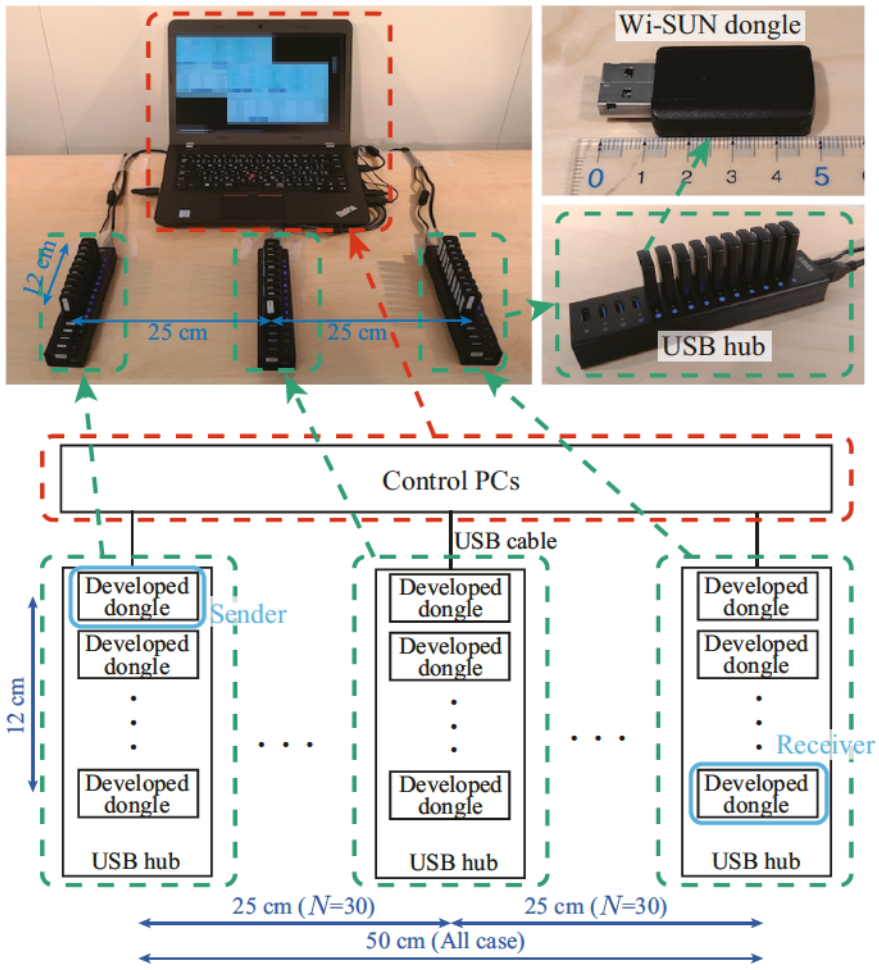

Figure 3.6: Configuration of experiments (N=30). ©2021 IEICE

3.3.2. Experimental Evaluation Results

The parameters of the experimental evaluation are shown in Table 3.3. The number of trials of communications for each parameter is 1.0×10^4. Figure 3.7 shows the measurement results of the transmission performances as a function of the MAC RIT Tx wait duration T_{TWD}. The measured transmission success rate is calculated from the ratio of successful receptions of DACK for the communication trials. When the MAC RIT Tx wait duration T_{TWD} is set to 5 s, which is the specified value of the JUTA profile in the Low-MAC, the JUTA F-RIT protocol can achieve the transmission success rate of over 90% in cases of N =10, 20, 30. When N =20, the transmission success rate of around 94% is achieved. As the MAC RIT Tx wait

Table 3.3: Parameters of experimental evaluation.

Parameter	Values
Wireless frequency	923.7, 925.7, 927.7 (MHz)
Number of terminals N	10–50
RIT data request frame length (RNO command)	28 byte
RIT data response frame length (SREQ command)	25 byte
Data frame length (RACK command)	22 byte
Data frame length (DATA command)	250 byte
Data frame length (DACK command)	22 byte
MAC RIT period T_{RIT}	5 s
Average data generation interval	30 s
MAC RIT Tx wait duration T_{TWD}	5–25 (s)
Pre-CS length T_{CS}	0.13 ms

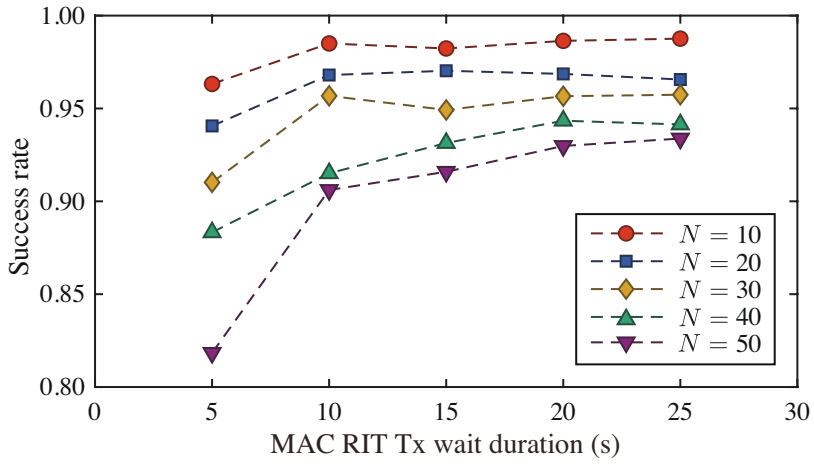

Figure 3.7: Experimental results of transmission success rate. ©2021 IEICE

duration T_{TWD} is prolonged, the transmission success rate tends to converge to a certain rate for each number of terminals (e.g., the transmission success rate of around 98.5% in the case of N =10). When the MAC RIT Tx wait duration T_{TWD} is set to 25 s, the transmission success rate over 90% is achieved without the re-establishment of the communication link and re-transmission of data frames in all cases of numbers of terminals N. The measurement results of the transmission success rate show a tendency similar to the simulation results discussed in Sect. 3.2.5, while the differences between the measurement results and the simulation results are within 5.0%.

3.4 Consideration of Performances in Prototype

In this section, the transmission performances in prototypes are considered in detail to provide the reference for better implementation or upper layer design. Focusing mainly on the Low-MAC, the transmission performance of data frames and the timeout incident is discussed.

3.4.1. Frame Transmission Performance

It is important to understand the frame transmission performance in the Low-MAC because the backoff is omitted in the Wi-SUN JUTA profile. Especially the results of the Pre-CS before transmitting data frames may be utilized for the link control of the protocol (e.g., re-transmission of data frames) controlled from the upper layer. Note that the main aim of this chapter is to grasp the performance in the Low-MAC for the upper layer design, and the impact of the link control design in the High-MAC is out of the scope of this chapter.

In this section, the transmission performances of data frames with DATA and DACK commands are discussed from the theoretical analysis and the experimental results. As discussed in Sect. 3.2.3, the incident rate of the carrier detection and the incident rate of the collision are calculated from (3.1) and (3.2), respectively. In the experiments in Sect. 3.3, the transmission results of data frames with DATA and DACK commands can be obtained from the information reported to the application (i.e., the numbers of transmission trials, carrier detections, and successful receptions).

Figures 3.8 and 3.9 show the incident rate characteristics of carrier detection and the collision, respectively. Theoretically, both characteristics increase linearly to the amount of interference (i.e., the number of terminals N). While there is some deviation between the theoretical analysis results and experimental results that may be caused by processing delay in actual modules, the experimental results show a similar tendency with theoretical analysis in both incident rates of the carrier detection and the collision. For example, when the number of terminals N is 50, the collision occurs with probability from 0.34% to 0.64% in the experimental results, while the rate is 0.49% in the theoretical result as shown in Fig. 3.9. Such incident rates of the collision are not small that cannot be ignored compared to the incident rates of the carrier detection, which occur from 2.4% to 3.4% in experimental results as shown in Fig. 3.8.

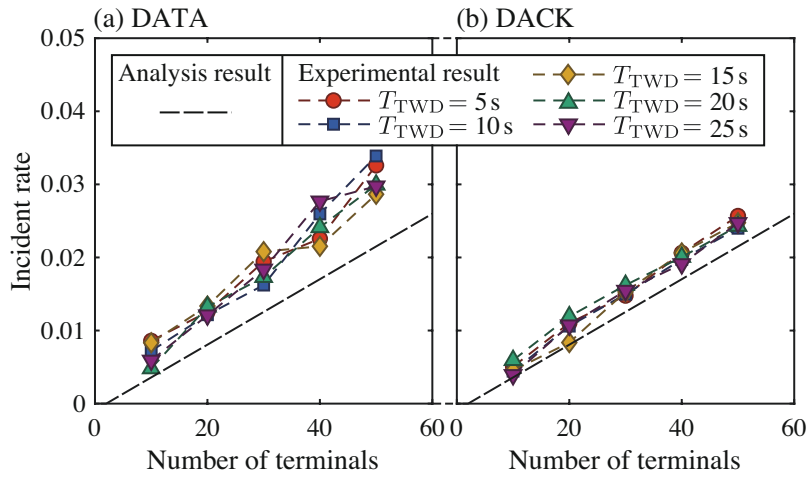

Figure 3.8: Incident rate of carrier detection. ©2021 IEICE

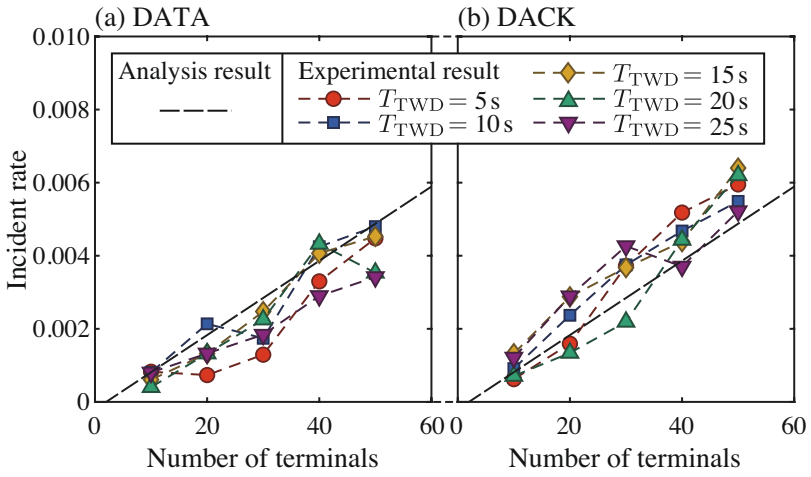

Figure 3.9: Incident rate of collision. ©2021 IEICE

From the above results, it is shown that the collision frequently occurs with a high probability of around one-fifth of the case of the carrier detection in theoretically in the JUTA F-RIT protocol at the Low-MAC, where the most of air traffic are occupied by short and frequently transmitted RIT data request frames. Therefore, it is preferable to design the upper layer on the assumption that collisions will occur frequently.

3.4.2. Timeout Incident

In this section, the transmission characteristics of the JUTA F-RIT protocol are discussed with regard to the RIT unique timeout problem. Comparing Figs. 3.5 and 3.7, it can be found that the transmission success rate shows that the measured transmission success rate is lower than simulation results. Also, the transmission performances of data frames after the establishment of the communication link cannot be the main reason for the deterioration in the experimental results because the performance can be explained from a theoretical approach as discussed in Sect. 3.4.1. Mainly, the reason for the deterioration in the experimental results is the timeout problem, which occurs in the process of establishing the communication link. The timeout is one of the major causes of transmission failures in RIT-based systems that occurs when the sender does not receive the RIT data request frame from the receiver during the Tx wait duration [30].

Figure 3.10 shows the incident rate of the timeout as a function of the MAC RIT Tx wait duration T_{TWD} in the simulation and the experimental results. In the simulation results, the MAC RIT period is slightly randomized intentionally in the simulator. On the other hand, the MAC RIT period deviates in actual modules by clock variations. Therefore, the MAC RIT period is affected by individual specificity. Furthermore, the clock is affected by temperature fluctuations. In such a condition, the timeout incidents in the experiment are not simply discussed.

To discuss the timeout problem in actual modules, an example of the wake-up duration characteristics of a sender for several communication links is shown in Fig. 3.11. This example is obtained when the MAC RIT Tx wait duration T_{TWD} is 25 s, and the number of terminals N is 20. In this example, the wake-up durations are around 25 s at the communication link index (i.e., the index of trials at the sender) from 2,061 to 2,085. In this period, the sender cannot receive RIT data request frames from the receiver due to the collision with interference frames from a specific terminal as shown in Fig. 3.12. Such continuous collisions sometimes occur, and the incident rate of timeout in the measurement results is higher than the simulation results. Due to the bias of the continuous timeout incident, the success rate depending on the parameters does not make sufficiently clear in the experimental results. Figure 3.13 shows the simulation and the experimental results of the transmission success rate that exclude the timeout incident from the number of trials. The degradation of the transmission success rate from the simulation results due to causes other than the

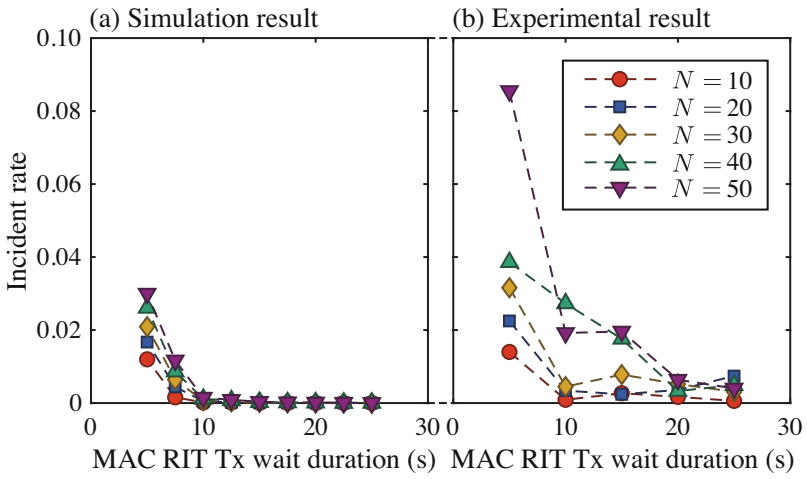

Figure 3.10: Comparison of incident rate of timeout in simulation and experimental results. ©2021 IEICE

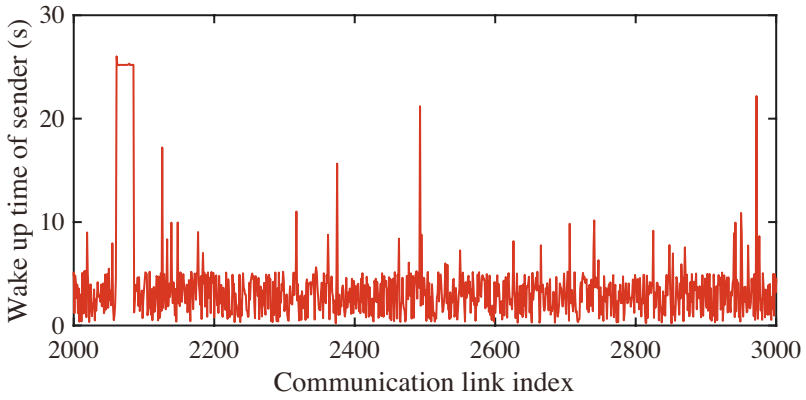

Figure 3.11: Example of experimental result of wake-up time of sender. ©2021 IEICE

timeout is evaluated from these characteristics. The differences in the transmission success rate are within 1.5%. The deterioration of the frame transmission performance described in Sect. 3.4.1 can be considered a reason for the differences in the transmission success rate, excluding timeout.

In this way, continuous collisions, which is the problem unique to the RIT protocol, may cause continuous timeouts in the actual devices. This problem cannot be detected by the carrier sense and can occur over a longer period of time if the terminal has a high-accuracy clock. Therefore, it is preferable to take measures such as periodically

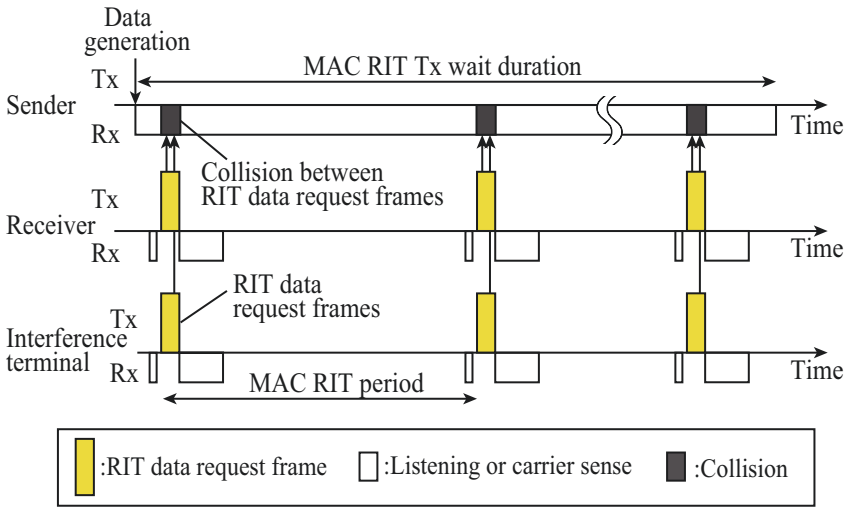

Figure 3.12: Mechanism of timeout incident due to continuous collision between RIT data request frames. ©2021 IEICE

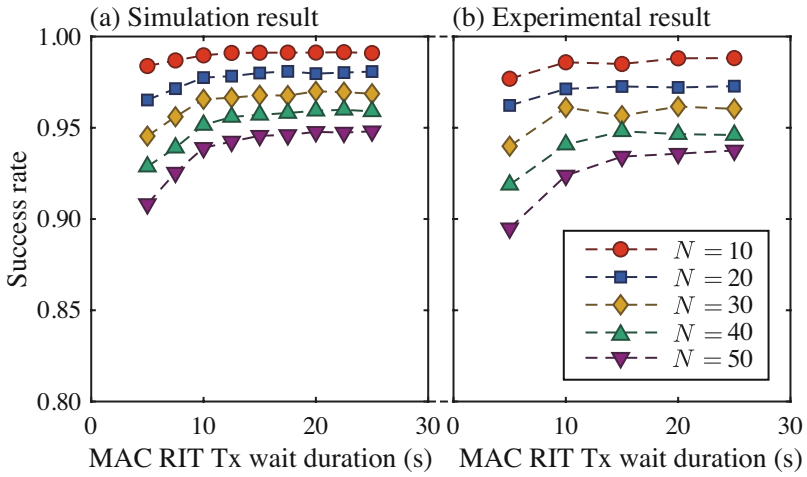

Figure 3.13: Comparison of the simulation and experimental results of transmission success rate excluding case of timeout. ©2021 IEICE

resetting the initial timing to transmit the RIT data request frames in consideration of the timeout problem.

3.5 Conclusion

In this chapter, the world's first experimental evaluation of the JUTA F-RIT protocol was conducted. Firstly, the transmission success rate in an interference environment was evaluated by the developed theoretical analysis and computer simulations. It was shown that theoretical analysis and simulation showed a similar tendency on the transmission performance of the JUTA F-RIT protocol. Then, the world's first Wi-SUN dongle-type prototype that hosts the JUTA F-RIT protocol was developed. The experimental results in an interference environment showed that the transmission success rate at the Low-MAC was around 94% when the specification of the JUTA profile was given, and the number of terminals was 20. When the waiting time for the establishment of the communication link was extended over 10 s, the JUTA F-RIT protocol can achieve the transmission success rate of over 90% without the re-establishment of the communication link and re-transmission of data frames. Moreover, the frame transmission performances and the timeout incident in the prototype were discussed in detail to provide references for better implementation and upper layer design.

Chapter 4
Efficient Polling Communications for Low-Power Data Collections

4.1 Introduction

Apart from the MAC operation, the data collection approach can also give impact on communication performances. In multi-hop networks, there are two types of approaches to collect data for better performance, whether routing is performed based on the routing tables or the centralized metrics described in Sect. 2.3.3. One is the push-type data collection approach using only uplink communications [13], [14], [23]–[27]. In this approach, terminals generate their data and send them to the coordinator independently. While this approach is a straightforward way, it has a significant problem of collisions that occurs when multiple terminals try to access a terminal simultaneously [13], [23]. It leads to the decline of communication reliability because the communication timing is limited by the low-power operation but wasted by collisions. On the other hand, the pull-type data collection approach (i.e., a polling communication) would be effective to avoid collisions [34]. However, there are only a few reports about the performance of the polling communications on the multi-hop networks based on receiver-initiated MAC protocols [48], nevertheless some actual metering systems utilize polling communications for data collection [22]. In the pull-type approach, the problem is distinct from the push-type approach, especially when routing is performed based on the centralized metrics between each terminal and the coordinator. A problem is the larger communication delay and current consumption caused by the round-trip operation of polling communications, while the collision problem in the push-type approach is avoided [34]. To achieve the frequent data collection or the longer lifetime of devices within a limited battery capacity, the delay and the current consumption related to the data collection should be improved.

In this chapter, two schemes are proposed to improve the delay and the current consumption for polling communications in multi-hop networks with receiver-initiated MAC protocol [29]. The first is an enhanced source routing scheme that

focuses on downlink communications from a coordinator to each terminal. In the proposed scheme, the route is not identified uniquely and multiple terminals can be assigned as candidates of the relay terminal. The improvement of the delay and the current consumption is expected by shortening the waiting time for communication timings. The second is a round-trip delay reduction scheme based on the wake-up interval modification that focuses on the bi-directionality of polling communications. In the proposed scheme, the terminal that succeeds the data transferring in downlink shortens the transmission interval for frames in RIT operation to improve the round-trip delay. Here, the two proposed schemes can be applied jointly in polling communications because the delay is improved by different and independent approaches. Therefore, this thesis also proposes the combined use of the enhanced source routing scheme and the round-trip delay reduction scheme. To show the impact of the proposed schemes, a multi-hop network based on the F-RIT protocol is evaluated by computer simulations. In this chapter, polling communications under a stable radio environment are assumed. Evaluation results show that the communication delay and the current consumption are improved by the proposed schemes.

The rest of this chapter is organized as follows. The problems in multi-hop networks based on receiver-initiated MAC protocols are discussed in detail in Sect. 4.2 to reveal the motivation of this section. Then, the MAC protocol and the multi-hop network assumed in this chapter are described in Sect. 4.3. In Sect. 4.4, the enhanced source routing scheme for downlink communications is proposed and evaluated by computer simulations. Next, the round-trip delay reduction scheme is proposed and evaluated in Sect. 4.5. Then, the cases that the two proposed schemes are jointly applied are evaluated in Sect. 4.6. Finally, this chapter is concluded in Sect. 4.7.

4.2 Problems in Multi-Hop Networks Based on Receiver-Initiated MAC Protocols

In this section, the problems in multi-hop networks based on receiver-initiated MAC protocols are defined in detail. From the discussion on the network management type and the data collection approaches, the motivation to achieve efficient polling communications in the network managed by the centralized metric is explained.

4.2.1. Network Type Based on Management Scheme

As discussed in Sect. 2.3.3, two network type can be considered with different management scheme (i.e., the table-based networks and the centralized metric-based networks). In term of the scalability, the metric-based networks have the merit of smaller load on each terminal excluding a coordinator for the infrequent exchange of the tables and light management of the neighbor's information. However, as implied in Sect. 2.3.3, the problem of the bi-directionality arises. In uplink communications from each terminal to a coordinator, routing is achieved utilizing the advantage of potential receivers in the receiver-initiated MAC protocols. To the contrary, downlink communications are not available if only using the centralized metrics. This is because only the coordinator is discriminated from the centralized metrics, but each terminal cannot be identified uniquely. Therefore, downlink communications cannot be simply driven by using only the centralized metrics, but there are few related works. For downlink communications, a scheme that uses multiple metrics for multi-sink networks has been proposed [93], but it cannot be applied to simple networks managed by a single coordinator. Thus, practical simple systems often use the source routing in downlink communications using past communication data or network topology acquired by a coordinator. A problem may occur that the potential receivers are not available in the source routing which specifies the route uniquely. It can bring on a reduction of communication reliability or an increase in the current consumption.

4.2.2. Data Collection Approach

Apart from the network designs, the approach of data collection (i.e., the push-type and the pull-type approaches) is essential for the network performances as described in Sect. 4.1. In this section, highly reliable polling communications in the centralized metric-based networks are discussed. When the centralized metric-based network design and the approach of polling communication are combined, the following problem occurs. The first is the delay because the polling communications require a larger delay than the push-type approach due to the round-trip operation [34]. Also, the source routing that specifies the route in downlink communications is the cause of the increase of the delay since the multiple potential receivers to shorten the delay are not available. To realize the frequent polling communications, the communication delay per one polling trial should be shortened. The second is the current consumption. In receiver-initiated MAC protocols, the larger communication delay increases the

current consumption because the terminals which holds data to be transferred is in the wake-up state. Obviously, the current consumption should be improved to prolong the lifetime of terminals or achieve the frequent data collection. It can be indirectly achieved by improving the communication delay in receiver-initiated MAC protocols. Therefore, we improve the delay and the current consumptions focusing on the source routing scheme in downlink communications, and round-trip operations of polling communications.

4.3 Target Multi-Hop Network

In this section, the target multi-hop network supposed in this chapter is introduced. In the MAC layer, the Wi-SUN JUTA profile-compliant F-RIT protocol with the communication sequence based on the U-Bus Air [28] is adopted as a concrete receiver-initiated MAC protocol. In the network layer, downlink and uplink communications are performed based on the routing protocol in a centralized metric-based network.

4.3.1. MAC Protocol

In this chapter, the Wi-SUN JUTA profile-compliant F-RIT protocol is adopted as a MAC protocol. The overview was introduced in Sects. 2.5.3 and 3.2.2, but the re-establishment of a communication link is introduced as different from evaluation in Chapter 3. In addition, some components are adopted to provide reliable and practical multi-hop communications based on the F-RIT protocol. First is an anomaly detection of the continuous check code, which is a part of the function in the U-Bus Air, is adopted. This function is adopted to evade the collision that occurs when multiple terminals try to access a terminal simultaneously. Each terminal records the number of consecutive anomaly times k that the terminal cannot receive a frame correctly in the data wait duration, and loads the number in the RIT data request frame. The number of consecutive anomaly times k is initialized if the terminal does not detect any signal or receives a frame correctly. The sender that receives the RIT data request frame transmits the RIT data response frame at the probability of

$$p(k) = \begin{cases} 1/2^k & k \leq 5, \\ 1/2^5 & k > 5. \end{cases} \tag{4.1}$$

Second is the retransmission of DATA. If the sender never receives DACK after the transmission of DATA, the sender retransmits DATA again. This retransmission

can be repeated for several times. Last is the reestablishment of the communication sequence. If the sender never receives DACK in one communication sequence and the sequence ends in failure, the sender gets back to the Tx wait duration and waits for the RIT data request frame. As long as the MAC RIT Tx wait duration is not counted up, the sender tries to reestablish the communication sequence each time it receives an RIT data request frame from the receiver to transfer the data.

4.3.2. Routing Protocol

In this chapter, a network that all terminals have a metric called rank as a location indicator in the network is assumed. The rank indicates the number of transfers to the coordinator from each terminal, so the coordinator has the rank of 0. Terminals broadcast the RIT data request frame that loads the own rank information. Each terminal can assess the state of the neighbor terminals by receiving RIT data request frames. Each terminal decides its own rank as the number of the minimum rank of its neighbors adding one.

In uplink communications to the coordinator, the data is transferred to the terminal with a smaller rank. Once a terminal (i.e., the sender) starts the transfer process, the sender starts the Tx wait duration. The sender decides whether to transfer the holding data or not by a routing function when the terminal receives an RIT data request frame from a neighbor terminal. In other words, the forwarding destination is not decided uniquely at the start, and routing is achieved opportunistically by receiver-initiated operation in the MAC layer. In this chapter, a routing function designed based on the U-Bus Air is considered. Each terminal transfers its holding data if the following condition is satisfied:

$$\begin{cases} r(y) = r(x) - 1 & t \leq T_{\mathrm{TWD}}/2, \\ r(x) - 1 \leq r(y) \leq r(x) & t > T_{\mathrm{TWD}}/2. \end{cases} \tag{4.2}$$

Here, $r(x)$ is a sender's own rank, and $r(y)$ is the rank contained in the received RIT data request frame. Also, t is the elapsed time from the start of the Tx wait duration. T_{TWD} is defined as the maximum length of the Tx wait duration (i.e., the MAC RIT Tx wait duration). If the condition satisfies (4.2), the sender tries to transfer the data to the source of the RIT data request frame (i.e., the receiver) using the communication sequence shown in Fig. 2.7. During the communication sequence after receiving an RIT data request frame until exchanging DACK, the sender never tries to transfer the data to the terminal other than the receiver. If the sender receives DACK from the receiver successfully, the transfer process ends. If the sender never receives DACK in

the communication sequence, the sender gets back to the Tx wait duration and continues to try to transfer the holding data to one of the potential receivers until the MAC RIT Tx wait duration is counted up. Multiple potential receivers provide more communication opportunities during the MAC RIT Tx wait duration compared to the case that the receiver is specified uniquely. The sender transfers the holding data to one of the potential receivers in the successful transfer case as a result of the receiver-initiated mechanism of the MAC protocol. Each terminal that transfers the data for uplink communications adds 8 bytes of information about the own address and the rank to the routing information in the DATA payload.

As mentioned in Sect. 4.2.1, the source routing that specifies the route from the coordinator to the destination terminal is required for downlink communications. Hereinafter, the destination of the end-to-end downlink communications is called the target terminal. The specified route information to the target terminal is loaded in DATA. In this chapter, the coordinator makes a record of routes in uplink communications from routing information for uplink communications. The source routing information is built by loading the reverse of information of relay terminals included in the most used uplink route and adding the information of the target terminal. The routing information volume for one terminal is 8 bytes as same as uplink communications. Each terminal that receives DATA for downlink communications transfers to the neighbor terminal following to the routing information if the own address is different from the address of target terminal.

4.4 Enhanced Source Routing Scheme for Efficient Downlink Communications

In this section, the enhanced source routing scheme is proposed to improve the delay and the current consumption in downlink communications [29]. Computer simulations are carried out and the results show the effectiveness of the proposed enhanced source routing scheme.

4.4.1. Proposed Enhanced Source Routing Scheme

For efficient downlink communications, the enhanced source routing scheme is proposed to improve the delay and the current consumption by enabling multiple potential receivers to achieve the opportunistic routing. Hereinafter, the source routing scheme that specifies the route uniquely is called the conventional scheme in this

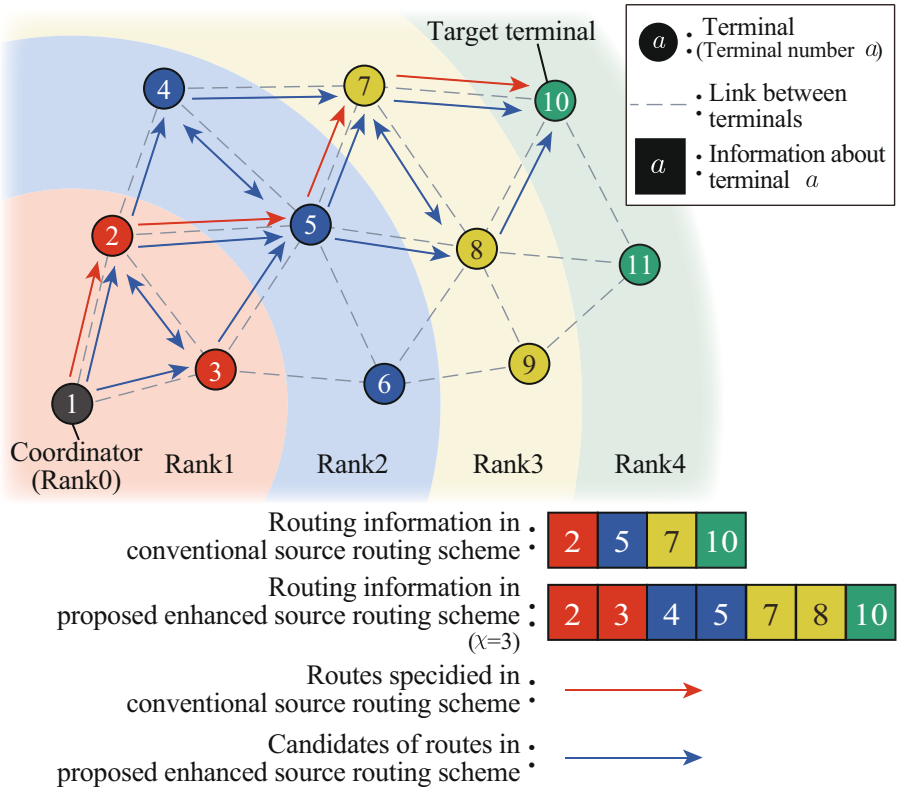

Figure 4.1: Overview of conventional and proposed enhanced source routing schemes. ©2021 IEICE

section. In the enhanced source routing scheme, information about multiple terminals in the same rank is loaded in the routing information for the source routing. Figure 4.1 shows an overview of the conventional scheme and the enhanced source routing scheme. In the proposed enhanced source routing scheme, the relay terminals are decided from candidates by the receiver-initiated operation in the MAC layer.

As a parameter for the enhanced source routing scheme, the maximum number of additional addresses, χ, is introduced. This is the maximum number of terminals that are newly added to the routing information in comparison with the conventional scheme. Hence, $\chi = 0$ expresses for the conventional scheme. Various methods can be considered to construct the routing information. In this chapter, terminals are chosen from the routes frequently used in uplink communications. Algorithm 4.1 shows the process to make a set of terminals Ω_d for the enhanced source routing information of which the target terminal has the terminal number of d. Here, $\Psi_{d,i}$ denotes the set of relay terminal numbers in the i-th most used in uplink communications from the terminal number of d. $n(A)$ is defined as the number of

Algorithm 4.1 Selection of Terminals for Route Configuration.

$i \leftarrow 1,\ \Omega_d \leftarrow d$
while $n(\Omega_d) \leq r(d) + \chi$ and $n\left(\Psi_{d,i}\right) > 0$
  if $n\left(\Psi_{d,i}\right) = = r(d) - 1$
    if $n(\Omega_d \cup \Psi_{d,i}) \leq r(d) + \chi$
      $\Omega_d \leftarrow \Omega_d \cup \Psi_{d,i}$
    end if
  end if
  $i = i + 1$
end while

elements of set A. The routing information for the proposed enhanced source routing scheme in downlink communications is constructed by loading the information about terminals in set Ω_d in order of their rank.

The relay terminal which transfers data decides whether to transfer of not by a routing function as same as uplink communications. In this chapter, the routing function for downlink communications is designed as the reverse of the routing function for uplink communications, so expressed as

$$\begin{cases} r(y) = r(x) + 1 & t \leq T_{\mathrm{TWD}}/2, \\ r(x) \leq r(y) \leq r(x) + 1 & t > T_{\mathrm{TWD}}/2. \end{cases} \tag{4.3}$$

If the rank loaded in the RIT data request frame from a neighbor terminal satisfies (4.3) and y is included in Ω_d, the terminal tries to transfer the data to the source terminal of the RIT data request frame.

In the overview of the conventional and the enhanced source routing scheme illustrated in Fig. 4.1, a network consists of 11 terminals with the maximum rank is 4 is assumed. The target terminal is the terminal of which terminal number d is 10 and rank $r(d)$ is 4. Here, the maximum number of additional addresses χ of 3 is considered. In the conventional scheme, information about 4 terminals are loaded in routing information to specify the route for the downlink communication. On the other hand, information about 7 terminals is loaded in routing information for the enhanced source routing scheme. There are multiple candidates of routes, so the route actually used is determined by the routing function at each terminal.

While the volume of routing information of the enhanced source routing scheme is larger than that of the conventional scheme, potential receivers can be utilized when

more than one multiple candidates of the relay terminal are available. Therefore, as in the case of the opportunistic routing for uplink communications, more communication chances are provided than in the case that the receiver is specified uniquely. If there are multiple potential receivers to transfer the data, the expected waiting time for the RIT data request frame from the receivers decreases. The feature of the receiver-initiated MAC protocol is that the waiting time at the Tx wait duration is dominant for the delay and the current consumption [20]. The larger routing information due to the proposed scheme may increase the delay and the current consumption required for transferring DATA, but this is generally small compared to the effect of shortening the waiting time for the RIT data request frame at the Tx wait duration. Therefore, the improvement of the delay and the current consumption is expected by setting multiple candidates to transfer data in downlink communications. Moreover, data transferring is continued even if one communication trial for a terminal fails, because the sender may have additional communication chances to another terminal, which has another link. The proposed scheme modifies only the routing scheme, and the MAC protocol does not need to be changed. Therefore, the proposed scheme can extract the advantage of the MAC protocol without making changes in the concrete and highly-interoperable MAC protocols.

4.4.2. System Model for Evaluations

In this chapter, a multi-hop network that collects data by polling communications is evaluated. A coordinator is installed in a corner of a field of which size is 1,000 m × 1,000 m, and 49 terminals are randomly set in the field. Parameters for evaluations are shown in Table 4.1. A Stable channel is considered between terminals. Received signal strength indicator (RSSI) between terminals is calculated from the path-loss by the two-rays ground reflected model. The judgment of a neighbor or not (i.e., the terminals can communicate directly or not) is decided by an RSSI threshold. When the threshold is –91 dBm, a multi-hop network in which the maximum rank of the terminals is 4, is constructed as shown in Fig. 4.2. In this chapter, the terminal arrangement shown in Fig. 4.2 is used for all evaluations.

The data which includes the user data of 128 bytes are collected from each terminal by polling communications. In downlink communications, only routing information is loaded in the payload of DATA. In uplink communications, the user data and routing information are loaded in the payload of DATA as described in Sects. 4.3.2 and 4.4.1. The coordinator starts a series of polling communications for each terminal in a fixed

Table 4.1: Simulation parameters.

Parameter	Values
Radio frequency	922.5 MHz
Modulation scheme	2-GFSK
Transmission rate	100 kbit/s
Modulation index	1.0
Gaussian filter *BT*	Tx: 0.5, Rx: 0.7
Channel model	AWGN
Antenna gain	2.15 dBi
Additional system noise	5.0 dB
Antenna height	1.0 m
Number of terminals	50
Field size	1,000 m × 1,000 m
Carrier sense threshold	–80 dBm
RSSI threshold for neighbor decision	–91 dBm
RIT data request frame length	28 bytes
RIT data response frame length	25 bytes
Data frame length (RACK)	22 bytes
Data frame length (DATA, exclude routing information and user data)	31 bytes
User data payload length	128 bytes
Data frame length (DACK)	22 bytes
MAC RIT period	5,000 ms
MAC RIT Tx wait duration	25,000 ms
Number of retransmission (only DATA)	3
Data lifetime	40,000 ms
Tx current	45 mA
Rx current	25 mA
Sleep current	4.0 μA

interval. Only after receiving an instruction from the coordinator by the downlink communication to send the user data, the target terminal sends DATA loading user data in uplink. The polling for each terminal is performed independently in one series of polling communications from the coordinator. The polling communications are managed by the index in the data frame. In the case that the collision occurs at transferring of DACK, the duplication of the data may occur. This is because the sender may judge that the transfer to a receiver results in failure by the non-arrival of DACK, but the receiver may successfully receive the data and start forwarding after transmitting DACK. To manage the duplication cases, the coordinator or the target

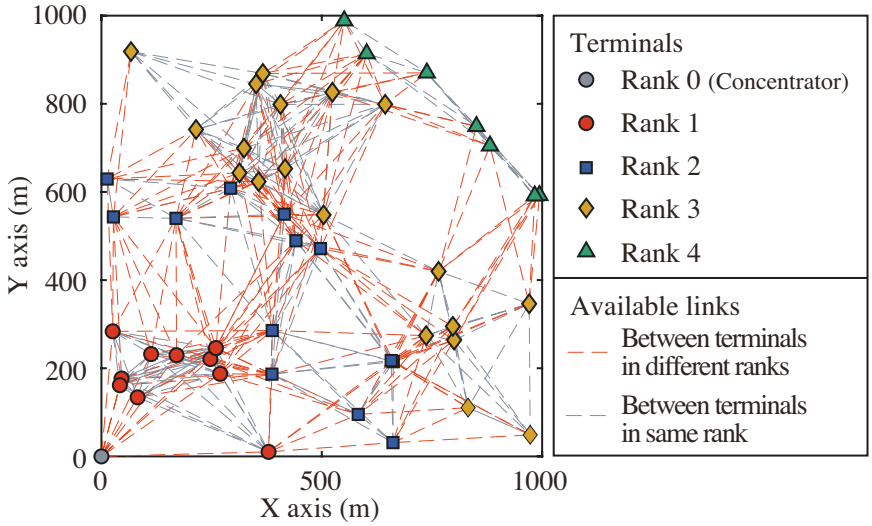

Figure 4.2: Arrangement of terminals in computer simulations. ©2021 IEICE

terminal discards all arrival data but the first one. Note that this is not the major case because the collision does not occur frequently even in a crowded condition [28]. Normally, the coordinator starts the polling for the next target terminal when it receives a user data by uplink communications from a target terminal. If the coordinator does not receive the uplink DATA from a target terminal for 80 s (i.e., twice of the DATA lifetime for downlink and uplink), it starts a polling for the next target terminal. In this chapter, the polling intervals from 900 s to 21,600 s are evaluated.

4.4.3. Configuration of Downlink Routing Information

The proposed enhanced source routing scheme that sets the maximum number of additional addresses χ provides the potential of usage of multiple routes. In other words, if there are no sufficient candidate terminals, the number of addresses for the proposed enhanced source routing scheme may not reach the maximum number of addresses χ. Therefore, the configuration of routing information should be evaluated. Table 4.2 shows the frequency distribution for the number of addresses in routing information and the target terminal's rank. This result is derived from the routing information for the downlink at the last series of polling when the maximum number of additional addresses χ is set to 9 and the polling interval is 900 s.

Table 4.2: Frequency distribution of number of addresses in routing information and target terminal's rank when $\chi = 9$ and polling interval is 900 s.

		Number of addresses in routing information for downlink source routing												
		1	2	3	4	5	6	7	8	9	10	11	12	13
Rank of target terminal	1	10	0	0	0	0	0	0	0	0	0			
	2		5	1	1	2	1	1	0	0	0	2		
	3			0	1	2	0	0	2	2	2	1	9	
	4				0	0	0	0	0	0	0	0	0	7

When the target terminals are in rank 1, the coordinator sets only one address in the routing information for all 10 terminals. This is because the multiple routes cannot be prepared for the target terminals which the coordinator can communicate directly (i.e., terminals in rank 1) as long as the additional hop is not considered. Therefore, the benefit of the proposed enhanced source routing scheme does not appear in the polling communications for target terminals in rank 1 since the modification of the hop number is not considered in this chapter. The same is true of 5 target terminals in rank 2, where the number of addresses in routing information for these terminals is 2. These target terminals in rank 2 have only one neighbor terminal in rank 1. To summarize, the routing for 15 terminals is as same as the conventional scheme.

The benefit of the proposed enhanced source routing scheme is expected to appear in the polling communications for the other 34 terminals. For target terminals in rank 2 or 3, the number of addresses in routing information for some target terminals are smaller than the sum of their rank and the maximum number of additional addresses $\chi = 9$. The routes to these terminals may not increase by setting a large maximum number of additional addresses.

4.4.4. Evaluation Results of Collection Success Rate

Figure 4.3 shows the collection success rate characteristics for polling intervals when the maximum number of additional addresses χ is set to 0, 3, 6, and 9. The collection success rates in all parameters achieve over 99.5%, which is a target rate of wireless systems for critical infrastructures [20], since the channel fluctuation is not considered in this chapter. The proposed enhanced source routing scheme may increase the frame length of DATA, but the collection success rate does not decrease because collisions are avoided by polling communications.

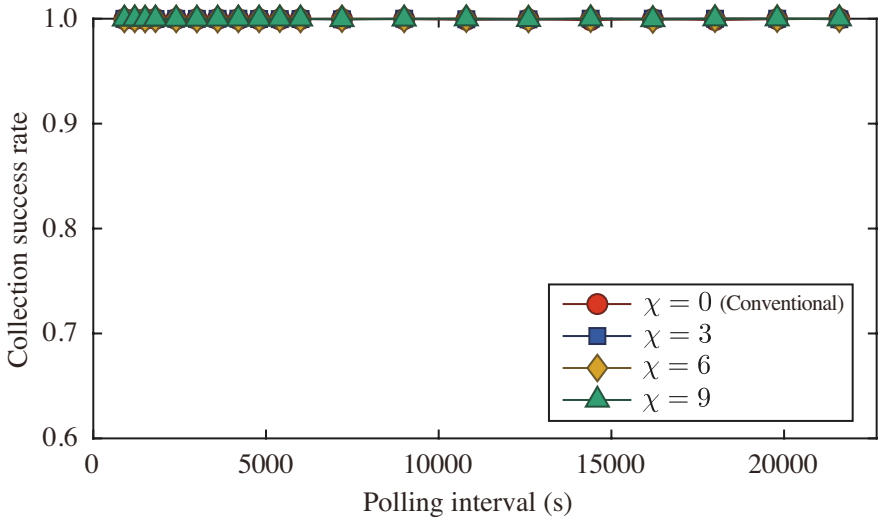

Figure 4.3: Collection success rate characteristics as a function of polling interval for each maximum number of additional addresses χ. ©2021 IEICE

4.4.5. Evaluation Results of Delay

Figure 4.4 shows the average downlink delay characteristics for polling intervals when the maximum number of additional addresses χ is set to 0, 3, 6, and 9. The downlink delay tends to decrease as the maximum number of additional addresses χ increases. There is no tendency for polling interval because collisions of data transmissions are avoided by polling communications.

To analyze detail, the downlink delay characteristics for the maximum number of additional addresses χ when the polling interval is 900 s are shown in Fig. 4.5. The downlink delay is averaged for the rank of the target terminal and all trials in this figure. In average downlink delay of all trials, the delay of the conventional scheme (i.e., $\chi = 0$) is 8.2 s. When the maximum number of additional addresses χ is set to 9, the average downlink delay is 5.5 s. Therefore, the proposed enhanced source routing scheme improves the delay by 32.2%. For the target terminals in rank 1, there is no improvement because the usage of multiple routes is not available. The improvement effect is small for the target terminals in rank 2 because not all target terminals benefit sufficiently by setting a large maximum number of additional addresses χ as analyzed in Sect. 4.4.3. The improvement of the delay especially appears when the rank of the target terminal is large because the number of candidates for relay terminals is enough. For the target terminals in rank 4, the downlink delay is 13.0 s in the

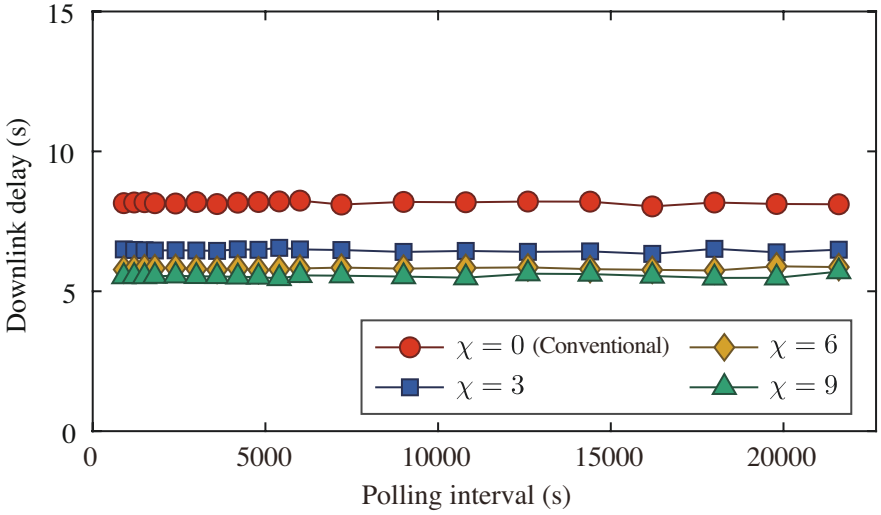

Figure 4.4: Downlink delay characteristics as a function of polling interval for each maximum number of additional addresses χ. ©2021 IEICE

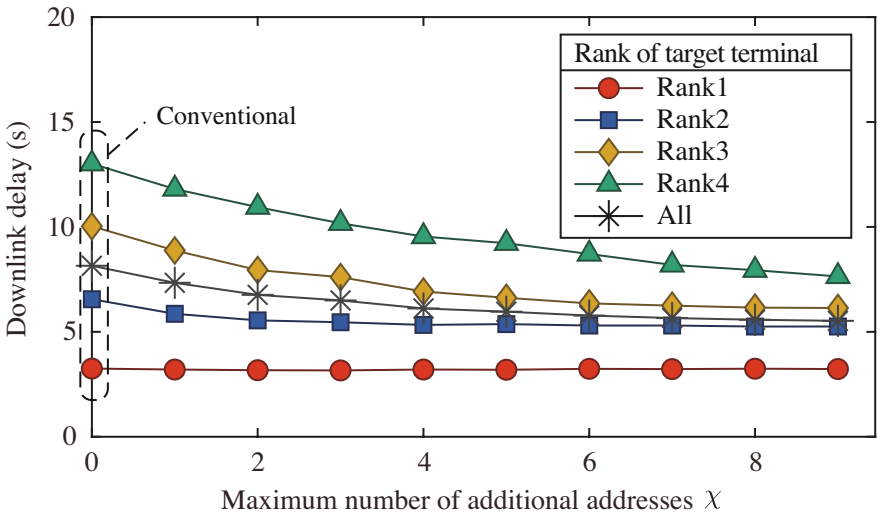

Figure 4.5: Downlink delay characteristics as a function of maximum number of additional addresses χ when polling interval is 900 s. ©2021 IEICE

conventional scheme (i.e., $\chi = 0$). On the other hand, the delay is 7.6 s when the maximum number of additional addresses χ is 9. This result shows the improvement of 41.3% by the proposed scheme from the conventional scheme.

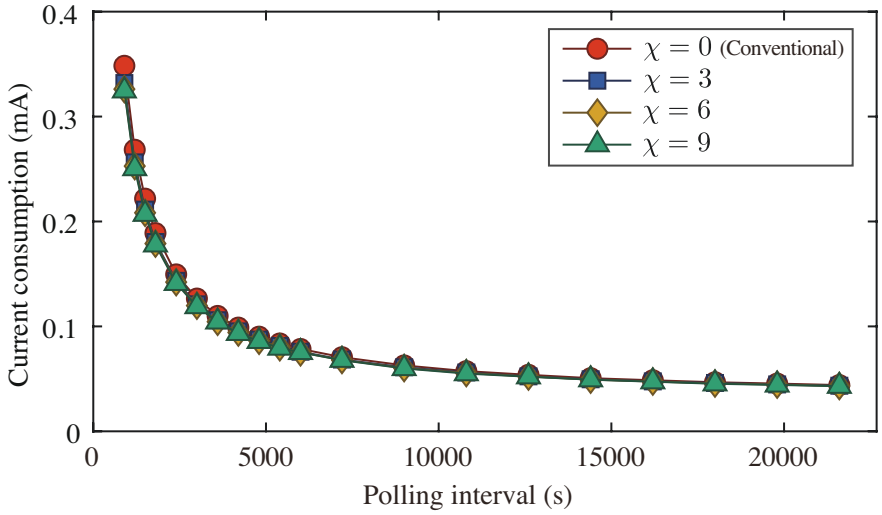

Figure 4.6: Current consumption characteristics as a function of polling interval for each maximum number of additional addresses χ. ©2021 IEICE

4.4.6. Evaluation Results of Current Consumption

The current consumption characteristics per unit time for polling intervals when the maximum number of additional addresses χ is set to 0, 3, 6, and 9 are shown in Fig. 4.6. Here, the current consumption is averaged for all terminals except for the coordinator. The current consumption tends to increase as the polling interval decreases (i.e., the polling frequency increases), regardless of the maximum number of additional addresses χ. In addition, the current consumption tends to decrease slightly as the maximum number of additional addresses χ becomes large.

We focus on the characteristics when the polling interval is 900 s to clarify the improvement effect of the proposed enhanced source routing scheme. Figure 4.7 shows the current consumption characteristics averaged for terminals in each rank and all terminals except for the coordinator. In the characteristics shown in Fig. 4.7, the current consumption averaged for all terminals except for the coordinator is 0.32 mA when the maximum number of additional addresses χ is set to 9. This is 6.8% more efficient than the conventional scheme (i.e., $\chi = 0$) that the current consumption is 0.35 mA. The improvement effect is clear at the terminals in rank 1, that transfer DATA frequently. The current consumption improves by 13.5% from the conventional scheme (i.e., $\chi = 0$) that the current consumption is 0.89 mA to the proposed enhanced

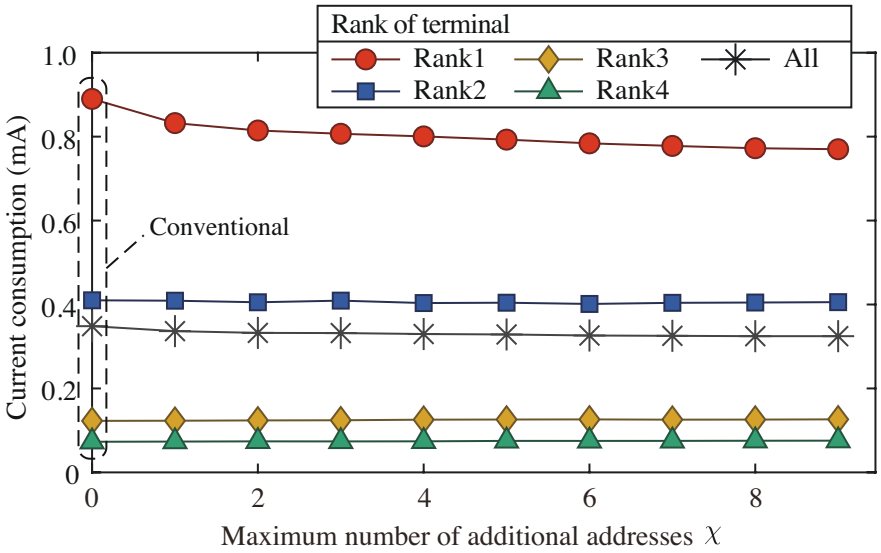

Figure 4.7: Current consumption characteristics as a function of maximum number of additional addresses χ when polling interval is 900 s. ©2021 IEICE

source routing scheme with $\chi = 9$ that the current consumption is 0.77 mA. On the other hand, the current consumption of terminals in rank 3 and 4 does not improve by the proposed enhanced source routing scheme. This is because terminals in rank 3 and 4 do not transfer DATA for downlink communications or should transfer DATA to a specified target terminal. It means that they do not benefit from the proposed enhanced source routing scheme since they never consider multiple candidates of receivers. For these terminals, the volume of DATA to transfer or receive in downlink communications may increase by the proposed enhanced source routing scheme, but the remarkable rise of the current consumption does not occur.

4.5 Round-Trip Delay Reduction Scheme Based on Wake-Up Interval Modification

In this section, the round-trip delay reduction scheme is proposed for efficient polling communications [29]. Computer simulations are carried out to show the effectiveness of the proposed round-trip delay reduction scheme.

4.5.1. Proposed Round-Trip Delay Reduction Scheme

The proposed round-trip delay reduction scheme improves the round-trip delay and the current consumption focusing on the bi-directionality of polling communications. Normally, the F-RIT protocol adopts the fixed MAC RIT period for the transmission interval of the RIT data request frames (e.g., 5 s in the Wi-SUN JUTA profile). In the proposed round-trip delay reduction scheme, the terminal which succeeds to transfer DATA in downlink communications modifies the transmission interval of RIT data request frames (i.e., the wake-up interval) to be smaller for a while. Hereinafter, the reduced transmission interval is called the reduced MAC RIT period T'_{RIT} in this chapter. Also, the case that the reduced MAC RIT period T'_{RIT} is set to 5 s (i.e., the same value as the MAC RIT period in the Wi-SUN JUTA profile) is defined as the conventional scheme in this section. If the terminal receives a returned DATA in uplink communications, the terminal reverts the transmission interval of RIT data request frames back to the original MAC RIT period.

In the F-RIT protocol, the transmission interval of RIT data request frames (i.e., the MAC RIT period) is the dominant parameter for the current consumption of terminals [20]. The shorter interval can reduce the delay and the power consumption to transfer DATA, because the listening state of the Tx wait duration to wait for the RIT data request from the destination terminals is shorten. However, the shorter interval increases the current consumption of the usual time (i.e., the time when the terminal does not try to transfer DATA) to transmit RIT data request frames frequently. Contrary, the larger interval requires the larger delay and current consumption to transfer DATA, but the current consumption of the usual time becomes smaller. The proposed round-trip delay reduction scheme is expected to improve not only the delay but also the current consumption avoiding this trade-off relationship on the transmission interval of RIT data request frames. In the proposed round-trip delay reduction scheme, the duration to reduce the interval is limited to a certain time, but the uplink communications may be achieved in shorter delay and lower current consumption. The proposed scheme does not use the default value specified in the Wi-SUN JUTA profile, thus deviates from the standard. However, the proposed scheme uses a very simple and autonomous modification that changes parameter temporarliy and provides additional communication opportunities to the conventional scheme. This results in high compatibility with the conventional scheme.

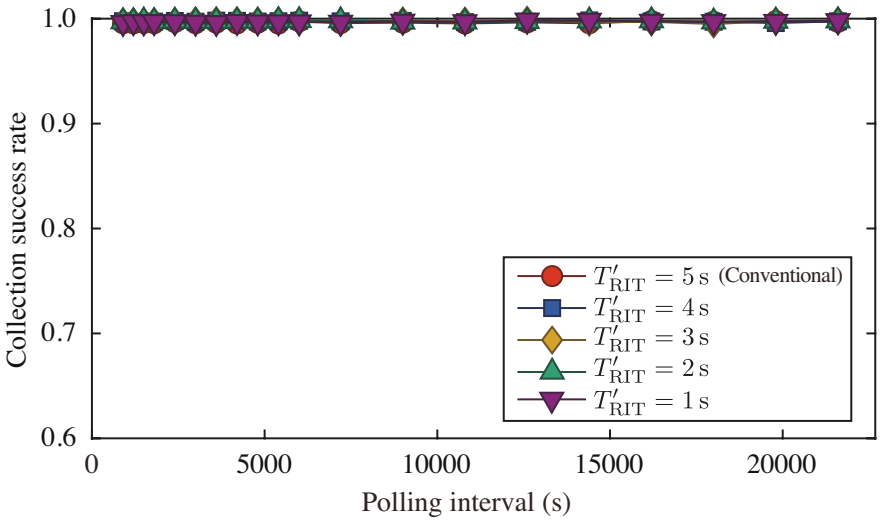

Figure 4.8: Collection success rate characteristics as a function of polling interval for each reduced MAC RIT period T'_{RIT}. ©2021 IEICE

4.5.2. Evaluation Results of Collection Success Rate

The effectiveness of the proposed round-trip delay reduction scheme is evaluated by computer simulations. The system model and evaluation parameters are as same as evaluations in Sect. 4.4.

The collection success rate characteristics for polling intervals are shown in Fig. 4.8. The deterioration of the collection success rate does not occur by reducing the MAC RIT period in the proposed round-trip delay reduction scheme, even it may increase the number of transmitted frames.

4.5.3. Evaluation Results of Current Delay

This section focuses on the round-trip delay because the proposed round-trip delay reduction scheme is developed based on the bi-directionality of the polling communications. Figure 4.9 shows the average round-trip delay characteristics for polling intervals. As the reduced MAC RIT period T'_{RIT} becomes smaller, the round-trip delay tends to decrease.

The detail is analyzed from the round-trip delay characteristics for the reduced MAC RIT period T'_{RIT} when the polling interval is 900 s shown in Fig. 4.10. In this graph, the round-trip delay is averaged for the rank of the target terminal and all trials.

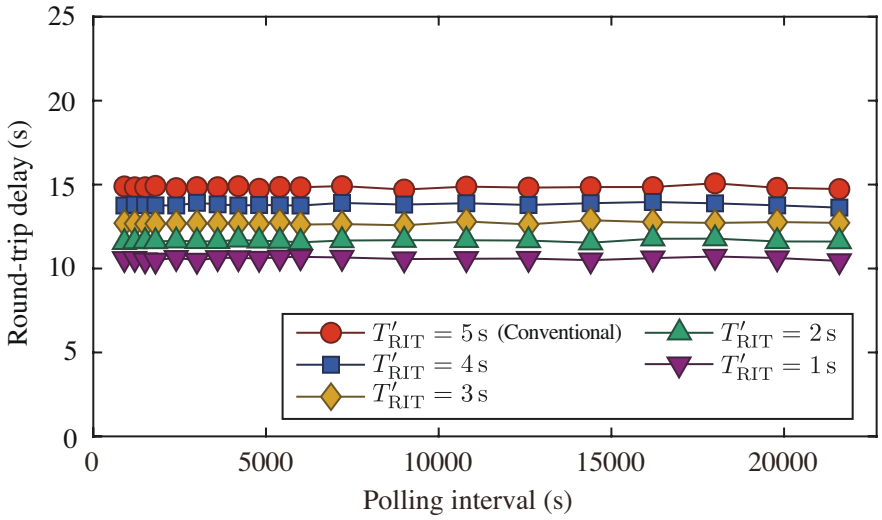

Figure 4.9: Round-trip delay characteristics as a function of polling interval for each reduced MAC RIT period T'_{RIT}. ©2021 IEICE

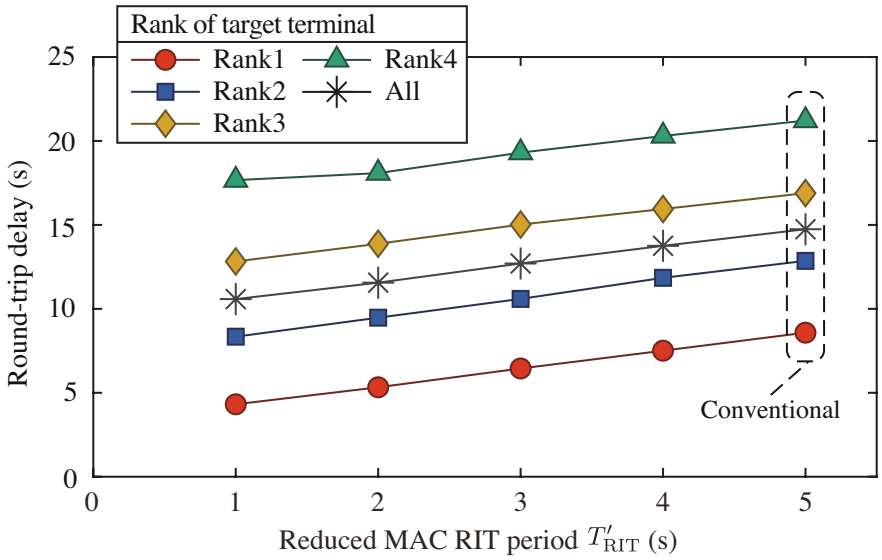

Figure 4.10: Round-trip delay characteristics as a function of reduced MAC RIT period T'_{RIT} when polling interval is 900 s. ©2021 IEICE

In the average for all cases, the round-trip delay in the conventional scheme (i.e., T'_{RIT} = 5 s) is 14.7 s. The proposed round-trip delay reduction scheme improves by 28.2% to 10.6 s when T'_{RIT} = 1 s. The improvement effect can be seen especially in

communications for target terminals in the lower rank. For target terminals in rank 1, the proposed round-trip delay reduction scheme improves by 49.7% from 8.6 s of the conventional scheme to 4.3 s when T'_{RIT} = 1 s.

4.5.4. Evaluation Results of Current Consumption

The current consumption characteristics per unit time averaged for all terminals except for the coordinator are shown in Fig. 4.11. The current consumption tends to increase as the polling interval decreases as same as Fig. 4.6. When the polling interval is small (i.e., the current consumption used for transferring DATA is large), the current consumption is improved as the reduced MAC RIT period T'_{RIT} becomes smaller.

The effect of the proposed round-trip delay reduction scheme is analyzed in detail from the current consumption characteristics for reduced MAC RIT period T'_{RIT} when the polling interval is 900 s shown in Fig. 4.12. The current consumption averaged for all terminals except for the coordinator is 0.24 mA when T'_{RIT} = 1 s. The proposed round-trip delay reduction scheme improves the current consumption by 30.9% from 0.35 mA in the conventional scheme (i.e., T'_{RIT} = 5 s). The improvement effect remarkably appears at terminals in rank 1, where the number of transfers is large. The current consumption of terminals in rank 1 is improved by 38.2% from 0.89 mA of the conventional scheme (i.e., T'_{RIT} = 5 s) to 0.55 mA of the proposed round-trip delay reduction scheme when T'_{RIT} = 1 s. Unlike the enhanced source routing scheme for downlink communications proposed in Sect. 4.4, the proposed round-trip delay reduction scheme based on polling communications can reduce the current consumption of terminals in larger ranks. The current consumption of terminals in rank 4 is improved by 21.6% from 0.072 mA of the conventional scheme (i.e., T'_{RIT} = 5 s) to 0.057 mA of the proposed round-trip delay reduction scheme when T'_{RIT} = 1 s.

4.6 Joint Evaluation of Proposed Schemes

The proposed schemes described in Sects. 4.4 and 4.5 (i.e., the enhanced source routing scheme and the round-trip delay reduction scheme) can improve the communication delay and the current consumption. Both schemes can be adopted simultaneously because the points to improve the delays are different. In this section, we propose the combined use of the enhanced source routing scheme proposed in Sect. 4.4 and the round-trip delay reduction scheme proposed in Sect. 4.5. The cases that both proposed schemes are jointly adopted are evaluated by computer simulations.

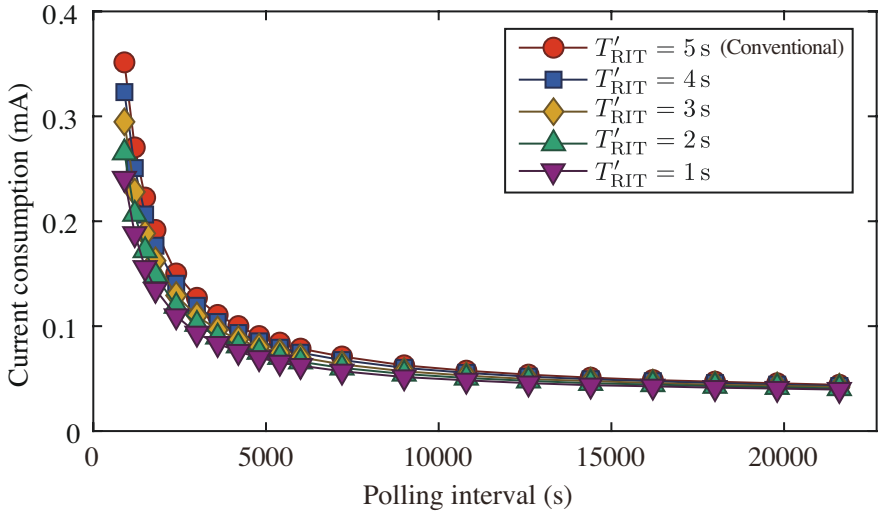

Figure 4.11: Current consumption characteristics as a function of polling interval for each reduced MAC RIT period T'_{RIT}. ©2021 IEICE

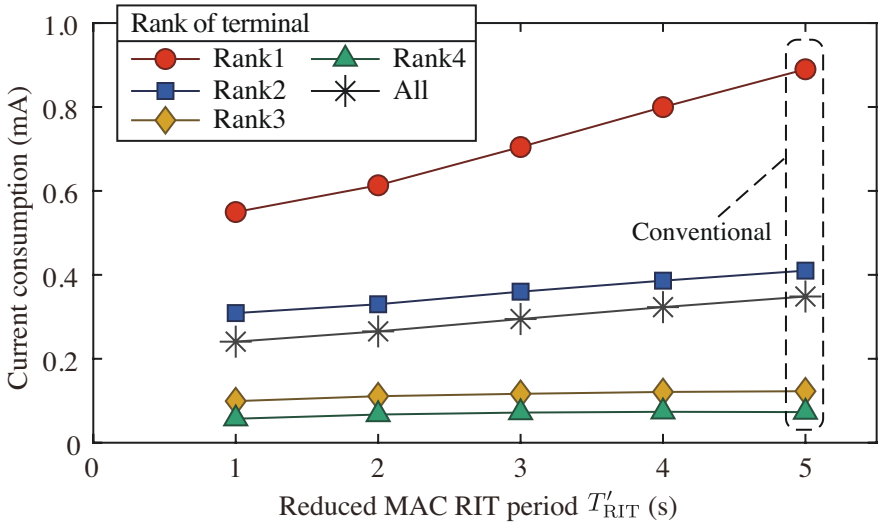

Figure 4.12: Current consumption characteristics as a function of reduced MAC RIT period T'_{RIT} when polling interval is 900 s. ©2021 IEICE

The system model and evaluation parameters are common with evaluations in Sects. 4.4 and 4.5. From evaluations in Sect. 4.4, it is revealed that a larger maximum number of additional addresses χ achieves better downlink delay and current consumption characteristics. Also, a smaller reduced MAC RIT period T'_{RIT} brings

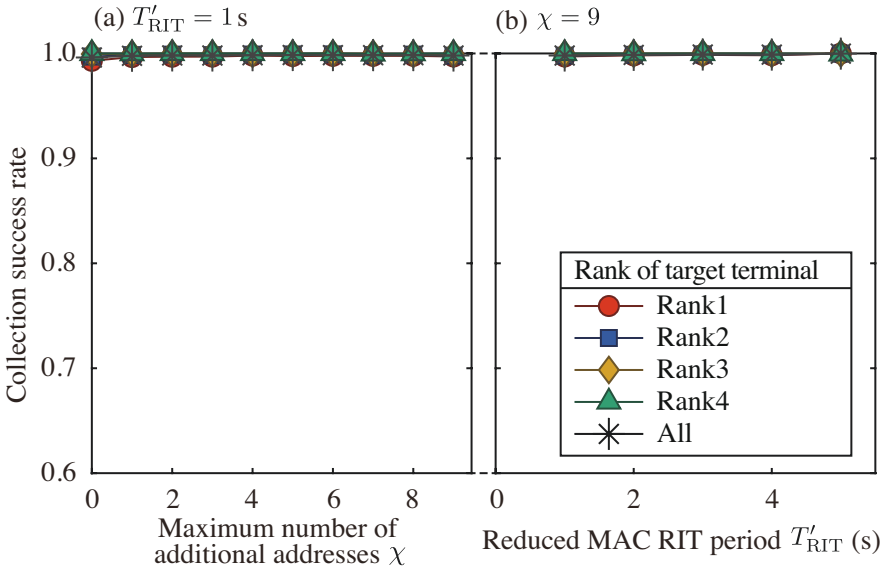

Figure 4.13: Collection success rate characteristics when polling interval is 900 s: (a) T'_{RIT} = 1 s, (b) χ = 9. ©2021 IEICE

on smaller round-trip delay and current consumption characteristics as discussed in Sect. 4.5. Therefore, we evaluate the case that the maximum number of additional addresses χ is 9 with various reduced MAC RIT periods T'_{RIT}, and the case that the reduced MAC RIT period T'_{RIT} is 1 s with various maximum number of additional addresses χ. In this section, the case of χ = 0 (i.e., the conventional scheme in Sect. 4.4) and T'_{RIT} = 5 s (i.e., the conventional scheme in Sect. 4.5) is referred to as the *conventional scheme*. In this section, the case of the polling interval of 900 s is discussed.

4.6.1. Evaluation Results of Collection Success Rate

The collection success rate characteristics when T'_{RIT} = 1 s and when χ = 9 are shown in Figs. 4.13(a) and 4.13(b), respectively. The collection success rate is averaged for the rank of the target terminal and all trials in this figure. In the average of all trials, the success rate of 99.5% is achieved under all parameters. This result shows that the high reliability of polling communications is achieved when both proposed schemes are adopted simultaneously.

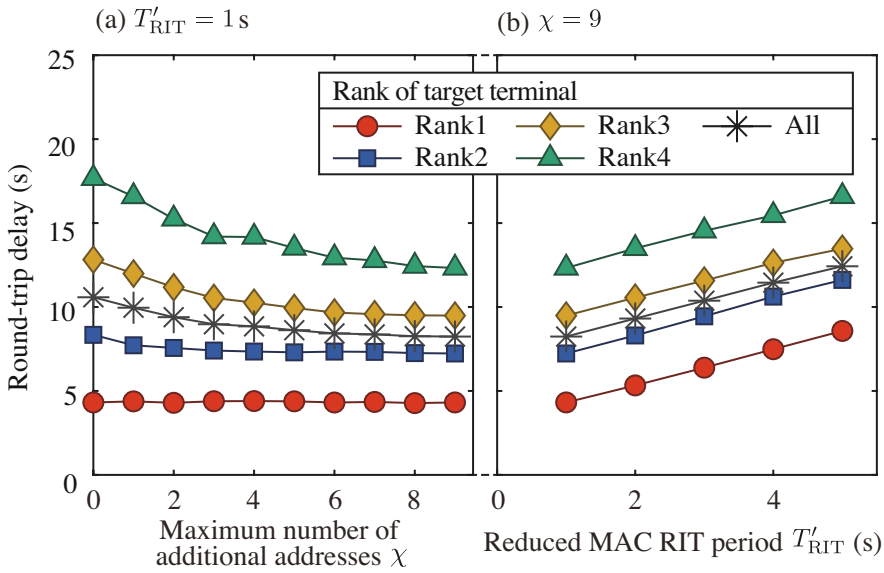

Figure 4.14: Round-trip delay characteristics when polling interval is 900 s: (a) T'_{RIT} = 1 s, (b) χ = 9. ©2021 IEICE

4.6.2. Evaluation Results of Delay

Figures 4.14(a) and 4.14(b) depict the round-trip delay characteristics of the cases that T'_{RIT} =1 s and χ =9, respectively. The round-trip delay is averaged for the rank of the target terminal and all trials. As discussed in Sects. 4.4 and 4.5, the delay is improved as the maximum number of additional addresses χ becomes larger and as the reduced MAC RIT period T'_{RIT} becomes smaller. When we focus on the average round-trip averaged for all trials, the round-trip delay is 14.7 s in the conventional scheme (i.e., χ = 0 and T'_{RIT} = 5 s) as shown in Fig. 4.10. Compared to that, the adoption of both proposed schemes improves the round-trip delay by 44.1% to 8.2 s when χ = 9 and T'_{RIT} = 1 s. This result means the combined use of the proposed schemes can fasten information collection from all terminals on a network. Not only the timeliness in automatic meter reading but also the effectiveness of the fieldwork using a handy terminal would be improved by the proposed schemes.

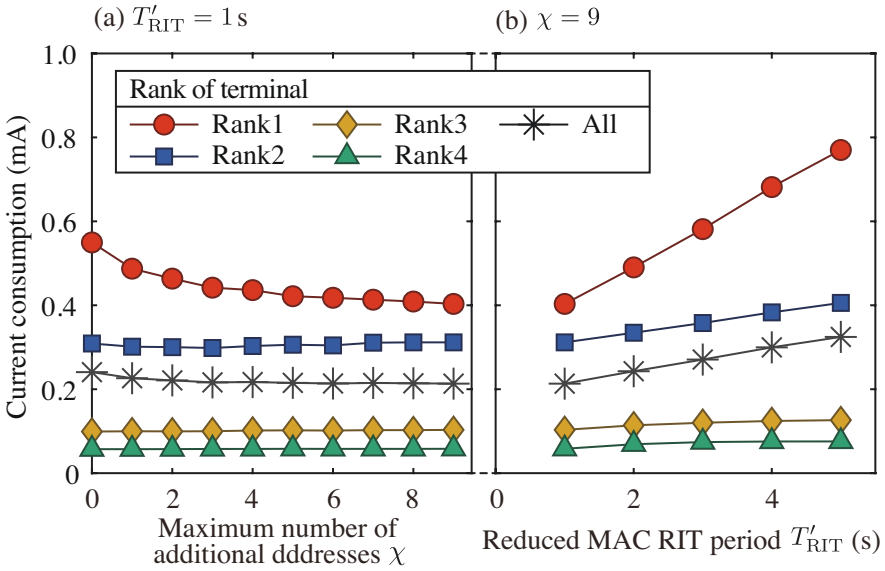

Figure 4.15: Current consumption characteristics when polling interval is 900 s: (a) T'_{RIT} = 1 s, (b) χ = 9. ©2021 IEICE

4.6.3. Evaluation Results of Current Consumption

The current consumption characteristics when T'_{RIT} = 1 s and χ = 9 are shown in Figs. 4.15(a) and 4.15(b), respectively. Here, the current consumption is averaged for terminals in each rank and all terminals except for the coordinator. The combined use of both proposed schemes is effective to reduce the current consumption. As shown in Fig. 4.12, the current consumption averaged for all terminals except for the coordinator is 0.35 mA in the conventional scheme (i.e., χ = 0 and T'_{RIT} = 5 s). Compared to that, the adoption of both proposed schemes reduces the current consumption by 38.7% to 0.21 mA when χ = 9 and T'_{RIT} = 1 s. The improvement appears clearly at terminals in rank 1 that should transfer many frames. In the conventional scheme, the current consumption of terminals in rank 1 is 0.89 mA as discussed in Sect. 4.5.4. It is improved by 54.7% to 0.40 mA in the case of χ = 9 and T'_{RIT} = 1 s that adopts the proposed schemes simultaneously. In general, the terminals near the coordinator runs out of its battery at first in multi-hop networks [94]. Therefore, the improvement of the current consumption in terminals with smaller ranks by the combined use of the proposed schemes is effective to extend the lifetime of the entire network. Alternatively, the proposed schemes enable more frequent data collection with limited batteries.

4.7 Conclusion

In this chapter, two schemes were proposed for efficient polling communications in multi-hop networks based on the F-RIT protocol. The first proposal, the enhanced source routing scheme, improves the delay and the current consumption by utilizing multiple routes based on the receiver-initiated operation in the MAC layer. Computer simulations were carried out and showed the effectiveness in improving the downlink delay and the current consumption. In the case that the polling interval was 900 s, the downlink delay for target terminals in rank 4 was improved by 41.3%, and the current consumption of terminals in rank 1 was improved by 13.5% when the maximum number of additional addresses χ was 9. The second proposal, the round-trip delay reduction scheme, can reduce the polling delay by setting a smaller transmission interval of RIT data request frames to wait for uplink communications. It was shown that the round-trip delay for terminals in rank 1 was improved maximum 49.7% by setting the reduced MAC RIT period T'_{RIT} to 1 s. Moreover, the combined use of the enhanced source routing scheme and the round-trip delay reduction scheme was proposed. By adopting the two proposed schemes when the polling interval was 900 s, the round-trip delay and the current consumption in average were improved by 44.1% and 38.7%, respectively.

Chapter 5
Enhanced F-RIT Protocol for High Traffic Bi-Directional Communications

5.1 Introduction

The capability for practical communication traffics is required in IoT systems. The evaluations in Chapters 3 and 4 do not consider the high traffic communications because there is little need for frequent communications on a device with a limited battery capacity in the usual time. However, AMI systems should support communications in times of emergencies (e.g., gas leak detection) and emergency operation of shut-off, in addition to the usual metering operation. In emergency communications, it is anticipated that the operation of several communication sessions per minute is required, unlike the several communications per one hour in usual. Also, such emergency communication requires bi-directional communication since the terminals transmit individually and the communication delay should be suppressed.

In a previous study, the communication performances of the conventional F-RIT protocol are evaluated focusing on the frequency of data transmissions [20]. This protocol is called the conventional F-RIT protocol in this chapter. In the evaluation, the conventional F-RIT protocol has been implemented into Wi-SUN modules, and its feasibility has been evaluated in terms of the transmission success rates and the power consumption in a one-way communication model [20]. That evaluation concluded that the conventional F-RIT protocol can achieve high transmission performance when the data generation rate is from 1.0×10^{-3} to 1.0×10^{-2} (s^{-1}), which indicates that the conventional F-RIT protocol can achieve several reliable communication sessions per hour. However, there are no evaluations of bi-directional RIT-based communications in high traffic environments assuming emergency situations.

In this chapter, the IEEE 802.15.4e-compliant conventional F-RIT protocol in the bi-directional communication model is evaluated by the computer simulations and experiments [30]. Firstly, Wi-SUN modules with bi-directional operation are

developed. The module is based on the IEEE 802.15.4/4g-compliant commercial Wi-SUN module with ARIB STD T-108 [6] and implements IEEE 802.15.4e-based conventional F-RIT protocol. Twenty Wi-SUN modules with the conventional F-RIT protocol (i.e., ten communication pairs) are set up in a radio anechoic chamber. To validate the measurement results, the same parameters of experimental equipment are applied to the computer simulator. The experimental and simulation results indicate that the conventional F-RIT protocol can achieve more than 90% transmission success rates in typical AMI systems operation environment. However, the transmission success rates decline as the traffic expands in the conventional F-RIT protocol and only about 60% of transmissions are succeeded when the data generation rate is 1.0×10^{-1} s^{-1} in both simulation and experimental evaluation.

To overcome the transmission success rate deterioration problem when the data generation rate is high for the emergency cases, the transmission failures in the F-RIT protocol is analyzed, and reveals that the timeout problem specific to RIT-based systems is the main factor of the transmission failures in the bi-directional communication model. This timeout problem occurs when the destination terminal is in the wait duration for the transmission mode as same as the sender, i.e., transmission deadlock incident occurs. Based on this analysis, an eF-RIT protocol is proposed to suppress the incident of the timeout problem when the data generation rate is high. The proposed eF-RIT protocol is evaluated and analyzed in the bi-directional communication model by the computer simulations and experiments as same as the IEEE 802.15.4e compliant F-RIT protocol. The measurement results show that the proposed eF-RIT protocol suppresses the incident of the timeout problem of 0.6% – 31%, and the transmission success rates increase from the conventional F-RIT protocol. Especially, when the data frame length is shorter than 20 ms and the data generation rate is smaller than 1.0×10^{-1} s^{-1}, the proposed eF-RIT protocol can achieve high transmission success rates of over 90%.

This chapter is organized as follows. Bi-directional communication characteristics of the conventional F-RIT protocol is evaluated by computer simulations and experiments in Sect. 5.2. In Sect. 5.3, the conventional F-RIT protocol is analyzed in detail to reveal the causes of the transmission success rate deterioration problem when the data generation rate is high. Then, to prove the problem of the conventional F-RIT protocol, the eF-RIT protocol is proposed. In Sect. 5.4, the proposed eF-RIT protocol is evaluated by computer simulations and experiments. Also, the proposed eF-RIT

protocol is analyzed in detail as same as the conventional F-RIT protocol and its effectiveness and feasibility are shown. Finally, Sect. 5.5 concludes this chapter.

5.2 Evaluations of Bi-Directional Transmission Performance of Conventional F-RIT Protocol

In this section, the bi-directional conventional F-RIT transmission performance characteristics are evaluated by computer simulations and experiments. The experimental evaluation is performed in a radio anechoic chamber by using the developed actual Wi-SUN RF modules equipped with the conventional F-RIT protocol to prove its effectiveness and feasibility. The measurement results are compared with simulation results for the validation of the experiments.

5.2.1. System Model

The bi-directional communication model for the evaluation in this chapter consists N terminals, i.e., $N/2$ communication pairs. Each terminal transmits data frames to its pair terminal based on the conventional F-RIT protocol. Since the system model uses a single channel for the operation, each communication pair has $(N/2-1)$ communication pairs that act as interference sources. Each terminal generates a data with a rate of λ that follows the Poisson distribution. When each terminal succeeds receiving the ACK frame after transmitting the data frame, this transmission of the data frame is judged as a success. In this evaluation, the capacity for the queueing is limited only one data frame, and if a terminal failed the transmission, it does not attempt the retransmission. The listening duration to wait for the RIT data request frame from the receiver is set equal to the MAC RIT period.

5.2.2. Conventional F-RIT Protocol Detail for Implementation

In this chapter, the lightweight F-RIT protocol (i.e., the conventional F-RIT protocol), which was designed in the works evaluating performance in interference environments with high data traffic [20], is used for evaluations. In the conventional F-RIT protocol for the implementation [20], two frames are appended to the communication sequence

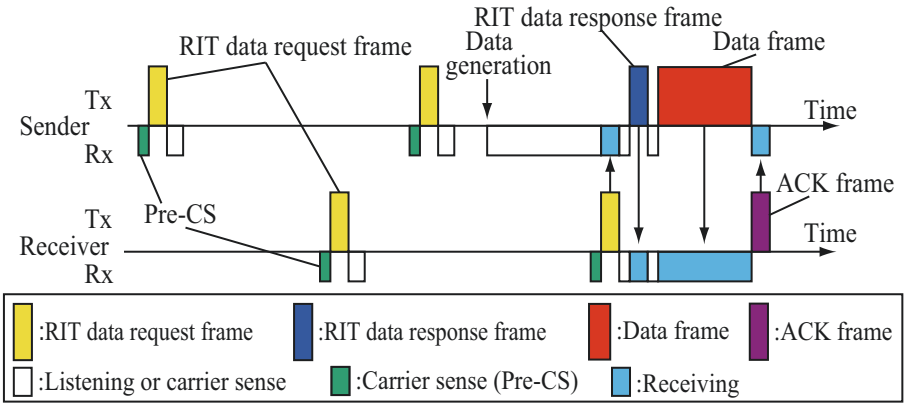

Figure 5.1: Overview of conventional F-RIT protocol for implementation. ©2018 IEICE

to evaluate the practical F-RIT protocol based on the IEEE standard MAC service. The overview of the conventional F-RIT protocol for the implementation is illustrated in Fig. 5.1. One is the RIT data response frame that is transmitted to reply to the RIT data request frame. The communication pair is established when the receiver accepts the RIT data response frame from the sender as shown in Fig. 5.1. In this chapter, the F-RIT protocol is developed based on IEEE 802.15.4/4e/4g [7], [17], [95], but IEEE 802.15.4-2015 [18] newly adopts the message sequence for the data transmission with the RIT data response command. The second is the ACK frame which is transmitted by the receiver that received the data frame correctly. The ACK frame confirms the successful reception and validation of the data [95], and it facilitates retransmission control in actual systems. The constitutions of all conventional F-RIT frames are shown in Fig. 5.2.

In the evaluations, the distance between each terminal is small and the hidden terminal does not exist. However, in realistic environments, the hidden terminal problem occurs [13]. It is reported that the collision between RIT data request frames and the data frame declines the transmission success rates. To take into the account of the hidden terminal problem, the conventional F-RIT protocol is evaluated in not only the mode performing the Pre-CS but also the mode ignoring the Pre-CS. The former mode is called Pre-CS ON, and the latter mode is called Pre-CS OFF. When the mode is Pre-CS OFF, the (N/2–1) communication pairs act as hidden terminals, and the transmission performance characteristics are the worst case of the hidden terminal problem occurrence in realistic environments.

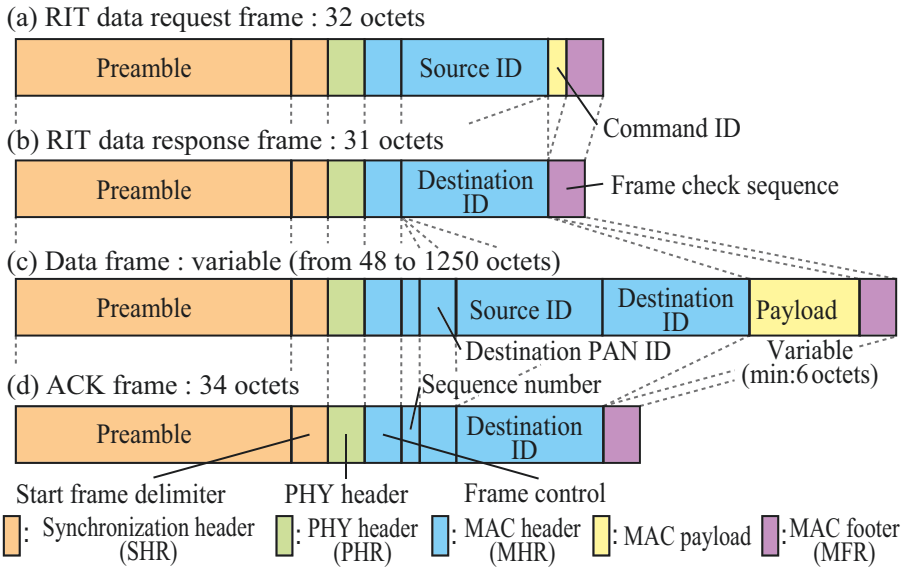

Figure 5.2: Constitutions of lightweight F-RIT frames. ©2018 IEICE

Table 5.1: Parameters for computer simulation.

Parameter	Values
Transmission rate	100 kbit/s
Pre-CS mode	ON, OFF
Number of terminals	20
Data generation rate	From 1.0×10^{-3} to 1.0×10^{-1} (s^{-1})
RIT data request frame length	2.56 ms
RIT data response frame length	2.48 ms
Data frame length	3.84, 20.0, 50.0, 100 (ms)
ACK frame length	2.72 ms
MAC RIT period	5.0 s
Pre-CS length	0.13 ms

5.2.3. Evaluation by Computer Simulations

Table 5.1 shows simulation parameters based on the implemented conventional F-RIT protocol. The data generation rate λ is set from 1.0×10^{-3} to 1.0×10^{-1} (s^{-1}). Typical AMI systems collect data frames more than one time per one hour, therefore the data generation rate of the evaluation satisfies this demand. The length of the data frame

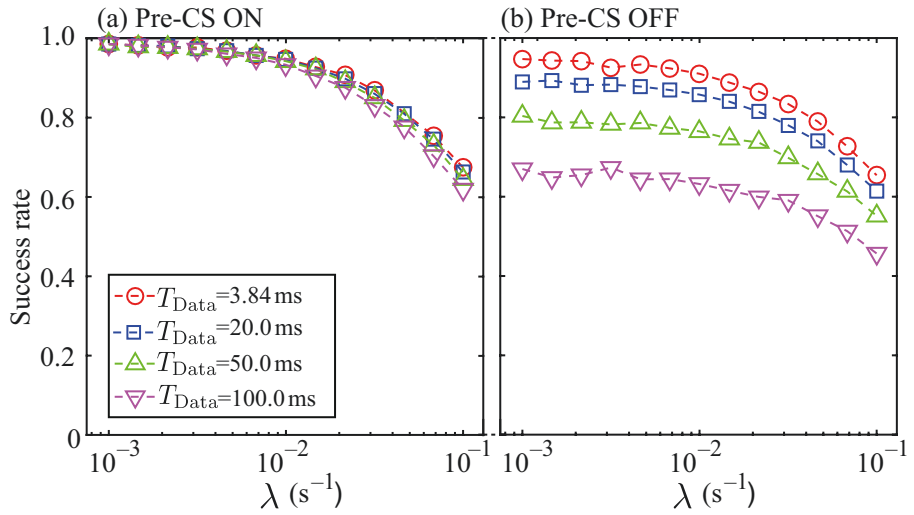

Figure 5.3: Transmission performance characteristics calculated by computer simulation. ©2018 IEICE

T_{Data} is set to 3.84, 20.0, 50.0 and 100 (ms). The data frame length in the computer simulation is set equal to the data frame length in the experimental evaluation as explained in Section 5.2.2. For example, the recommended maximum length of the PSDU is defined as 255 octets by ECHONET Lite [63], which is an application layer protocol for AMI in Japan. Therefore, T_{Data} of 20.0 ms is sufficient for practical AMI situations. The number of the terminals N is set to 20 because the report about the transmission performance of the AMI in a condominium [96] shows that the number of terminals in the direct communication area of the terminal located in a corner room is only 10 and a margin of 10 is considered.

Figure 5.3 shows the simulation results of the transmission success rate characteristics. The transmission success rate S is defined as follows:

$$S = n_{\mathrm{Success}}/(n_{\mathrm{Total}} - n_{\mathrm{Queue}}), \tag{5.1}$$

where n_{Success}, n_{Total} and n_{Queue} express for the number of transmission succeeds, the number of transmission trials, and the number of the data generations when a data frame is queued already, respectively. The transmission success rates decrease as the data generation rate increases regardless of whether the Pre-CS mode is ON or OFF when $\lambda > 1.0 \times 10^{-2}$ s^{-1}. Also, the transmission success rates decrease distinctly as the data frame length extends when the Pre-CS mode is OFF since the collision between the data frame and the RIT data request frame occurs. When the Pre-CS mode is ON,

Table 5.2: Specifications of Wi-SUN dongles.

Parameter	Values
USB dongle	Jorjin Technologies Inc. WSR35A1-00
RF module	ROHM Co., Ltd BP35A1
Host interface	UART (115,200 baud)
Wireless standard	Based on ARIB STD-T108
Modulation	2-GFSK
Wireless frequency	920 MHz band
Transmission rate	100 kbit/s
Transmission power	+20 mW
CS level	–77 dBm
Receiving sensitivity	–103 dBm (TYP.)(100 kbit/s, BER<0.1%)

the deterioration due to the data frame extension is improved. The simulation results indicate that the conventional F-RIT protocol can achieve transmission success rates highly at over 90% for all cases of the various data frame length when the Pre-CS mode is ON and $\lambda < 1.0 \times 10^{-2}$ s^{-1}. However, the transmission success rate declines as the traffic expands and only about 60% of the transmissions are in succeeds when $\lambda = 1.0 \times 10^{-1}$ s^{-1}.

5.2.4. Experimental Configuration

The conventional F-RIT protocol is implemented into the IEEE 802.15.4/4e/4g [7], [17], [95] compliant commercial Wi-SUN module with ARIB STD T-108 [6] compliant RF modules [20]. The specifications of the target Wi-SUN dongles are shown in Table 5.2. The overview of the implemented conventional F-RIT protocol and the constitutions of the conventional F-RIT frames are shown in Figs. 5.1 and 5.2, respectively. These frames are designed for the conventional F-RIT operation within the IEEE 802.15.4/4e. The payload length of the data frame is variable as shown in Fig. 5.2(c). The minimum length of the payload is defined by 6 octets for the performance measurement, i.e., the minimum length of the data frame is 3.84 ms. Experimental evaluation with variable data frame length can be performed by changing the payload length. The developed conventional F-RIT-based Wi-SUN modules are connected to a PC for the control via the USB interface.

Figure 5.4 shows the configuration of the experiment. The experimental platform consists of two experimental sets, i.e., experimental sets-A and -B operating in

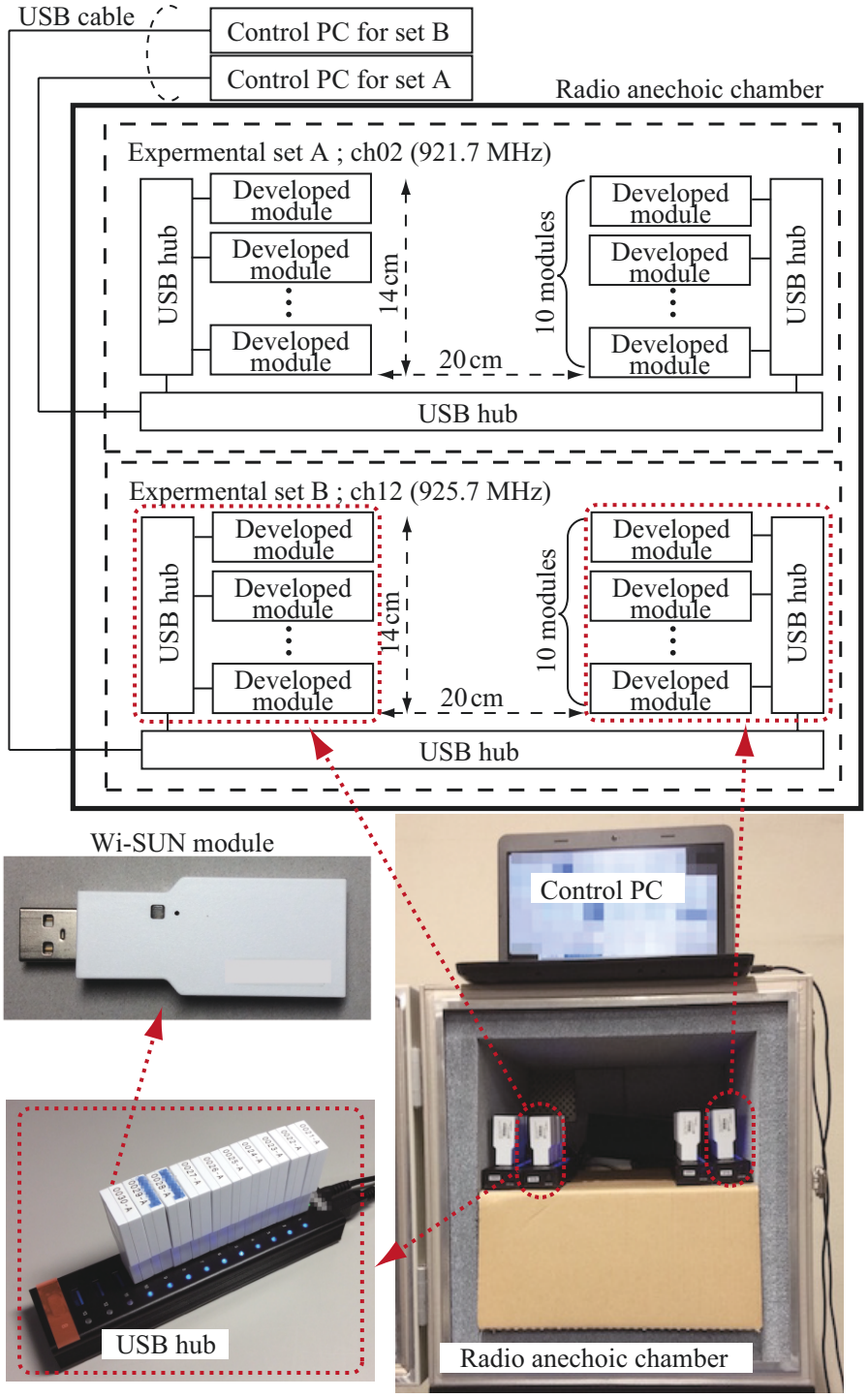

Figure 5.4: Configuration of experiments. ©2018 IEICE

channel-02 (center frequency is 921.7 MHz) and channel-12 (center frequency is 925.7 MHz), respectively. Each experimental set has ten communication pairs. These modules are set up in a radio anechoic chamber and controlled by the PCs via USB

Table 5.3: Parameters for experimental evaluation.

Parameter	Values
Transmission rate	100 kbit/s
Frequency	921.7, 925.7 (MHz)
Pre-CS mode	ON, OFF
Number of modules	20
Data generation rate	From 2.0×10^{-3} to 1.0×10^{-1} (s^{-1})
RIT data request frame length	2.56 ms
RIT data response frame length	2.48 ms
Data frame length	3.84, 20.0, 50.0, 100 (ms)
ACK frame length	2.72 ms
MAC RIT period	5.0 s

cables and hubs from the outside of the radio anechoic chamber. The distance between the communication pair terminals is set to 20 cm. The two experiments are performed in parallel using the two experimental sets. There is no inter-experimental sets interference because they are operated in different frequency channels.

5.2.5. Experimental Evaluation Results

Table 5.3 shows the parameters for the experimental evaluation. The conventional F-RIT protocol is evaluated in the various data frame size, the various data generation rate, and the Pre-CS mode of ON or OFF. The measurement results of the transmission success rate characteristics are shown in Fig. 5.5. By comparing with Figs. 5.3 and 5.5, it can be found that the differences in the transmission success rates between the experimental and simulation evaluations are within 5%. Especially, it appears that the measurement results of the transmission success rate characteristics tend to descend than the simulation results in the setting of parameters where achieve high transmission success rates. It is suspected that the control delay of the modules causes a little decline in the transmission success rates. Expect for these acceptable mismatches, the measurement results are almost the same as the simulation results.

The measurement results show that the transmission success rates of the conventional F-RIT protocol can be achieved over 90% when $\lambda<1.0\times10^{-2}$ s^{-1} and $T_{Data}<100$ ms. In the practical case, further reliable transmission can be expected because the re-transmission algorithm is applied in the systems. By the experimental evaluation, the effectiveness and feasibility of the conventional F-RIT protocol is shown when the traffic is not heavy. However, the deterioration of the transmission

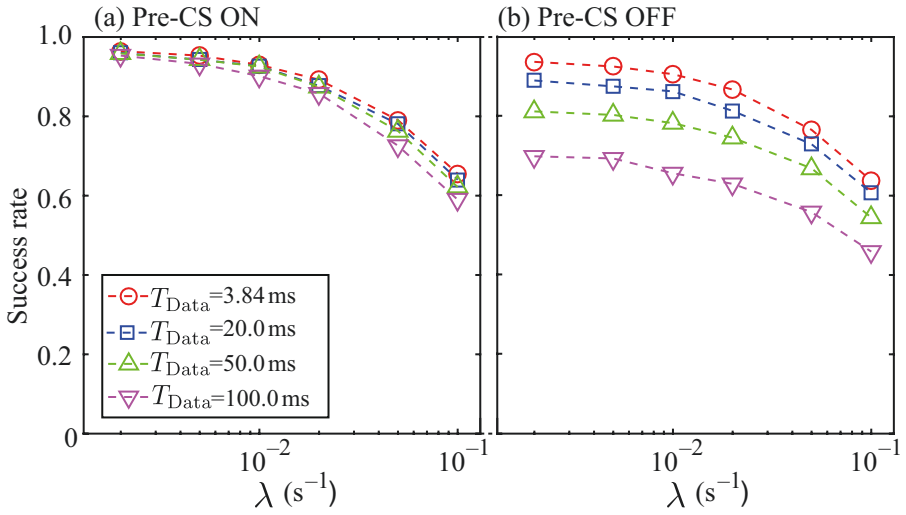

Figure 5.5: Experimental results of transmission performance characteristics in conventional F-RIT protocol. ©2018 IEICE

success rate depends on the data generation rate occurs as well as the results of the evaluations by computer simulations.

5.3 Proposed Enhanced F-RIT Protocol

In Sect. 5.2, the effectiveness and feasibility of the conventional F-RIT protocol are shown in the bi-directional communication environments when the traffic is not heavy like the usual gas AMI use cases. However, when the traffic is heavy (i.e., $\lambda=1.0\times10^{-1}$ s^{-1}) like the emergency cases of the gas AMI, it was found that the transmission success rate deteriorates. In this section, to overcome this problem, the factors of the transmission failures are extracted from the simulation and experimental results in Sect. 5.2, and it reveals the timeout problem incidents frequently in the conventional F-RIT bi-directional communication. Then, the eF-RIT protocol is newly proposed to suppress the incident of the timeout problem for the heavy traffic bi-directional communication use cases.

5.3.1. Classification of Transmission Characteristics in Conventional F-RIT Protocol

The factors of the transmission failures are extracted from the measurement results and analyzed to reveal the problem of the conventional F-RIT protocol. Firstly, the factors

of the transmission failures are classified into four categories, i.e., (A) Discarding data, (B) Carrier detection, (C) Timeout, and (D) No receiving ACK. The schematics of these failure factors are shown in Figs. 5.6(A), (B), (C) and (D), respectively.

(A) *Discarding data*: In this chapter, the capacity of the queue is set at one data frame length. Therefore, the data frame is discarded when the frame is generated before the transmission of an already queued data frame is judged as success or failure as shown in Fig. 5.6(A). This case is classified as the discarding data.

(B) *Carrier detection*: When any carriers are detected at the carrier sense process before the transmission of a data or RIT data response frame, the terminal suspends the transmission of the frame. As a result, the transmission is judged as failure as shown in Fig. 5.6(B). Of course, this failure factor can be removed by considering the re-transmission.

(C) *Timeout*: When the sender never receives the RIT data request frame from the receiver until the end of the listening duration of the MAC RIT period waiting for the RIT data request frame, the sender gives up the transmission of the data frame and stops listening. In this case, the transmission of the data frame is judged as a failure by the timeout as shown in Fig. 5.6(C).

(D) *No receiving ACK*: If the sender of a data frame cannot receive the ACK frame from the receiver due to the interference, the data frame is counted as the transmission failure as shown in Fig. 5.6(D).

5.3.2. Analyses of Transmission Failure Factors in Experimental Results

The incident rates of each above-mentioned failure factor in the measurement results are shown in Figs. 5.7, 5.8, 5.9, and 5.10. Incident rates from (A) to (D) are defined as follows:

$$p_{\mathrm{A}} = n_{\mathrm{A}}/n_{\mathrm{Total}}, \tag{5.2}$$

$$p_{\mathrm{B}} = n_{\mathrm{B}}/(n_{\mathrm{Total}} - n_{\mathrm{A}}), \tag{5.3}$$

$$p_{\mathrm{C}} = n_{\mathrm{C}}/(n_{\mathrm{Total}} - n_{\mathrm{A}}), \tag{5.4}$$

$$p_{\mathrm{D}} = n_{\mathrm{D}}/(n_{\mathrm{Total}} - n_{\mathrm{A}}), \tag{5.5}$$

where n_{A}, n_{B}, n_{C} and n_{D} express for each number of incidents of (A), (B), (C), and (D), respectively. Figure 5.7 shows the incident rate characteristics of the discarding data. The rates increase as the data generation rate increases. In the experiment, the transmission failure due to the discarding data occurs frequently since the capacity of

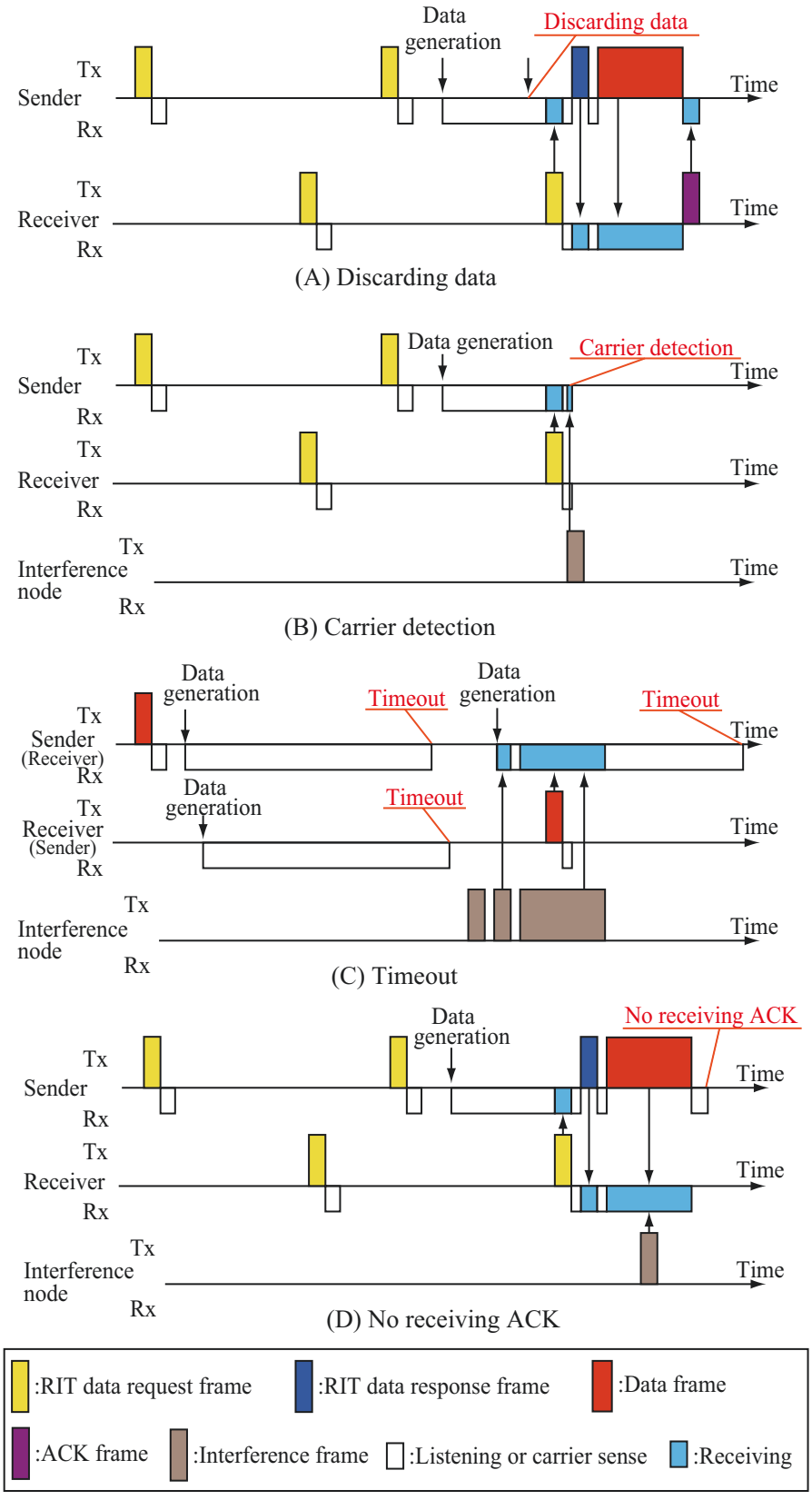

Figure 5.6: Factors of transmission failures in conventional F-RIT protocol. ©2018 IEICE

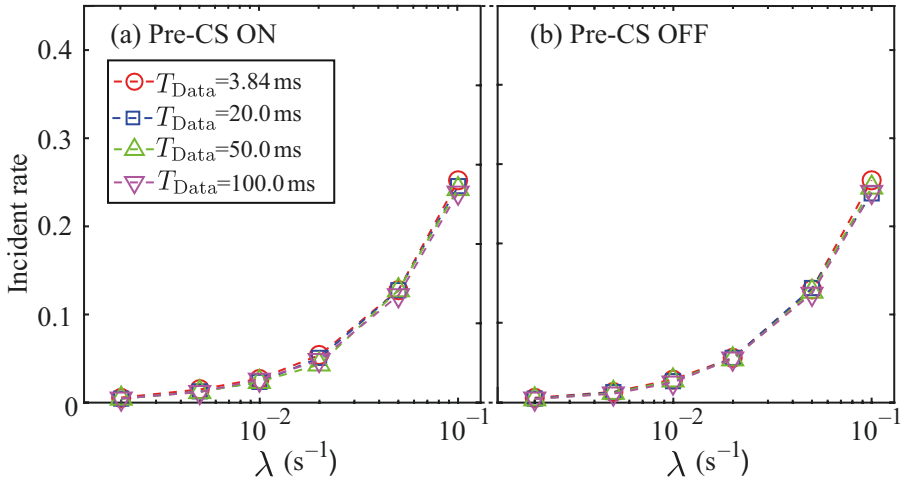

Figure 5.7: Incident rate of discarding data in conventional F-RIT protocol. ©2018 IEICE

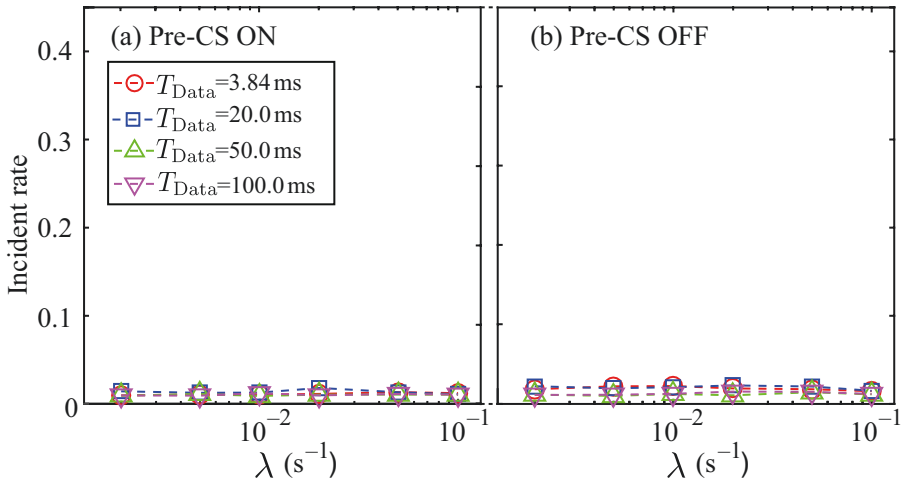

Figure 5.8: Incident rate of carrier detection in conventional F-RIT protocol. ©2018 IEICE

the queue is limited to only one data frame length. In practical systems, incidents of the discarding data can be reduced by expanding the queue capacity limitation. As shown in Fig. 5.8, the incident rates of the transmission failures due to the carrier detection are up to 2.0%. The rates have almost no correlation depending on the data frame length and the data generation rate.

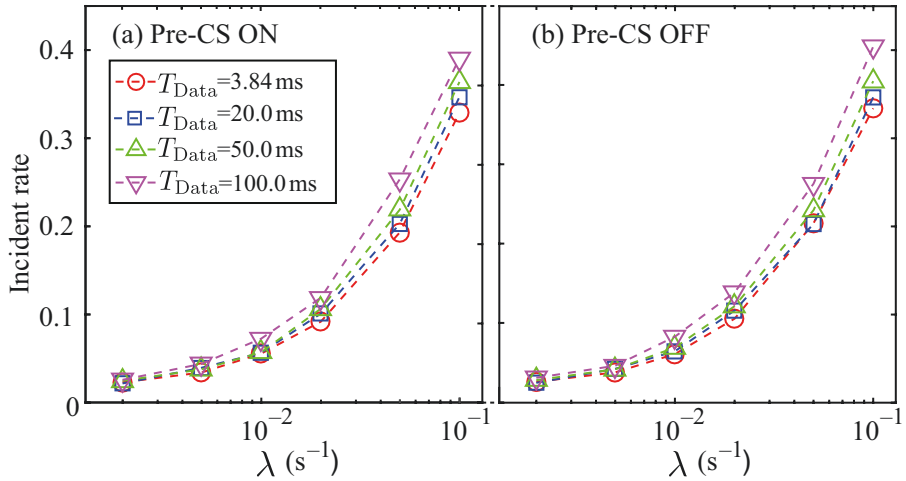

Figure 5.9: Incident rate of timeout in conventional F-RIT protocol. ©2018 IEICE

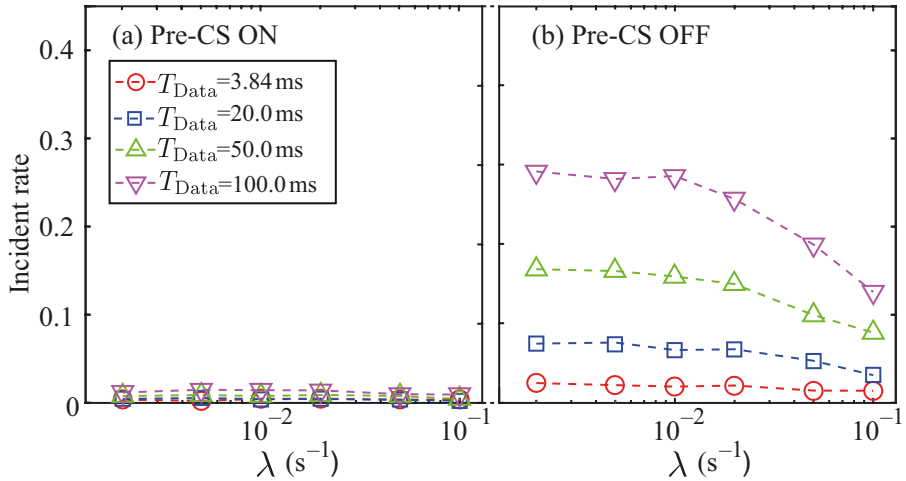

Figure 5.10: Incident rate of no receiving ACK in conventional F-RIT protocol. ©2018 IEICE

Figure 5.9 shows the incident rate characteristics of the timeout. The rates increase rapidly as the data generation rate increase when the Pre-CS mode is both ON and OFF. The timeout problem occurs due to the absence of the RIT data request frame from the destination terminal. It often occurs when the destination terminal is in the wait duration and it does not send the RIT data request frame. The deadlock of the transmission occurs in the case, and the incident of the case occurs depending on the data generation rate. Another reason for the absence of the RIT data request frame is

channel occupancy by interference frames. Therefore, the incident rates of the timeout also increase a little when the channel busy rates become large, i.e., the case of the data frame length extends because the chance to exchange the RIT data request frame is reduced. The timeout problem also occurs when the data traffic is not heavy. For example, the incident rate of the timeout is 2.3% when the Pre-CS mode is ON, λ=2.0 $\times 10^{-3}$ s^{-1}, T_{Data}=3.84 ms, and this accounts for around 65% of the factors of the transmission failures excluding the discarding data.

As shown in Fig. 5.10, when the Pre-CS mode is ON, the incident rates of the no receiving ACK are 0.2% to 1.5%. However, when the Pre-CS mode is OFF, the incident rates of the no receiving ACK tend to increase as the data frame length extends. The incident rates of the no receiving ACK are affected by the incident of the timeout, but the rates are roughly proportional to the data frame length. This result indicates that the transmission success rates would decline if the data frame length extends in realistic systems with hidden terminals. The worst value of the deterioration rates due to the hidden terminal problem is almost the same as the incident rates of the no receiving ACK when the Pre-CS mode is OFF. From the above analyses about the transmission failure factors in the measurement results, it is revealed that the main factor of the transmission failure is the timeout in the IEEE 802.15.4e compliant conventional F-RIT protocol.

5.3.3. Proposed eF-RIT Protocol

In the conventional F-RIT protocol complied with the IEEE 802.15.4e, a terminal cannot receive the data frame to oneself when it has a data frame to transmit and this behavior results to occur the timeout problem. This problem occurs because the terminal in the listening state of waiting for the RIT data request frame from the destination terminal does not transmit the RIT data request frame as shown in Fig. 5.11(a). The transmission failure may decrease the communication reliability or expand the delay and the power consumption. This problem especially occurs when two terminals communicate with each other as in Fig. 5.11(a), but it also occurs in the tree and mesh topology systems.

To resolve this problem, the eF-RIT protocol is proposed [30]. In the proposed protocol, the terminal that attempts to transmit its data frame to any terminal stops the listening and transmits an RIT data request frame when the timing to transmit an RIT data request frame arrives as shown in Fig. 5.11(b). If a terminal transmits its data frame after the transmitting of an RIT data request frame, the terminal receives the

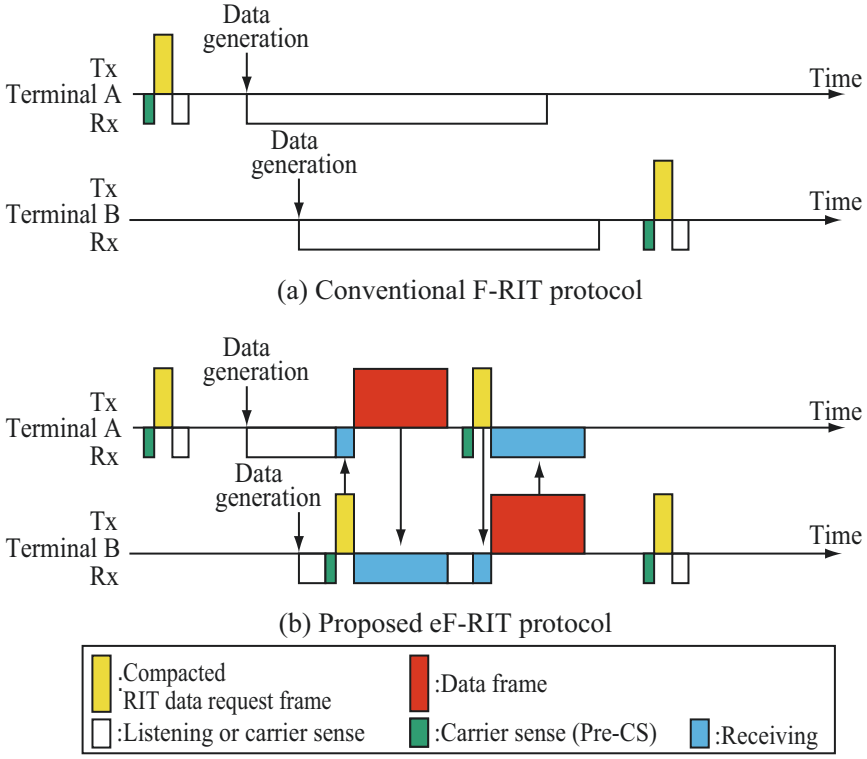

Figure 5.11: Comparison of conventional F-RIT protocol and proposed eF-RIT protocol. ©2018 IEICE

frame and it starts the listening again after the communication. If no terminal transmits the data frame, the terminal immediately starts the listening after the transmission of an RIT data request frame. Namely, the terminal in operation as a sender acts as a receiver for a short time. By this process, the transmission of the data frame to the terminal that has a data frame is achieved. In the proposed protocol, there is a possibility of missing the transmission opportunity as a sender by transmitting an RIT data request frame. However, the transmission time of an RIT data request frame as a receiver is sufficiently smaller than the waiting time to receive an RIT data request frame as a sender. In other words, it is expected that the opportunity to provide the communication chances by resolving the deadlock of the sender operation is larger than the case that the sender misses the transmission chances by inserting the operation as a receiver during the sender operation by waiting for the RIT data request frame from the destination terminal. Therefore, the proposed eF-RIT protocol can improve the transmission reliability by suppressing the frequency of communication failures that occurs depending on the state of the receiver. Since the proposed eF-RIT protocol

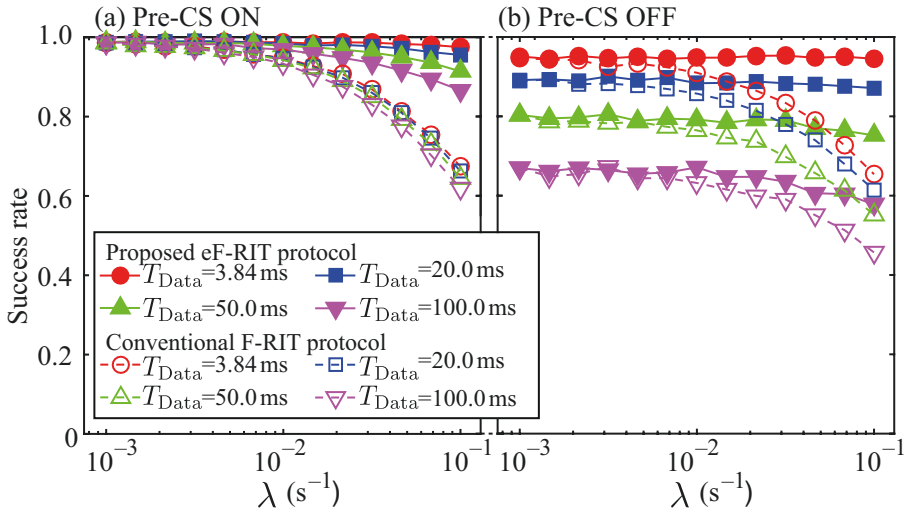

Figure 5.12: Transmission performance characteristics calculated in proposed eF-RIT and conventional F-RIT protocols. ©2018 IEICE

provides extra communication opportunities compared to the comventional F-RIT protocol, it is highly compatible with the conventional protocol, and also can be interconnected.

5.4 Evaluations of Bi-Directional Transmission Performance of Proposed eF-RIT Protocol

In this section, the proposed eF-RIT protocol is evaluated as same as the IEEE 802.15.4e compliant conventional F-RIT protocol. The evaluations reveal the effectiveness and feasibility of the proposed protocol.

5.4.1. Computer Simulation Results

The proposed eF-RIT protocol is evaluated by computer simulations as same as the evaluation of the conventional F-RIT protocol by computer simulations in Sect. 5.2.3. The simulation parameters are the same as the conventional F-RIT protocol and shown in Table 5.1. Figure 5.12 shows the computer simulation results of the transmission success rate characteristics of the conventional and proposed eF-RIT protocols. The transmission success rate S is defined in (5.1). In the proposed eF-RIT protocol, the deterioration due to the data generation rate increase is lessened from the conventional

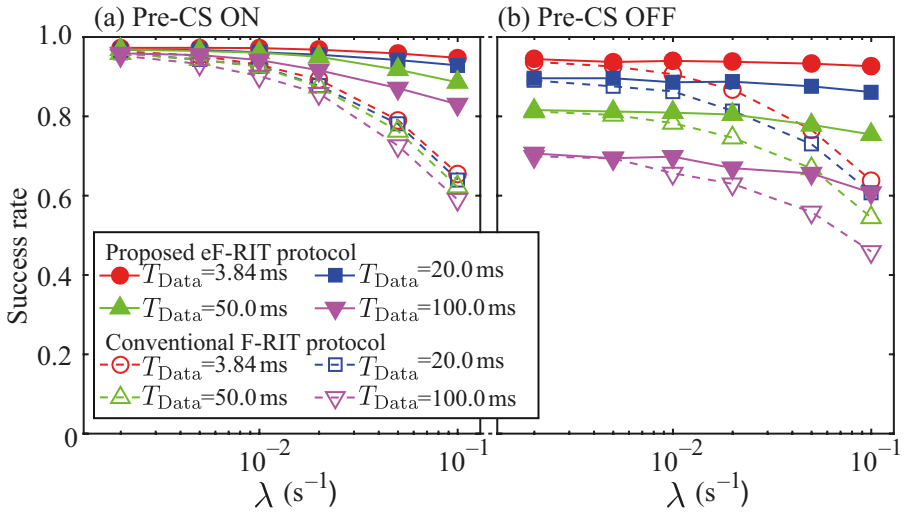

Figure 5.13: Experimental results of transmission performance characteristics in proposed eF-RIT protocol and conventional F-RIT protocols. ©2018 IEICE

F-RIT protocol. The proposed eF-RIT protocol achieves higher transmission success rates than the conventional F-RIT protocol and expands the data generation rate where the transmission success rates are higher than 90% to $\lambda<5.0\times10^{-2}$ s^{-1}.

5.4.2. Experimental Evaluation Results

Experimental evaluations are carried out in order to prove the feasibility of the proposed eF-RIT protocol as the same as the conventional F-RIT protocol in Sects. 5.2.5 and 5.3.2. The experimental configuration and the parameters for the evaluations are shown in Fig. 5.4 and Table 5.3, respectively. The measurement results of the transmission success rate characteristics are shown in Fig. 5.13. The differences of the transmission success rates between the simulation and experimental results are within 5% as same as the conventional F-RIT protocol. The measurement results prove that the proposed eF-RIT protocol can achieve over 90% of the transmission success rate when $\lambda<2.0\times10^{-2}$ s^{-1} and $T_{Data}<100$ ms. If the data frame length is limited shorter than 20 ms, the transmission success rates over 90% is achieved when $\lambda<1.0\times10^{-1}$ s^{-1}. In all measured data generation rate and data frame length, the proposed eF-RIT protocol achieved a superior success rate than the conventional F-RIT protocol. When $\lambda=1.0\times10^{-1}$ s^{-1} and the Pre-CS mode is ON, the proposed eF-RIT protocol improves the transmission success rates of 24% – 28 % from the conventional F-RIT protocol.

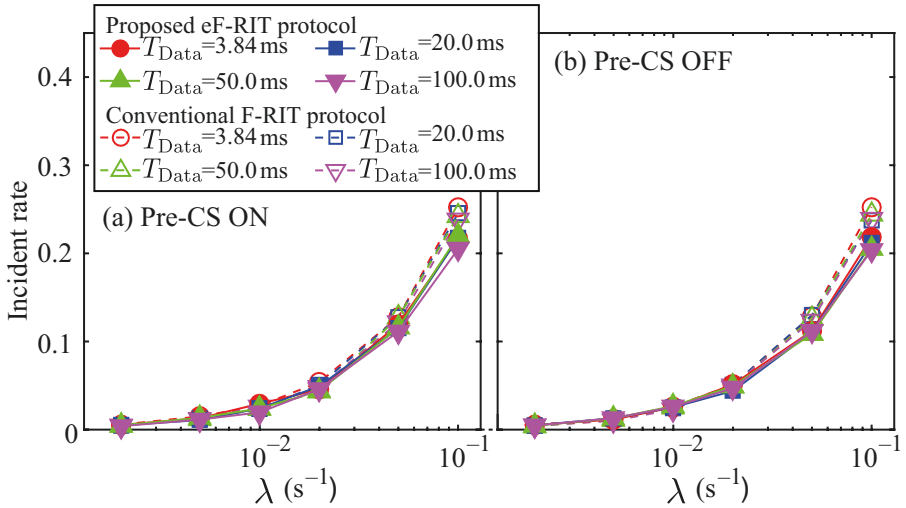

Figure 5.14: Incident rate of discarding data in proposed eF-RIT and conventional F-RIT protocols. ©2018 IEICE

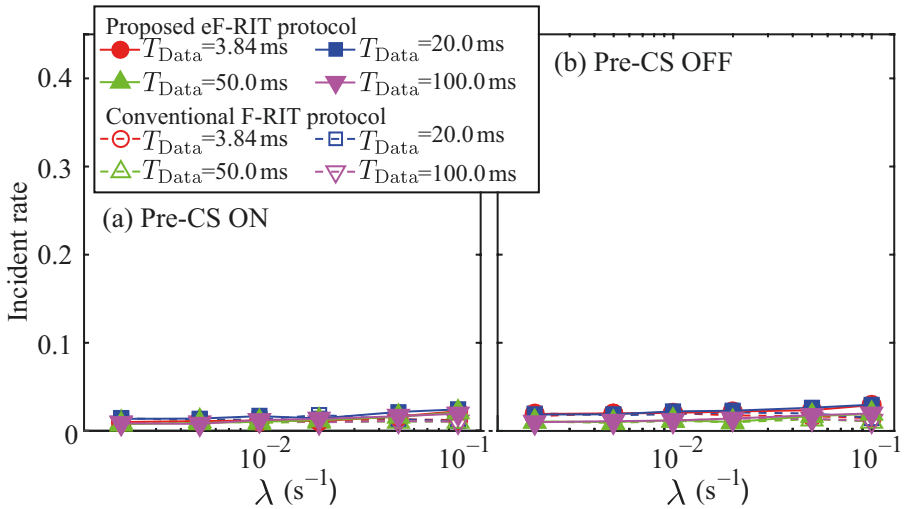

Figure 5.15: Incident rate of carrier detection in proposed eF-RIT and conventional F-RIT protocols. ©2018 IEICE

5.4.3. Analyses of Transmission Failure Factors in Experimental Results

The incident rates of each failure factor in the measurement results are shown in Figs. 5.14, 5.15, 5.16, and 5.17. Incident rates from (A) to (D) are as same as defined

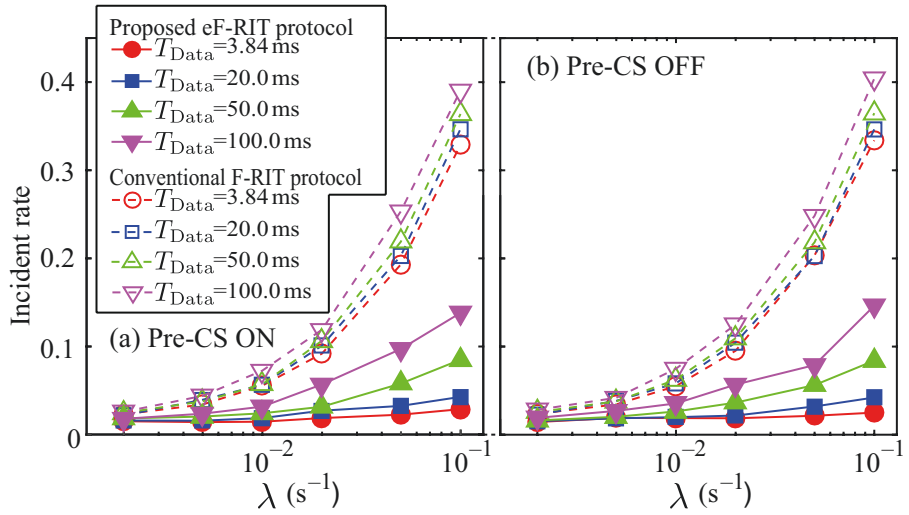

Figure 5.16: Incident rate of timeout in proposed eF-RIT and conventional F-RIT protocols. ©2018 IEICE

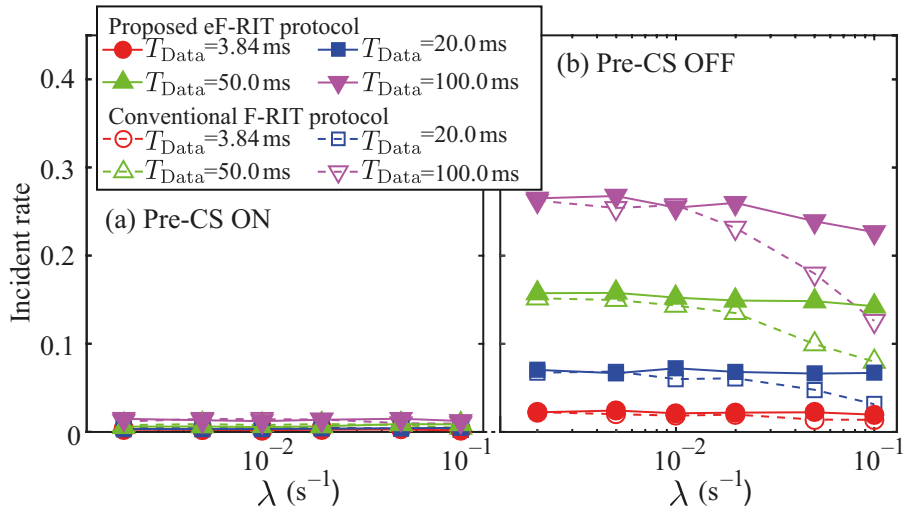

Figure 5.17: Incident rate of no receiving ACK in proposed eF-RIT and conventional F-RIT protocols. ©2018 IEICE

in (5.2), (5.3), (5.4), and (5.5). The incident rate characteristics of the discarding data are shown in Fig. 5.14. The trends of the proposed eF-RIT protocol and the conventional F-RIT protocol are almost the same and the rates increase as the data generation rate increases, but the incident rates decline a little in the proposed eF-RIT protocol since the wait duration of the transmission is shorter than the conventional F-

RIT protocol. Figure 5.15 shows the incident rates of the transmission failures due to the carrier detection. The incident rates in the proposed eF-RIT protocol are up to 3.0% and the trend is the same as the conventional F-RIT protocol.

Figure 5.16 shows the incident rate characteristics of the timeout. The reductions in the incident rates of the timeout by introducing the proposed eF-RIT protocol instead of the conventional F-RIT protocol are 0.6% – 31%, and the improvement effect is remarkable when the data generation rate is high. As illustrated in Fig. 5.17, when the Pre-CS mode is ON, the incident rates of the no receiving ACK are 0.1% to 1.5% in the proposed eF-RIT protocol. When the Pre-CS mode is OFF, the incident rates of the no receiving ACK tend to increase as the data frame length extends in the proposed eF-RIT protocol as same as the conventional F-RIT protocol. The incident rates of the no receiving ACK are affected by the incident of the timeout, and the incident rates of the No receiving ACK tend to increase in the proposed eF-RIT protocol than the conventional F-RIT protocol. This occurs since more data frames are transmitted due to the suppression of the timeout problem in the proposed eF-RIT protocol than the conventional F-RIT protocol.

From the above analyses about the transmission failure factors in the measurement results of the proposed eF-RIT protocol, it is revealed that the proposed eF-RIT protocol can reduce the incidents of timeout problem by up to about 31% when the traffic is heavy.

5.5 Conclusion

In this chapter, the conventional F-RIT protocol is evaluated in the bi-directional communication scenario by the computer simulations and the experiments. The measurement results showed that the conventional F-RIT protocol can achieve over 90% transmission success rates under the practical AMI specified conditions, but the transmission success rates decline to about 60% in high traffic environments like the emergency communication cases in AMI systems. Detailed analyses revealed that the timeout problem occurs frequently in high traffic environments due to the deadlock problem between communication pairs. To overcome the problem, the eF-RIT protocol was proposed. The proposed eF-RIT protocol offers improved transmission performance over the conventional F-RIT protocol, especially in high traffic environments. The proposed eF-RIT protocol could reduce the occasions of the timeout problem by up to 31% from the conventional F-RIT protocol. When the data

generation rate λ was 1.0×10^{-1} s^{-1} and the Pre-CS mode was ON, the proposed eF-RIT protocol improved the transmission success rates by up to 28% than the conventional F-RIT protocol. The proposed eF-RIT protocol achieved transmission success rates over 90%, for data frame lengths shorter than 20 ms when the Pre-CS mode is ON and $\lambda < 1.0 \times 10^{-1}$ s^{-1}.

Chapter 6
Conclusions

This thesis has focused on wireless mesh networks for IoT based on the receiver-initiated MAC protocol with efficient bi-directional communications. With the aim of contributing to the practical IoT networks, this thesis presented a two-stage discussion. First was the evaluation and analysis of the concrete standardized protocol. Second was the communication performance enhancement focusing on the practical communication traffics. Especially, the second topic was divided into two subtopics based on the traffic pattern: efficient data collections in the usual time and high traffic communications in the urgent time.

In Chapter 2, various wireless technologies related to IoT systems were discussed. In particular, regarding the low-power wireless mesh networks based on receiver-initiated MAC protocols, its principle, various research approaches, and standardization for practical use were introduced in detail. Through comparison with various technologies, it was emphasized that receiver-initiated MAC protocols have peculiar characteristics not only in terms of reducing power consumption but also in selecting a communication destination in a wireless mesh network.

In Chapter 3, the JUTA F-RIT protocol, which was a protocol complied with the Wi-SUN JUTA profile, was studied comprehensively for the feasibility study. One-way communications in an environment with multiple interference terminals were considered, and theoretical analysis focusing on the results of the carrier sense was developed. Also, the JUTA F-RIT protocol was evaluated by computer simulations and experiments with developed Wi-SUN dongles. The evaluation results proved the feasibility of the Wi-SUN JUTA F-RIT protocol to achieve a high transmission success rate in the interference environment. Furthermore, the characteristics of the JUTA F-RIT protocol was discussed in terms of frame transmission characteristics and timeout incidents. It was found that collisions often occurred even if the carrier was assessed as clear at the carrier sense compared to the case of the carrier detection, and the collision problem sometimes caused the continuous timeout incidents.

The efficient polling communications for the low-delay and low-power consumption data collections were presented in Chapter 4. To achieve efficient polling

communications by shortening delay, two schemes were proposed. First was the enhanced source routing scheme that enables the use of potential receivers in downlink communications. Second was the round-trip delay reduction scheme that can reduce the uplink delay by setting the reduced MAC RIT period temporarily focusing on the bi-directionality of polling communications. Two proposed schemes were designed independently and can be applied simultaneously. Computer simulation results showed that the combined use of the two proposed schemes achieved the low-delay and low-power polling communications.

In Chapter 5, the eF-RIT protocol was proposed to achieve high traffic bi-directional communications for emergency cases. Firstly, the conventional F-RIT protocol was evaluated in a bi-directional communication scenario by computer simulations and experiments with the developed dongles. Then, the experimental results were analyzed in detail, and it was shown that the timeout incident due to the deadlock of sender operation in both terminals in a communication pair was a cause of the transmission success rate failure in a high traffic environment. The proposed eF-RIT protocol solved the problem by transmitting the RIT data request frame in the Tx wait duration, i.e., the receiver operation was weaved in the sender operation to prevent the communication deadlock. The proposed eF-RIT protocol was evaluated by computer simulations and experiments as the same as the conventional F-RIT protocol. The results showed the feasibility of the proposed protocol under a high traffic environment.

From the above researches, the basic transmission characteristics of a receiver-initiated transmission MAC protocol and enhancements of its bi-directionality for practical data traffics were shown. Especially, the challenges on the enhancements of bi-directionality were coped with maintaining the asynchronousness of the RIT protocol and providing additional communication opportunities. Namely, the ideas to improve the communication characteristics in this thesis can be summarized in the enhancement of the ad-hocness of the protocol. The results showed that transmission characteristics based on an asynchronous MAC protocol can be improved with a simple approach. The author considers the low-power wireless mesh network that deals with bi-directional traffic both in usual and emergency cases can be achieved based on the concrete MAC protocol by combining these researches.

As a future work, there is still a need to improve the performance in the PHY and MAC layers. For the PHY layer, not only the OFDM with higher data rates has been standardized in the IEEE 802.15.4x, the FSK with higher data rates are being discussed.

Also, spectrum utilization is becoming more important as the spreading of IoT systems, and condition-aware communications employing the spectrum resource information by the SRM in the IEEE 802.15.4s can be a solution. The author considers the ad-hocness of the receiver-initiated MAC protocols is useful for proper implementation of such technologies even in low-performance terminals. For example, loading spectrum information for link control on the sequential frame exchange of the U-Bus Air may be effective. By adopting the faster modulation that can be achieved depending on the link state, it may be possible to reduce the current consumption due to the shorter frame transmission time. Since there is a certain amount of uncertainty in wireless communications, the author considers that there are cases where the less and looser controlled way like the receiver-initiated MAC protocol can provide a better solution.

Moreover, integration with various IoT systems is also an important work. Smart metering systems, which have been developed separately for electricity, gas, and water, can be integrated in the future. Trials are also being made to accommodate other applications like water level monitoring in the river on smart metering systems. Although these applications use fixed IoT terminals, a dense mesh network consists of fixed terminals has the potential to accommodate mobile IoT terminals such as wearable sensors. For such integrated IoT systems, it is necessary to build a network from various terminals including existing ones, and to allow the coexistence of various protocols. The ad-hocness of the receiver-initiated MAC protocols, that a receiver has the initiative of communication, can be a good solution for low-performance or mobile terminals. In terms of the coexistence of protocols, it is easy to connect a terminal operating with a receiver-initiated MAC protocol by simply sending a beacon and performing an appropriate receiving at the terminal that bridges the different systems. For such deployments, there is a need to develop functions like topology management to accommodate various terminals seamlessly.

In this way, the receiver-initiated MAC protocol and its ad-hocness may be adopted in various and advanced wireless applications although the current main deployment scenario is for gas and water smart metering. The bi-directionality to connect terminal in an efficient way would be still important in various applications. The author hopes that the discussions in this thesis to enhance the bi-directionality of communications will support future wireless access technologies.

Bibliography

[1] H. Harada, K. Mizutani, J. Fujiwara, K. Mochizuki, K. Obata, and R. Okumura, "IEEE 802.15.4g based Wi-SUN communication systems," *IEICE Trans. Commun.*, vol.E100-B, no. 7, pp. 1032–1043, Jul. 2017.

[2] K. Akabane, N. Mochizuki, S, Teruhi, M. Kobayashi, S, Yoshino, M. Shimizu, and K. Uehara, "High-capacity wireless access networks using 920 MHz band for wide-area IoT/M2M services," *IEICE Trans. Commun.*, vol. E99-B, no. 9, pp. 1920–1929, Sept. 2016.

[3] M. Chen, Y. Miao, H. Yixue, and K. Hwang, "Narrow band Internet of things," *IEEE Access*, vol. 5, pp. 20557–20577, Sept. 2017.

[4] A. Lavric, A. I. Petrariu, and V. Popa, "Long range SigFox communication protocol scalability analysis under large-scale, high-density conditions," *IEEE Access*, vol. 7, pp. 35816–35825, Mar. 2019.

[5] F. Adelantado, X. Vilajosana, P. Tuset-Peiro, B. Martinez, J. Melia-Segui, and T. Watteyne, "Understanding the limits of LoRaWAN," *IEEE Commun. Mag.*, vol. 55, no. 9, pp. 34–40, Sept. 2017.

[6] Association of Radio Industries and Business, "920 MHz-Band Telemeter, Telecontrol and Data Transmission Radio Equipment ARIB STD-T108 Version 1.3," Apr. 2019.

[7] IEEE Computer Society, "IEEE Std 802.15.4g^{TM}-2012," Apr. 2012.

[8] M. Carratù, M. Ferro, V. Paciello, A. Pietrosanto, and P. Sommella, "Performance analysis of wM-Bus networks for smart metering," *IEEE Sensors Journal*, vol. 17, no. 23, pp. 7849–7856, Dec. 2017.

[9] Japan Utility Telemetering Association, "U-Bus Air communications specification draft ver. 2.0," Jun. 2012 (in Japanese).

[10] Japan Utility Telemetering Association, "U-Bus Air functions specification draft ver. 1.1," Aug. 2012 (in Japanese).

[11] Japan Utility Telemetering Association, http://www.teleme-r.or.jp/index.html

[12] X. Fafoutis, A. D. Mauro, M. D. Vithanage, and N. Dragoni, "Receiver-initiated medium access control protocols for wireless sensor networks," *Computer Networks*, vol. 76,

pp. 55–74, Jan. 2015.

[13] D. Kominami, M. Sugano, M. Murata, and T. Hatauchi, “Energy-efficient receiver-driven wireless mesh sensor networks,” *Sensors*, vol. 11, no. 1, pp. 111–137, Dec. 2011.

[14] T. Hatauchi, Y. Fukuyama, M. Ishii, and T. Shikura, “A power efficient access method by polling for wireless mesh network,” *IEEJ Trans. EIS*, vol. 128, no. 12, pp. 1761–1766, Dec. 2008 (in Japanese).

[15] T. Hatauchi, “PHY and MAC proposals for battery-operated SUN,” doc.: IEEE 802.15-09-0285-00-004g, May 2009, https://mentor.ieee.org/802.15/dcn/09/15-09-0285-00-004g-mac-and-phy-proposal-for-802-15-4g- for-smart-utility-networks.ppt

[16] F. Kojima, H. Harada, T. Hatauchi, M. Tanabe, K. Sakamoto, A. Kashiwagi, T. Banno, and H. Nishiyama, “MAC proposals for low-power consumption,” doc.: IEEE 802.15-09-0514-00-004e, Jul. 2009, https://mentor.ieee.org/802.15/dcn/09/15-09-0514-00-004e-mac-proposals-for-low-power-consumption.pdf

[17] IEEE Computer Society, “IEEE Std 802.15.4e™-2012,” Apr. 2012.

[18] IEEE Computer Society, “IEEE Std 802.15.4™-2015,” Dec. 2015.

[19] J. Fujiwara, H. Harada, T. Kawata, K. Sakamoto, S. Tsuchiya, and K. Mizutani, “An ultra-low power consumption MAC protocol complied with IEEE 802.15.4/4e for wireless smart utility networks,” *IEEJ Trans. EIS*, vol. 136, no. 11, pp. 1555–1566, Nov. 2016 (in Japanese).

[20] J. Fujiwara, R. Okumura, K. Mizutani, and H. Harada, “Feasibility study of F-RIT low-power MAC protocol complied with IEEE 802.15.4/4e for wireless smart utility network,” *IEEJ Trans. EIS*, vol. 137, no. 11, pp. 1461–1471, Nov. 2017 (in Japanese).

[21] Wi-SUN Alliance, https://wi-sun.org

[22] A. Otokawa, T. Suzuki, K. Yamaguchi, and S. Yasuzawa, “An effort of utilizing electricity smart meter telecommunication system to gas and water metering,” *IEE Tech. Rep.*, CMN-20-020, Jan. 2020 (in Japanese).

[23] T. Moriyama, T. Nakayama, and T. Fujii, “Intermittent interval feedback design for multi-stage wireless sensor network,” *Mobile Netw Appl*, vol. 22, no. 5, pp. 970–982, Oct. 2017.

[24] H. Sanada, T. Fujii, R. Aizawa, and T. Kawata, “Routing redundancy reducing method for U-Bus Air using cloud coorperation,” in Proc. 2018 Tenth International Conference on Ubiquitous and Future Networks (ICUFN), pp. 223–228, Jul. 2018.

[25] D. Kominami, M. Sugano, M. Murata, and T. Hatauchi, “Controlled and self-organized routing for large-scale wireless sensor networks,” *ACM Trans. on Sensor Networks*, vol. 10, no. 1, pp. 1–27, Nov. 2013.

[26] R. Tanabe, T. Kawaguchi, R. Takitoge, and K. Ishibashi, “Energy-aware receiver-driven medium access control protocol for wireless energy-harvesting sensor networks,” in *Proc. 15th IEEE Annual Consumer Communication & Networking Conference (CCNC)*, pp. 1–6, Jan. 2018.

[27] A. Fujimoto, Y. Masui, T. Yoshihiro, and F. Uchio, “Beacon scheduling in receiver-initiated MAC protocols for low-delay and energy-efficient WSNs,” in *Proc. 2017 IEEE Wireless Communications and Networking Conference (WCNC)*, pp. 1–6, Mar. 2017.

[28] R. Okumura, K. Mizutani, and H. Harada, “Feasibility study of Wi-SUN JUTA profile-compliant F-RIT protocol,” *IEICE Trans, Commun*. (to be published).

[29] R. Okumura, K. Mizutani, and H. Harada, “Efficient polling communications for multi-hop networks based on receiver-initiated MAC protocol,” *IEICE Trans. Commun.*, vol.E104-B, no. 5 , May 2021 (to be published).

[30] R. Okumura, J. Fujiwara, K. Mizutani, and H. Harada, “Enhanced F-RIT protocol for wireless smart utility networks with high traffic bi-directional communications,” *IEICE Trans. Commun.*, vol.E101-B, no. 12, pp. 2487–2497, Dec. 2018.

[31] K. Mochizuki, K. Obata, K. Mizutani, and H. Harada, “Development and field experiment of wide area Wi-SUN system based on IEEE 802.15.4g,” in *Proc. 2016 IEEE 3rd World Forum on Internet of Things (WF-IoT)*, pp. 1–6, Dec. 2016.

[32] R. Okumura, T. Habara, K. Obata, K. Mochizuki, K. Mizutani, H. Harada, and T. Shiba, “Field experiment of IEEE 802.15.4g based system for water smart metering systems”, *IEICE Tech. Rep*., vol. 116, no. 46, RCS2016-26, pp. 13–18, May 2016 (in Japanese).

[33] R. Okumura, T. Habara, K. Samejima, A. Dan, K. Mizutani, K. Mizutani, H. Harada, and T. Shiba, “Field experiment of IEEE 802.15.4g-based system in open space for water smart metering systems,” *IEICE Tech. Rep*., vol. 117, no. 363, SRW2017-63, pp. 19–24, Dec. 2017 (in Japanese).

[34] R. Okumura, K. Mizutani, and H. Harada, “Transmission route configuration and access schemes for multi-hop networks based on receiver-initiated MAC protocol,” *IEICE Tech. Rep*., vol. 119, no. 73, SRW2019-8, pp. 41–46, Jun. 2019 (in Japanese).

[35] H. Wang and A. O. Fapojuwo, “A survey of enabling technologies of low power and long

range machine-to-machine communications," *IEEE Communications Surveys & Tutorials*, vol. 19, no. 4, pp. 2621–2639, Jun. 2017.

[36] A. K. Sultania, P. Zand, C. Blondia, and J. Famaey, "Energy modeling and evaluation of NB-IoT with PSM and eDRX," in *Proc. 2018 IEEE Globecom Workshops (GC Wkshps)*, pp. 1–7, Dec. 2018.

[37] S. S. I. Samuel, "A review of connectivity challenges in IoT-smart home," in *Proc. 2016 3rd MEC International Conference on Big Data and Smart City (ICBDSC)*, pp. 1–4, Mar. 2016.

[38] U. Raza, P. Kulkarni, and M. Sooriyabandara, "Low power wide area networks: An overview," *IEEE Commun. Surveys & Tutorials*, vol. 19, no. 2, pp. 855–873, Jan. 2017.

[39] L. Qiao, Z. Zheng, W. Cui, and L. Wang, "A survey on Wi-Fi HaLow technology for Internet of things," in *Proc. 2018 2nd IEEE Conference on Energy Internet and Energy System Integration (EI2)*, pp. 1–5, Oct. 2018.

[40] A. G. Ramonet and T. Noguchi, "IEEE 802.15.4 now and then: evolution of the LR-WPAN standard," in *Proc. 2020 22nd International Conference on Advanced Communication Technology (ICACT)*, pp. 1198–1210, Apr. 2020.

[41] IEEE Computer Society, "IEEE Std 802.15.4d™," Apr. 2009.

[42] T. Winter, P. Thubert, A. Brandt, J. Hui, R. Kelsey, P. Levis, K. Pister, R. Struik, JP. Vasseur, and R. Alexander, "RFC6550; RPL: IPv6 routing protocol for low-power and lossy networks," Mar. 2012.

[43] IEEE Computer Society, "IEEE 802.15.10™," Apr. 2017.

[44] IEEE Computer Society, "IEEE Std 802.15.4x™," Mar. 2019.

[45] IEEE Computer Society, "IEEE Std 802.15.4s™," Feb. 2018.

[46] V. C. Gungor and G. P. Hancke, "Industrial wireless sensor networks: challenges, design principles, and technical approaches," *IEEE Trans. on Industrial Electronics*, vol. 56, no. 10, pp. 4258–4265, Oct. 2009.

[47] H. Hayashi, "Evolution of next-generation gas metering system in Japan," in *Proc. 2014 IEEE MTT-S International Microwave Symposium (IMS2014)*, pp. 1–4, Sept. 2014.

[48] K. Kamimura, H. Hayashi, and T. Hatauchi, "Determination of adjacent nodes for power efficient wireless sensor networks," *IEEJ Trans. EIS*, vol. 134, no. 5, pp. 612–619, May

2014 (in Japanese).

[49] J. S. Lee, “Performance evaluation of IEEE 802.15.4 for low-rate wireless personal area networks,” *IEEE Trans. on Consumer Electronics*, vol. 52, no. 3, pp. 742–749, Aug. 2006.

[50] É. Morin, M. Maman, R. Guizzetti, and A. Duda, "Comparison of the device lifetime in wireless networks for the Internet of things," *IEEE Access*, vol. 5, pp. 7097–7114, Apr. 2017.

[51] A. Mavromatis, G. Z. Papadopoulos, X. Fafoutis, A. Elsts, G. Oikonomou, and T. Tryfonas, “Impact of guard time length on IEEE 802.15.4e TSCH energy consumption,” in *Proc. 2016 13th Annual IEEE International Conference on Sensing, Communication, and Networking (SECON)*, pp. 1–3, Jun. 2016.

[52] A. Elsts, S. Duquennoy, X. Fafoutis, G. Oikonomou, R. Piechocki, and I. Craddock, “Microsecond-accuracy time synchronization using the IEEE 802.15.4 TSCH protocol,” in *Proc. 2016 IEEE 41st Conference on Local Computer Networks Workshops (LCN Workshops)*, pp. 156–164, Nov. 2016.

[53] F. Kojima and H. Harada, “A study on IEEE 802.15.4e compliant low-power multi-hop SUN with frame aggregation,” in *Proc. 2013 IEEE International Conference on Communications (ICC)*, pp. 4041–4045, Jun. 2013.

[54] P. Huang, L. Xiao, S. Soltani, M. W. Mutka, and N. Xi, “The evolution of MAC protocols in wireless sensor networks: A Survey,” *IEEE Communications Surveys & Tutorials*, vol. 15, no. 1, pp. 101–120, Jan. 2013.

[55] Y. Kawamoto, T. Matsunaga, and Y. Kado, “MAC protocol with clock synchronization correction for a practical infrastructure monitoring system,” *International Journal of Distributed Sensor Networks*, vol. 14, no. 4, pp. 1–14, Apr. 2018.

[56] K. Samejima, R. Okumura, K. Mizutani, and H. Harada, “Evaluation of CSL-based low power MAC protocol for wireless smart metering networks,” in *Proc. 17th IEEE Annual Consumer Communication & Networking Conference (CCNC)*, pp. 1–6, Jan. 2020.

[57] C. Perkins, E. Belding-Royer, and S. Das, “RFC3561; Ad hoc on-demand distance vector (AODV) routing,” Jul. 2003.

[58] T. Clausen and P. Jacquet, “RFC3626; Optimized link state routing protocol (OLSR),” Oct. 2003.

[59] S. Matsui, “Technology trends and applications of IoT systems,” *IEICE Trans. on Commun.*

(Japanese Edition), vol. J100-C, no. 4, pp. 151–158, Apr. 2017 (in Japanese).

[60] S. Deering and R. Hinden, “RFC8200; Internet protocol, version 6 (IPv6) specification,” Jul. 2017.

[61] JP. Vasseur, M. Kim, K. Pister, N. Dejean, and D. Barthel, “RFC6551; Routing metrics used for path calculation in low-power and lossy networks,” Mar. 2012.

[62] T. Habara, K. Mizutani, and H. Harada, “A load balancing algorithm for layer 2 routing in IEEE 802.15.10,” *IEICE Trans. Commun.*, vol.E101-B, no. 10, pp. 2131–2141, Oct. 2018.

[63] The Telecommunication Technology Committee, “JJ-300.10 Home Network Communication Interface for ECHONET Lite (IEEE 802.15.4/4e/4g 920 MHz-band Wireless),” Mar. 2015.

[64] R. Okumura, K. Mizutani, and H. Harada, “Experimental evaluation of co-existence for wireless communication systems using 920 MHz-band,” *IEICE Tech. Rep.*, vol. 118, no. 283, SRW2018-29, pp. 37–42, Nov. 2018 (in Japanese).

[65] S. Duquennoy, A. Elsts, B. A. Nahas, and G. Oikonomo, “TSCH and 6TiSCH for Contiki: challenges, design and evaluation,” in *Proc. 2017 13th International Conference on Distributed Computing in Sensor Systems (DCOSS)*, pp. 11–18, Jun. 2017.

[66] S. Petersen and S. Carlsen, “WirelessHART versus ISA100.11a: the format war hits the factory floor,” *IEEE Industrial Electronics Mag.*, vol. 5, no. 4, pp. 23–34, Dec. 2011.

[67] IETF 6TiSCH WG, https://datatracker.ietf.org/wg/6tisch/documents

[68] X. Vilajosana, T. Watteyne, M. Vučinić, T. Chang, and K. S. J. Pister, "6TiSCH: Industrial performance for IPv6 Internet-of-things networks," *Proc. IEEE*, vol. 107, no. 6, pp. 1153–1165, Jun. 2019.

[69] A. Musaddiq, Y. B. Zikria, Zulqarnain, and S. W. Kim, “Routing protocol for low-power and lossy networks for heterogeneous traffic network,” *EURASIP J. on Wireless Commun. and Networking*, no. 21, pp. 1–23, Jan. 2020.

[70] W. Robby, R. Okumura, K. Mizutani, and H. Harada, “A scheduling scheme for channel hopping in Wi-SUN FAN systems toward data throughput enhancement,” in *Proc. IEEE 91st Vehicular Technology Conference (VTC)*, pp. 1–5, May 2020.

[71] R. Okumura, K. Mizutani, and H. Harada, “Analysis of MAC protocols for battery-powered devices in wireless field area network,” *IEICE Tech. Rep.*, vol. 120, no. 138, SRW2020-18, pp. 45–50, Aug. 2020 (in Japanese).

[72] E. A. Lin, J. M. Rabaey, and A. Wolisz, “Power-efficient rendez-vous schemes for dense wireless sensor networks,” in *Proc. 2004 IEEE International Conference on Communications (ICC)*, pp. 3769–3776, Jun. 2004.

[73] E. A. Lin, J. M. Rabaey, S. Wiethoelter, and A. Wolisz, “Receiver initiated rendezvous schemes for sensor networks,” in *Proc. '05. IEEE Global Telecommunications Conference (GLOBECOM)*, pp. 3117–3122, Nov. 2005.

[74] T. Hatauchi, T. Shikura, M. Kishiro, and Y. Fukuyama, “A study on the number of peripheral nodes and channel margin in mesh network,” in *Proc. IEICE Society Conf.*, B-21-22, Sept. 2007.

[75] Y. Sun, O. Gurewitz, and D. B. Johnson, “RI-MAC: a receiver-initiated asynchronous duty cycle MAC protocol for dynamic traffic loads in wireless sensor networks,” in *Proc. 6th ACM conference on Embedded network sensor systems (SenSys)*, pp. 1–14, Nov. 2008.

[76] D. Kominami, M. Sugano, M. Murata, and T. Hatauchi, “Robustness of receiver-driven multi-hop wireless network with soft-state connectivity management,” in *Proc. 2010 Fifth International Conference on Systems and Networks Communications (ICSNC)*, pp. 46–51, Aug. 2010.

[77] A. A. Lata and M. Kang, “A survey on the evolution of opportunistic routing with asynchronous duty-cycled MAC in wireless sensor networks,” *Sensors*, vol. 20, no. 15, pp. 1–30, Aug. 2020.

[78] R. Okumura, K. Mizutani, and H. Harada, “A broadcast protocol for IEEE 802.15.4e RIT based Wi-SUN systems,” in *Proc. IEEE 85th Vehicular Technology Conference (VTC)*, pp. 1–5, Jun. 2017.

[79] M. Nakagawa, A. Keida, and G.Tanaka, “Design and simulation analysis of and asynchronous flooding protocol based on receiver-initiated media access control,” *IEICE Trans. Fundamentals (Japanese Edition)*, vol.J102-A, no. 3, pp. 133–148, Mar. 2019 (in Japanese).

[80] J. Li, D. Zhang, and L. Guo, “DCM: A duty cycle based multi-channel MAC protocol for wireless sensor networks,” in *Proc. IET International Conference on Wireless Sensor Network (IET-WSN) 2010*, pp. 233–238, Nov. 2010.

[81] L. Guntupalli, D. Ghose, F. Y. Li, and M. Gidlund, “Energy efficient consecutive packet transmissions in receiver-initiated wake-up radio enabled WSNs,” *IEEE Sensors J.*, vol. 18, no. 11, pp. 4733–4745, Jun. 2018.

[82] R. Singh and B. Sikdar, “A receiver initiated low delay MAC protocol for wake-up radio enabled wireless sensor networks,” *IEEE Sensors J.*, vol. 20, no. 22, pp. 13796–13807, Nov. 2020.

[83] X. Fafoutis and N. Dragoni, “ODMAC: an on-demand MAC protocol for energy harvesting-wireless sensor networks,” in *Proc. 8th ACM Symposium on Performance evaluation of wireless ad hoc, sensor, and ubiquitous networks (PE-WASUN)*, pp. 49–55, Nov. 2011.

[84] R. Duan, D. Fang, and X. Chen, “A wakeup adapting traffic and receiver-initiated duty cycle protocol for WSN,” in *Proc. 2015 IEEE 12th Intl Conf on Ubiquitous Intelligence and Computing and 2015 IEEE 12th Intl Conf on Autonomic and Trusted Computing and 2015 IEEE 15th Intl Conf on Scalable Computing and Communications and Its Associated Workshops (UIC-ATC-ScalCom)*, pp. 1753–1759, Aug. 2015.

[85] T. Wada, I. T. Lin, and I. Sasase, “Asynchronous receiver-initiated MAC protocol exploiting stair-like sleep in wireless sensor networks,” *IEICE Trans. Commun.*, vol.E96-B, no. 1, pp. 119–126, Jan. 2013.

[86] T. Hayamizu, D. Kominami, M. Sugano, M. Murata, and T. Hatauchi, “Performance improvement by collision avoidance of control packets in receiver-driven multihop wireless mesh networks,” in *Proc. 2012 IEEE 9th International Conference on Mobile Ad-Hoc and Sensor Systems (MASS 2012)*, pp. 473–474, Oct. 2012.

[87] S. Horie and H. Higaki, “Wake-up schedule modification for shorter-delay intermittent wireless sensor networks,” in *Proc. 2018 International Conference on Information Networking (ICOIN)*, pp. 134–139, Jan. 2018.

[88] C. Cano, D. Malone, B. Bellalta, and J. Barceló, “On the improvement of receiver-initiated MAC protocols for WSNs by applying scheduling,” in *Proc. 2013 IEEE 14th International Symposium on A World of Wireless, Mobile and Multimedia Networks (WoWMoM)*, pp. 1–3, Jun. 2013.

[89] L. Tang, Y. Sun, O. Gurewitz, and D. B. Johnson, “PW-MAC: an energy-efficient predictive-wakeup MAC protocol for wireless sensor networks,” in *Proc. The 30th IEEE International Conference on Computer Communications (INFOCOM)*, pp. 1305–1313, Jun. 2012.

[90] L. Amwine, M. T. R. Khan, M. A. Yaqub, S. H. Ahmed, and D. Kim, “RIED-MAC: Receiver-initiated MAC based on energy-efficient duty cycling for UWSNs,” in *Proc. 2018 OCEANS - MTS/IEEE Kobe Techno-Oceans (OTO)*, pp. 1–5, May 2018.

[91] R. Zhang, H. Moungla, J. Yu, and A. Mehaoua, “Medium access for concurrent traffic in wireless body area networks: protocol design and analysis,” *IEEE Trans. Veh. Technol.*, vol. 66, no. 3, pp. 2586–2599, Mar. 2017.

[92] S. Ghafoor, N. Boujnah, M. H. Rehmani, and A. Davy, “MAC protocols for terahertz communication: a comprehensive survey,” *IEEE Commun. Surveys & Tutorials*, Aug. 2020.

[93] S. Toyonaga, D. Kominami, M. Sugano, and M. Murata, “Potential-based routing for supporting robust any-to-any communication in wireless sensor networks,” *EURASIP J. on Wireless Commun. and Networking*, vol. 2013, no. 1, pp. 1–13, Dec. 2013.

[94] C. Damdinsuren, D. Kominami, M. Sugano, M. Murata, and T. Hatauchi, “Lifetime extension based on residual energy for receiver-driven multi-hop wireless network,” *Cluster Comput.*, vol. 16, no. 3, pp. 469–480, Sept. 2013.

[95] IEEE Computer Society, “IEEE Std 802.15.4™-2011,” Sept. 2011.

[96] T. Kawata, “Development and its future prospects of gas smart meter using Wi-SUN technology,” *IEICE Tech. Rep.*, vol. 116, no. 481, SRW2016-79, pp. 65–68, Mar. 2017 (in Japanese).

Author's Publication List

Journal Papers

1. R. Okumura, J. Fujiwara, K. Mizutani, and H. Harada, "Enhanced F-RIT protocol for wireless smart utility networks with high traffic bi-directional communications," *IEICE Trans. Commun.*, vol.E101-B, no. 12, pp. 2487–2497, Dec. 2018.

2. R. Okumura, K. Mizutani, and H. Harada, "Efficient polling communications for multi-hop networks based on receiver-initiated MAC protocol," *IEICE Trans. Commun.*, vol.E104-B, no. 5, May 2021, accepted.

3. R. Okumura, K. Mizutani, and H. Harada, "Feasibility study of Wi-SUN JUTA profile-compliant F-RIT protocol," *IEICE Trans. Commun.*, accepted.

4. H. Harada, K. Mizutani, J. Fujiwara, K. Mochizuki, K. Obata, and R. Okumura, "IEEE 802.15.4g based Wi-SUN communication systems," *IEICE Trans. Commun.*, vol.E100-B, no. 7, pp. 1032–1043, Jul. 2017.

5. J. Fujiwara, R. Okumura, K. Mizutani, and H. Harada, "Feasibility study of F-RIT low-power consumption MAC protocol complied with IEEE 802.15.4/4e for wireless smart utility network," *IEEJ Trans. EIS*, vol. 137, no. 11, pp. 1461–1471, Nov. 2017 (in Japanese).

6. Y. Xiang, R. Okumura, K. Mizutani, and H. Harada, "Data rate enhancement of FSK transmission scheme for IEEE 802.15.4 based field area network," *IEEE Sensors Journal*, vol. 21, no. 7, pp. 9600–9611, Apr. 2021.

International Conference Papers

1. R. Okumura, J. Fujiwara, K. Mizutani, and H. Harada, "Experimental evaluation and analysis of F-RIT low power MAC protocol complied with IEEE 802.15.4e," in *Proc. IEEE Wireless Communications and Networking Conference (WCNC)*, pp. 1–6, San Francisco, CA, U.S.A, Mar. 2017.

2. R. Okumura, K. Mizutani, and H. Harada, "A broadcast protocol for IEEE 802.15.4e RIT

based Wi-SUN systems," in *Proc. IEEE 85th Vehicular Technology Conference (VTC)*, pp. 1–5, Sydney, Australia, Jun. 2017.

3. R. Okumura, K. Mizutani, and H. Harada, "Analysis and experimental verification of F-RIT protocol for wireless smart utility network," in *Proc. 16th IEEE Annual Consumer Communication & Networking Conference (CCNC)*, pp. 1–6, Las Vegas, NV, U.S.A, Jan. 2019.

4. R. Okumura, K. Mizutani, and H. Harada, "Dependable source routing scheme for multi-hop networks based on receiver-initiated MAC protocol," in *Proc. 17th IEEE Annual Consumer Communication & Networking Conference (CCNC)*, pp. 1–4, Las Vegas, NV, U.S.A, Jan. 2020.

5. J. Fujiwara, R. Okumura, K. Mizutani, H. Harada, S. Tsuchiya, and T. Kawata, "Ultra-low power MAC protocol complied with RIT in IEEE 802.15.4e for wireless smart utility networks," in *Proc. IEEE 27th Annual International Symposium on Personal, Indoor, and Mobile Radio Communications (PIMRC)*, pp. 1–6, Valencia, Spain, Sept. 2016.

6. T. Junjalearmvong, T. Habara, R. Okumura, K. Mizutani, and H. Harada, "A dynamic routing protocol supporting mobile nodes in Wi-SUN FAN systems," in P*roc. 20th International Symposium on Wireless Personal Multimedia Communications (WPMC)*, pp. 324–330, Yogyakarta, Indonesia, Dec. 2017.

7. K. Samejima, R. Okumura, T. Habara, K. Mizutani, and H. Harada, "Practical analysis of CSL low power MAC protocol based on IEEE 802.15.4e frame structure," in *Proc. 21st Wireless Personal Multimedia Communications (WPMC)*, pp. 636–640, Chiang Rai, Thailand, Nov. 2018.

8. T. Junjalearnvong, R. Okumura, K. Mizutani, and H. Harada, "Performance evaluation of multi-hop network configuration for Wi-SUN FAN systems," in *Proc. 16th IEEE Annual Consumer Communication & Networking Conference (CCNC)*, pp. 1–6, Las Vegas, NV, U.S.A, Jan. 2019.

9. T. Hayashida, R. Okumura, K. Mizutani, and H. Harada, "Possibility of dynamic spectrum sharing system using VHF-band radio sensor and machine learning," in *Proc. 2019 IEEE DySpan Workshop on Data-Driven Dynamic Spectrum Sharing*, pp. 1–6, Newark, NJ, U.S.A, Nov. 2019.

10. D. Hotta, R. Okumura, K. Mizutani, and H. Harada, "Stabilization of multi-hop routing

construction in Wi-SUN FAN systems," in *Proc. 17th IEEE Annual Consumer Communication & Networking Conference (CCNC)*, pp. 1–6, Las Vegas, NV, U.S.A, Jan. 2020.

11. K. Samejima, R. Okumura, K. Mizutani, and H. Harada, "Evaluation of CSL-based low power MAC protocol for wireless smart metering networks," in *Proc. 17th IEEE Annual Consumer Communication & Networking Conference (CCNC)*, pp. 1–6, Las Vegas, NV, U.S.A, Jan. 2020.

12. K. Mizutani, R. Okumura, K. Mizutani, and H. Harada, "A heterogeneous wireless networks management scheme of Wi-SUN FAN and Wi-Fi systems," in *Proc. 17th IEEE Annual Consumer Communication & Networking Conference (CCNC)*, pp. 1–4, Las Vegas, NV, U.S.A, Jan. 2020.

13. K. Samejima, R. Okumura, K. Mizutani, and H. Harada, "Wireless smart ubiquitous network by CSL-based low power MAC protocol," in *Proc. 17th IEEE Annual Consumer Communication & Networking Conference (CCNC)*, pp. 1–2, Las Vegas, NV, U.S.A, Jan. 2020.

14. R. Wayong, R. Okumura, K. Mizutani, and H. Harada, "A scheduling scheme for channel hopping in Wi-SUN FAN systems toward data throughput enhancement," in *Proc. IEEE 91st Vehicular Technology Conference (VTC)*, pp. 1–5, Online, May 2020.

15. Y. Xiang, R. Okumura, K. Mizutani, and H. Harada, "Data rate enhancement for IEEE 802.15.4 based FSK transmission scheme," in *Proc. 2020 IEEE World Forum on Internet of Things (WF-IoT)*, pp. 1–6, Online, Jun. 2020.

16. K. Mizutani, R. Okumura, K. Mizutani, and H. Harada, "Coexistence of synchronous and asynchorous MAC protocols for wireless IoT systems in sub-gigaherz band," in *Proc. 2020 IEEE World Forum on Internet of Things (WF-IoT)*, pp. 1–6, Online, Jun. 2020.

17. H. Ochiai, K. Mizutani, R. Okumura, K. Mizutani, and H. Harada, "A high-speed Wi-SUN FAN network by highly-dense frequency hopping," in *Proc. IEEE 92nd Vehicular Technology Conference (VTC)*, pp. 1–5, Online, Nov. 2020.

18. R. Wayong, R. Okumura, K. Mizutani, and H. Harada, "A routing protocol toward reliable mobile communication in Wi-SUN FAN," in *Proc. 18th IEEE Annual Consumer Communication & Networking Conference (CCNC)*, pp. 1–6, Online, Jan. 2021.

Technical Reports and Local Conference Papers

1. R. Okumura, K. Mizutani, and H. Harada, "A broadcast protocol for IEEE 802.15.4e RIT based Wireless smart utility networks," *IEICE Tech. Rep*., vol. 115, no. 474, SRW2015–93, pp. 131–136, Mar. 2016 (in Japanese).

2. R. Okumura, T. Habara, K. Obata, K. Mochizuki, K. Mizutani, H. Harada, and T. Shiba, "Field experiment of IEEE 802.15.4g based system for water smart metering systems", *IEICE Tech. Rep*., vol. 116, no. 46, RCS2016-26, pp. 13–18, May 2016 (in Japanese).

3. R. Okumura, J. Fujiwara, K. Mizutani, and H. Harada, "Implementation and experimental evaluation of F-RIT low power MAC protocol for wireless smart utility networks -Bidirectional transmission characteristics under interference environments-," *IEICE Tech. Rep*., vol. 116, no. 249, SRW2016-54, pp. 59–64, Oct. 2016 (in Japanese).

4. R. Okumura, J. Fujiwara, K. Mizutani, and H. Harada, "Implementation and experimental evaluation of F-RIT low power MAC protocol for wireless smart utility networks -Improvement of transmission characteristics under high traffic environment-," *IEICE Tech. Rep*., vol. 116, no. 374, SRW2016-62, pp. 31–36, Dec. 2016 (in Japanese).

5. R. Okumura, J. Fujiwara, K. Mizutani, and H. Harada, "Many-to-one transmission characteristics of F-RIT low power MAC protocol for wireless smart utility networks," *IEICE Tech. Rep.*, vol. 116, no. 481, SRW2016-73, pp. 29–34, Mar. 2017 (in Japanese).

6. R. Okumura, K. Mizutani, and H. Harada, "Feasibility study of JUTA profile for Wi-SUN compliant F-RIT protocol," *IEICE Tech. Rep.*, vol. 117, no. 297, SRW2017-47, pp. 17–22, Nov. 2017 (in Japanese).

7. R. Okumura, T. Habara, K. Samejima, A. Dan, K. Mizutani, K. Mizutani, H. Harada, and T. Shiba, "Field experiment of IEEE 802.15.4g-based system in open space for water smart metering systems," *IEICE Tech. Rep.*, vol. 117, no. 363, SRW2017-63, pp. 19–24, Dec. 2017 (in Japanese).

8. R. Okumura, K. Mizutani, and H. Harada, "Experimental evaluation of co-existence for wireless communication systems using 920 MHz-band," *IEICE Tech. Rep.*, vol. 118, no. 283, SRW2018-29, pp. 37–42, Nov. 2018 (in Japanese).

9. R. Okumura, K. Mizutani, and H. Harada, "Transmission route configuration and access schemes for multi-hop networks based on receiver-initiated MAC protocol," *IEICE Tech. Rep*., vol. 119, no. 73, SRW2019-8, pp. 41–46, Jun. 2019 (in Japanese).

10. R. Okumura, K. Mizutani, and H. Harada, “Dependable downlink route configuration scheme for multi-hop networks based on receiver-initiated MAC protocol,” *IEICE Tech. Rep.*, vol. 119, no. 166, SRW2019-13, pp. 1–6, Aug. 2019 (in Japanese).

11. R. Okumura, K. Mizutani, and H. Harada, “Improvement of uplink delay for polling-based multi-hop networks with receiver-initiated MAC protocol,” *IEICE Soc. Conf.*, B-18-1, Sept. 2019 (in Japanese).

12. R. Okumura, K. Mizutani, and H. Harada, “A study on MAC protocols for battery-powered devices in wireless field area network,” *IEE Tech. Rep.*, CMN-20-013, pp. 67–72, Jan. 2020 (in Japanese).

13. R. Okumura, K. Mizutani, and H. Harada, “Analysis of MAC protocols for battery-powered devices in wireless field area network,” *IEICE Tech. Rep.*, vol. 120, no. 138, SRW2020-18, pp. 45–50, Aug. 2020 (in Japanese).

14. T. Habara, R. Okumura, K. Obata, K. Mochizuki, K. Mizutani, H. Harada, and T. Shiba, “Transmission characteristics of IEEE 802.15.4g based device-to-device communication systems in smart water-metering environments”, *IEICE Tech. Rep*., vol. 116, no. 88, SRW2016-32, pp. 39–44, Jun. 2016 (in Japanese).

15. T. Junjalearmvong, T. Habara, R. Okumura, K. Mizutani, and H. Harada, “A dynamic routing protocol supporting mobile nodes in Wi-SUN FAN systems,” *IEICE Tech. Rep.*, vol. 117, no. 178, SRW2017-9, pp. 1–6, Aug. 2017.

16. K. Samejima, R. Okumura, T. Habara, K. Mizutani, and H. Harada, “Analysis of CSL low power MAC protocol for wireless smart metering networks,” *IEICE Tech. Rep.*, vol. 117, no. 458, SRW2017-87, pp. 93–98, Feb. 2018 (in Japanese)

17. T. Junjalearmvong, T. Habara, R. Okumura, K. Mizutani, and H. Harada, “Experimental performance evaluation of multi-hop configuration and transmission in Wi-SUN FAN devices,” *IEICE Tech. Rep.*, vol. 117, no. 458, SRW2017-88, pp. 87–92, Feb. 2018.

18. K. Mizutani, R. Okumura, K. Mizutani, and H. Harada, “A home area network integrated 920MHz-band and 2.4GHz-band wireless systems,” *IEICE Tech. Rep*., vol. 118, no. 283, SRW2018-36, pp. 71–76, Nov. 2018 (in Japanese).

19. K. Samejima, R. Okumura, K. Mizutani, and H. Harada, “Routing metric calculation schemes for wireless mesh network based on IEEE 802.15.10 L2R protocol,” *IEICE Tech.*

Rep., vol. 118, no. 476, SRW2018-58, pp. 19–24, Mar. 2019 (in Japanese).

20. T. Hayashida, R. Okumura, K. Mizutani, and H. Harada, "Outdoor position clustering by machine learning with wide area radio profile," *IEICE Tech. Rep*., vol. 119, no. 62, SR2019-2, pp. 9–16, May 2019 (in Japanese).

21. D. Hotta, R. Okumura, K. Mizutani, and H. Harada, "Experimental evaluation on multi-hop route construction in Wi-SUN FAN systems," *IEICE Tech. Rep.*, vol. 119, no. 62, SR2019-13, pp. 79–86, May 2019 (in Japanese).

22. K. Mizutani, R. Okumura, K. Mizutani, and H. Harada, "Co-existence of synchronous and asynchronous protocols for wireless IoT systems in 920 MHz-band," *IEICE Tech. Rep.*, vol. 119, no. 73, SRW2019-7, pp. 35–40, Jun. 2019 (in Japanese).

23. R. Wayong, R. Okumura, K. Mizutani, and H. Harada, "A channel hopping scheduling toward throughput enhancement in Wi-SUN FAN systems," *IEICE Tech. Rep*., vol. 119, no. 73, SR2019-9, pp. 47–52, Jun. 2019.

24. Y. Xiang, R. Okumura, K. Mizutani, and H. Harada, "Field experiment of IEEE 802.15.4 based high-speed FSK transmission scheme," *IEICE Tech. Rep.*, vol. 119, no. 363, SRW2019-52, pp. 7–12, Jan. 2020.

25. H. Ochiai, K. Mizutani, R. Okumura, K. Mizutani, and H. Harada, "A highly dense frequency hopping for high-speed Wi-SUN FAN network," *IEICE Tech. Rep.*, vol. 119, no. 363, SRW2019-53, pp. 13–18, Jan. 2020 (in Japanese).

26. Y. Xiang, R. Okumura, K. Mizutani, and H. Harada, "Feasibility study of IEEE 802.15.4 based high-speed FSK transmission scheme for broadband wireless field area network," *IEE Tech. Rep.*, CMN-20-014, pp. 73–78, Jan. 2020.

27. H. Masaki, K. Mizutani, R. Okumura, K. Mizutani, and H. Harada, "Indoor transmission experiment of IEEE 802.15.4g systems for use in medical and nursing care," *IEICE Tech. Rep.*, vol. 119, no. 450, SRW2019-70, pp. 51–56, Mar. 2020 (in Japanese).

28. R. Hirakawa, K. Mizutani, R. Okumura, K. Mizutani, and H. Harada, "A routing method for improvement of transmission performance in Wi-SUN FAN network," *IEICE Tech. Rep.*, vol. 119, no. 450, SRW2019-73, pp. 69–74, Mar. 2020 (in Japanese).

29. R. Wayong, R. Okumura, K. Mizutani, and H. Harada, "A routing protocol toward seamless handover for mobile nodes in Wi-SUN FAN systems," *IEICE Tech. Rep.*,

vol. 120, no. 138, SR2020-10, pp. 7–12, Aug. 2020.

30. H. Masaki, R. Okumura, K. Mizutani, and H. Harada, “Fundamental transmission characteristics of contact detection system using short-range wireless communication technology,” *IEICE Tech. Rep.*, vol. 120, no. 138, SRW2020-19, pp. 51–56, Aug. 2020 (in Japanese).

31. H. Masaki, R. Okumura, K. Mizutani, and H. Harada, “Influence of obstacles on contact detection system using short-range wireless communication technology,” *IEICE Tech. Rep.*, vol. 120, no. 260, SRW2020-39, pp. 67–72, Nov. 2020 (in Japanese).

32. S. Kadoi, H. Ochiai, R. Okumura, K. Mizutani, and H. Harada, “IEEE 802.15.4-based OFDM transmission scheme toward adaptive IoT wireless communication systems,” *IEICE Tech. Rep.*, vol. 120, no. 406, SRW2020-77, pp. 88–93, Mar. 2021 (in Japanese).

Awards

1. IEICE SRW Student Award, Presented by The Institute of Electronics, IEICE Technical Committee on Short Range Wireless Communication (SRW), Aug. 2016.

2. IEEE VTS Tokyo Chapter Young Researcher’s Encouragement Award, Presented by IEEE Vehicular Technology Society (VTS) Tokyo Chapter, Jun. 2017.

3. The Telecom System Technology Student Award, The Telecommunication Advancement Foundation, Mar. 2019.

Scholarships and Financial Support

1. Category 1 scholarship from JASSO, Apr. 2012–Mar. 2016.

2. Category 1 scholarship from JASSO (Exemption from refund by outstanding achievements), Apr. 2016–Mar. 2018.

3. The Murata Science Foundation Grants for Overseas Research, Jun. 2017.

4. Grant in aid for JSPS research fellow: Grant number JP18J23198, Apr. 2018–Mar. 2021.